Assessment of Seismic Vulnerability of Building Structures in Almaty, Kazakhstan

Muhammad Sajjad Rashid, M.Eng

Submitted in fulfillment of the requirements
for the degree of Master of Science
in Civil & Environmental Engineering

School of Engineering and Digital Sciences
Department of Civil & Environmental Engineering
Nazarbayev University

53 Kabanbay Batyr Avenue,
Astana, Kazakhstan, 010000

Supervisor: Dr. Dichuan Zhang
Co-supervisor: Dr. Sung-Woo Moon

April 2023

DECLARATION

I hereby declare that this manuscript, entitled “Assessment of Seismic Vulnerability of Building Structures in Almaty, Kazakhstan”, is the result of my own work except for quotations and citations which have been duly acknowledged.

I also declare that, to the best of my knowledge and belief, it has not been previously or concurrently submitted, in whole or in part, for any other degree or diploma at Nazarbayev University or any other national or international institution.

Name: Muhammad Sajjad Rashid

Date: April 07, 2023

Abstract

Kazakhstan's southern and southern-eastern regions exhibit intraplate seismicity, which is characterized by numerous destructive earthquakes. The major metropolis in this area, Almaty, features a variety of buildings with different materials for construction and seismic-resistant systems. Numerous buildings were constructed during the Soviet Union era with inadequate seismic-resisting design, necessitating an empirical and analytical evaluation of their ability to withstand significant earthquakes. Thus, it is necessary to evaluate the seismic risks associated with these structures. This study adopted both empirical and analytical techniques to assess the seismic vulnerability of these structures in two phases.

In the first phase, the macro-level seismic assessment was conducted on residential, industrial, and commercial buildings. The European Macroseismic Scale was used to categorize these structures according to their seismic vulnerability. Different earthquake intensities and peak ground accelerations led to the development of vulnerability curves as well as the probability of damage for each damage grade chart. The likelihood of damage in the Almaty region was established for design basis and maximum considered earthquakes. Residential buildings made of unreinforced masonry and wood sustain significant damage, and in some cases, complete collapse when subjected to earthquakes of the maximum magnitude that are normally taken into account. While industrial and commercial buildings made of unreinforced masonry sustain the heavy to very heavy damage. Since damaged and precast concrete buildings are likely to sustain heavy to very heavy damages, an additional analytical assessment was necessary.

In the second phase, the analytical assessment was carried out to study the detailed performance and behavior of the pre-cast emulated moment frame buildings under the earthquakes. For this purpose, two pre-cast emulated moment frames were selected named VP and VT series, which were constructed between the 1970s to 1990s. Based on the data collected from the government agency, OPENSEES was used to produce two-dimensional nonlinear models for these buildings. The next step was to conduct increased amplitude dynamic analyses using 16 previously recorded strong ground motions, which share similar fault features with the Almaty. The results of the investigation were used to produce fragility curves using two parameter lognormal distribution function for Immediate occupancy, life safety and collapse prevention as per FEMA 356, which were subsequently used to evaluate the building structures' ability to withstand seismic activity.

Moreover, Immediate occupancy refers to minor/light damage, life safety refers to moderate and collapse prevention refers to severe damage. Furthermore, the probability of the global and local failure of the structural elements were calculated at both design basis earthquake and maximum considered earthquake using maximum inter-storey drift as evaluation criteria for global failure and plastic rotation for local failure. For global failure mode, it has been found that the pre-cast moment frame buildings have 100% chances of sustaining light damage for both DBE and MCE. While the probability of sustaining moderate damage for these buildings is more than 70% at DBE and more than 95% at MCE. Similarly, the probability of sustaining severe damage is more than 15% at DBE and more than 50% at MCE for both VT and VP series buildings.

Correspondingly, for local failure of structural elements it has been found that the columns of VT series buildings have a probability of 100% to undergo a severe damage at both DBE and MCE predicting that the buildings will collapse in future seismic event having spectral acceleration equivalent to DBE or MCE. Conversely, the structural elements of VP series buildings have a probability of more than 90% to sustain moderate damage and probability of more than 80% to suffer severe damage at DBE while this probability increases to 100% for both moderate and severe damage at MCE. Therefore, it is recommended that these reinforced concrete structures need to be strengthened or torn down based on further cost analysis.

Keywords: Macroseismic Assessment, Mean Damage, Probability of Damage, Vulnerability, Increment Dynamic Analysis (IDA), Reinforced Concrete, Fragility Curves

Acknowledgement

I would like to express my deepest gratitude to my thesis supervisors, **Dr. Dichuan Zhang** and **Dr. Sung-Woo Moon** for their invaluable guidance, support, and encouragement throughout the duration of my thesis. Their expertise and insights have been instrumental in shaping my research and have helped me to navigate the challenges that came with it. Their patience, dedication and willingness to go above and beyond to help me has been truly inspiring.

Dr. Dichuan Zhang has been an amazing mentor and a constant source of inspiration. Their guidance and support have been instrumental in helping me to navigate the complexities of my research. On the other hand, Dr. Sung-Woo Moon has been invaluable in the development of my research. Their guidance and support have been instrumental in helping me to navigate the complexities of my research and their dedication to my success has been truly inspiring.

I am grateful for their willingness to share their knowledge and expertise, and for the time they have invested in providing constructive feedback on my work. This thesis would not have been possible without the support and guidance of both my thesis supervisor and co-supervisor. Thank you both for your invaluable contributions and for being amazing mentors.

Also, I want to express my sincere gratitude to my parents, **Abdul Rashid** and **Nusrat Bano**, for their unflagging support and affection as I pursued my academic goals. Their never-ending support and inspiration have been crucial in helping me stay committed and focused on achieving my academic objectives.

Table of Content

List of Abbreviations and Variables

CP	Collapse Prevention
DBE	Design Basis Earthquake
DPM	Damage Probability Matrix
D1	Damage grade 1 (slight damage)
D2	Damage grade 2 (moderate damage)
D3	Damage grade 3 (heavy damage)
D4	Damage grade 4 (very heavy damage)
D5	Damage grade 5 (destruction)
EMS	European Macro-seismic Scale
ERD	Earthquake Resistant Design
GNDT	Group of National Defense against Earthquake
IDA	Increment Dynamic Analysis
IDR	Inter-storey Drift Ratio
IO	Immediate Occupancy
I	Earthquake Intensity
LLRS	Lateral Load Resisiting System
LS	Life Safety
λ	Mean
MCE	Maximum Considered Earthquake
p	Probability of damage
PGA	Peak Ground Acceleration

Q	Ductility Index
RC	Reinforced Concrete
Sa	Spectral Acceleration
ζ	Standard Deviation
V	Vulnerability Index
μ_D	Mean damage

List of Tables

List of Figures

Chapter 1 - Introduction

1.1 Problem statement

In the last few decades, economic loss and human casualties are increased to a great extent because of natural disasters[1]. Natural disasters pose an ever-present danger to human life as well as the infrastructure and worth land's economy; earthquakes are among the most catastrophic and fatal natural catastrophes around the globe[2][3]. The death toll from the 2010 Haiti earthquake was estimated by the CATDAT destructive earthquake database to be between 46,000 and 316,000 people. The Tohoku earthquake in Japan, which occurred 12 months later, claimed the lives of 20,475 individuals and left 1.108 million people homeless. In addition to casualties, $140 billion was lost as a result of the earthquake that struck Tohoku, Japan, in 2011[4]. There are a variety of factors taken into consideration while evaluating a certain structure. These factors are concerned with the structural system, seismic capability, soil condition, plane and elevation regularity, and the acquisition of restricted field data. These parameters offer a picture or a realistic estimate of the structural system's behavior. When it comes to seismological hazards, the risks are the potential for significant losses during a certain interval of time. Construction tagging processes are used to identify differences in building and structural safety induced by earthquake degradation after significant seismic activity. These approaches assist in determining the degree to which buildings and structures may have been damaged as a result of earthquakes. These approaches can be utilized to assure the safety of a structure [5]. The seismic performance of buildings during the earthquake attracted the attention of many authors as the buildings were vulnerable to withstand earthquakes all over the world in the past decade. This becomes a major concern over the vulnerability speculation of infrastructure everywhere in the world [6]. So, it becomes very important and the needs of the time to work on the development of methodologies that identify the damages to the buildings because of earthquakes and devise some standards or approaches related to the seismic assessment of the buildings.

1.1.1 Rationale for Project

It is well known that earthquakes are caused by the movement of geological faults. In the waters, earthquakes are confined to small regions, frequently on single faults that define the boundary of the Earth's plates. In contrast, earthquakes within continents, notably in the Central Asia region, are dispersed over hundreds of kilometers on intricate networks of thousands of faults

that move less regularly than one another. In light of this, it is considerably more challenging to locate these faults and comprehend the seismic hazard. On the continents, it can be thousands of years between earthquakes along the same fault. Before the 2003 earthquake in Bam, Iran, there was no documented or archaeological evidence of any major earthquakes in the past 2,000 years. The last significant earthquake in Kazakhstan, which largely damaged Almaty, occurred in 1911, more than a century ago. The absence of recent earthquakes often leads to the erroneous conclusion that a territory is not influenced by earthquakes.

This research is aimed especially at Kazakhstan as Kazakhstan's southern and south-eastern areas are in a seismically active zone. High seismic zones cover around 42.9 percent of Kazakhstan's land area. Over 7 million people reside here, more than 40% of the country's industrial capacity is concentrated here, and over 400 communities are situated here, including the country's major industrial and cultural hub, Almaty, with a population of more than 2.0 million. There were a lot of strong earthquakes in the late nineteenth and early twenty-first centuries in Almaty. The earthquake includes the 1887 earthquake with a magnitude of 7.2, the 1889 earthquake with a magnitude e 8.3, the 1911 earthquake with a magnitude e 8.2 earthquake, and a lot of smaller earthquakes[7].

An earthquake in the neighborhood of Almaty, such as the Verny earthquake, may bring catastrophic damage and a substantial loss of life. Because the Almaty area and its surrounding territory are located at the junction of several faults, stressing their vulnerability to potential seismic events (as shown in Figure 1), the probability of big earthquakes around the region has grown and emphasizing its susceptibility to potential devastating earthquakes. The cause of such catastrophic hazards is not only the intensity of a prospective earthquake, but also the underestimation of seismic danger, the selection of building locations, and other variables. A lot of research has been done on developing shallow and deep foundations in Kazakhstan [8], [9],[10], [11] but little has been done on determining how vulnerable buildings built during the Soviet Union's era are. As a result, it is critical for government decision-makers to assess the seismic risks to buildings in order to create an effective system for reducing catastrophe risk, particularly in urban areas with dense populations like the region around Almaty.

Recently, the Chinese government devised a plan for the construction of the New Silk Road Economic Belt, with the aim of fostering connectivity and cooperation particularly among Eurasia's

nations. The projected route for the New Silk Road is 8,445 kilometers long, with 2,787 kilometers passing through Kazakhstan territory[12]. Kazakhstan's government has committed to speeding up the rollout of China's New Silk Road initiative, with particular attention paid to the road connecting Western Europe and Western China, and to additional transit routes traversing Central Asia. One of the most vital nodes of the proposed New Silk Road is the city of Almaty. The building of structures in the Almaty region is expected to rise quickly in the next years to meet the demand for economic development along the New Silk Road Economic Belt. Since Almaty is located in a highly seismic region, it is crucial to reduce the seismic risk of existing and newly constructed structures in this area.

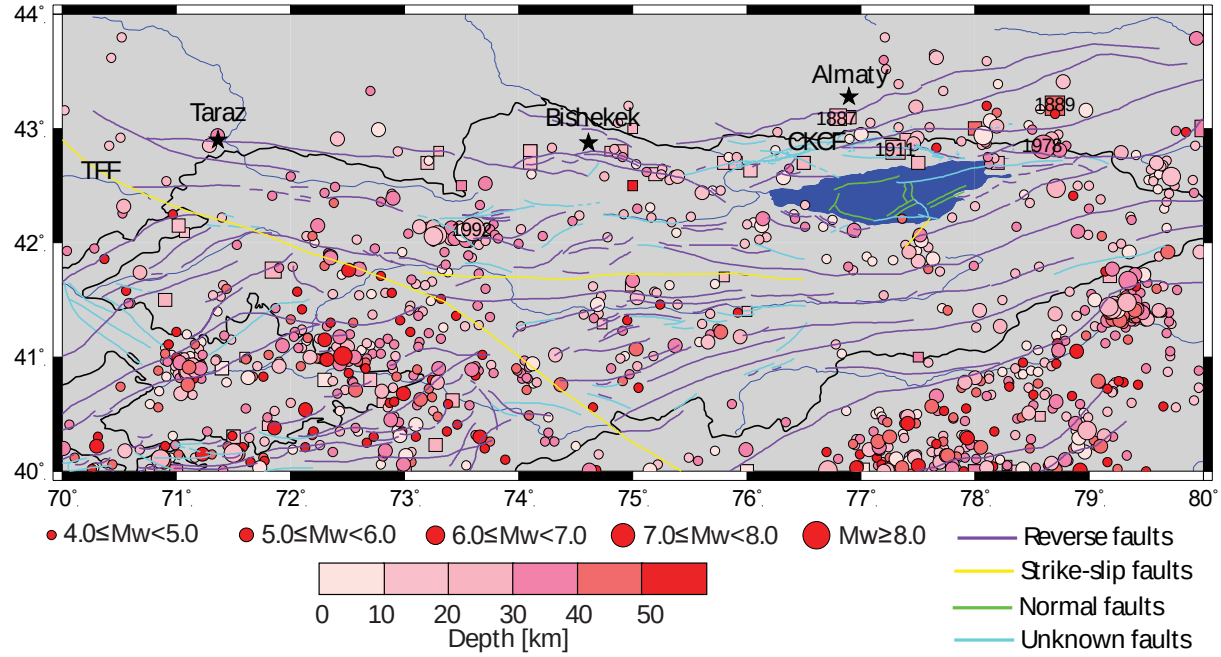

Figure 1-1 Seismic map of Almaty region[7], [8]

Assessing the structural seismic susceptibility in the Almaty area is the first step in reducing seismic risks. To facilitate the growth of the Silk Road Economic Belt, which connects China, Eurasia, and Europe, the Kazakhstani government needs this information to create an effective system for reducing disaster risk in the Almaty region.

1.2 Hypothesis

1. Several types of building structures in the Almaty region are vulnerable to earthquakes.
2. Pre-cast concrete emulated moment resisting frame buildings constructed in the 1970s and 1990s may not have sufficient capacity to resist large earthquakes.

1.3 Objectives

The objective of this study are;

1. Categorization of the building structures in the Almaty region.
2. Development of vulnerability curves based on Macroseismic assessment.
3. Development of structural models for pre-cast concrete emulated moment frame buildings.
4. Evaluation of the seismic performance of representative buildings through incremental dynamic analyses.
5. Development of seismic fragility curves for representative buildings based on incremental dynamic analyses results for
    a) Immediate occupancy,
    b) Life safety and
    c) Collapse prevention

1.4 Organization of the Thesis

Background knowledge, problem statement, the rationale for the study, hypothesis, and objectives are provided in **chapter 1**. **Chapter 2** provides a summary of the research that has already been conducted on seismic vulnerability, including the methods that have been developed to assess it and the measures that have been developed to reduce it in structures. It also includes the information regarding European Macroseismic Scale (EMS-98) used for macro level empirical study for the buildings located in Almaty. Furthermore, seismic information and activity of Almaty, has also been discussed in this chapter. **Chapter 3** discusses the building categorization, their link to EMS-98, the development of vulnerability curves for both earthquake intensity and PGA. Beside that the bar chart for probability of each damage grade versus spectral acceleration is also presented at 475 year and 2475 years return period. Recommendations are also given for residential, industrial, and commercial buildings based on these results. **Chapter 4** includes the analytical method of seismic assessment. This chapter discusses about the selection of prototype buildings,

ground motion selection, general results which includes hysteretic plot, plastic hinge formation and plastic deformation in columns and beams for a particular earthquake with different values of g. Fragility curves for different performance limits i.e., Immediate occupancy (IO), life safety (LS) and collapse prevention (CP) are also presented in this chapter. **Chapter 5** discuss the conclusion and limitations of this study.

Chapter 2 - Literature review

2.1 Seismic risk assessment—why?

The economic toll of natural disasters keeps climbing in tandem with the world's expanding population, accelerating rate of urbanization, and expansion of megacities[13]. International disaster management experts met in Sendai, Japan in 2015 to establish the Sendai Framework for Disaster Risk Reduction in response to the growing threat posed by natural disasters around the world [14], a global strategy with the goal of significantly lowering the risk of natural disasters by the year 2030. Financing for programs that aim to reduce the risk of catastrophes occurring in the first place is still difficult to come by, despite the fact that disaster costs continue to rise [15]. According to Danielll [16], earthquake events account for a large share of the growing economic effects, harm to cultural and social contexts, fatalities, injuries, and the destruction of homes and livelihoods [13]. Due to high levels of construction vulnerability, middle-income countries, especially those with fast expanding cities, are ever more vulnerable to earthquake disaster [17]

Evaluations of seismic risk at the urban, regional, and national levels try to quantify the probable magnitude of future earthquake impacts so that policymakers and society can take measures to better protect themselves [18]. The dynamic nexus between a city’s-built environment, its residents, and the many networks that exist makes risk assessment a particularly difficult task [19][20].

The assessment of the physical vulnerability of structures is a crucial step in reducing seismic risk. Regardless of whether you live in a location with a high or low seismic hazard, urban-scale seismic risk assessment is an essential first step toward earthquake-resilient communities. The term "resilience" does not refer only to the safety of the occupants, but the ability of systems to recover from the seismic event and return to their pre-earthquake performance[21][22]. Even minor damage may result in production halts and communication disruptions, with long-term effects on regional development. An urban system's potential damage from a seismic event may be estimated using hypothetical scenarios. As a result, effective proactive interventions may be performed, hence boosting overall resilience[23]. Assessing seismic risk on a big scale is a difficult and time-consuming procedure that requires a breadth of expertise. Exposure, seismic vulnerability, and hazard (Figure 2-1) are the factors to be considered while assessing the risk [24].

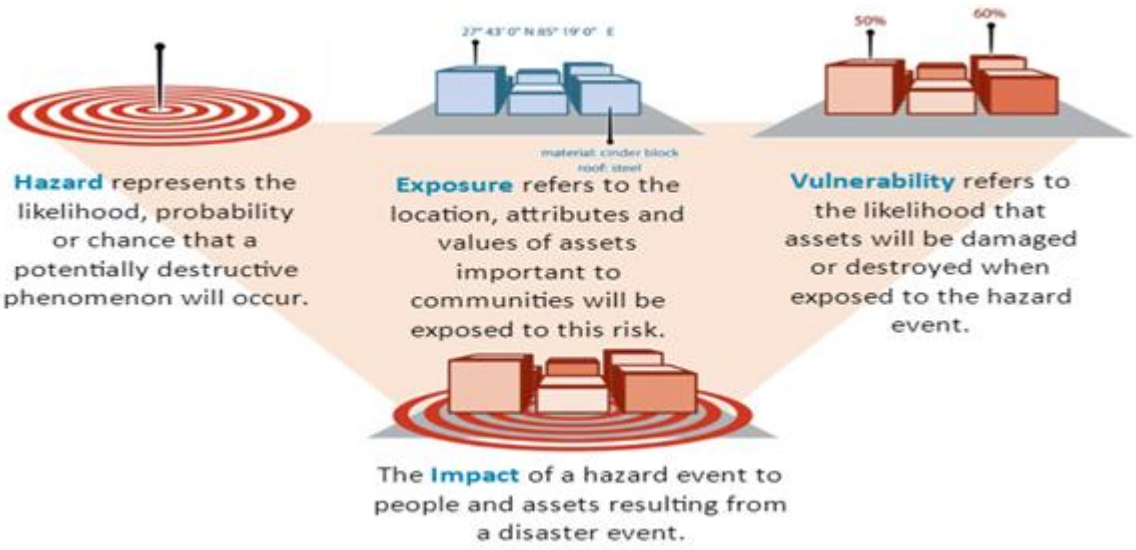

Figure 2-1 Factors used for evaluating seismic risk

The seismic risk may be conceptualized in terms of the relationship shown in Equation 2-1 [25].

$$Seismicis = Hazard\ x\ Vulnerability\ x\ Exposure \quad \text{.....} \textbf{\textit{Equation 2-1}}$$

More precisely, a building's seismic risk may be quantified as its likelihood of collapsing within a certain time interval Figure 2-1.

Figure 2-2 Seismic risk components

A comprehensive seismic risk assessment is a technically challenging and costly operation that incorporates a large number of buildings, their geometrical properties, and heterogeneity in terms of the structural design and seismic behavior characteristics within metropolitan regions[26]. Numerous approaches (qualitative and quantitative) have been developed over the last several decades, including those offered by Italy's Gruppo Nazionale for Difesa dei Terremoti[27], and the Federal Emergency Management Agency (FEMA) in USA [28] in addition to the European RISK-UE technique[29][30], have been established based on the assessment's resources and size. These approaches, which may be fine-tuned to reflect the specifics of regional building vulnerabilities as long as a thorough building inventory is provided, have been extensively utilized across the globe. In situ field surveys give the most trustworthy and detailed building inventories, although they are generally very costly. Furthermore, these issues are increased in areas with moderate seismic risks, where the resources available for seismic assessments are restricted.

2.2 How is the seismic vulnerability of a building determined?

The purpose of seismic vulnerability assessments is to provide an estimate of a building's vulnerability to damage from earthquakes. The first stage is to categorize structures into several categories with comparable seismic responses to reduce the amount of required computations (if classification were not employed, an evaluation would be required for each individual structure). Seismic vulnerability functions are then developed that connect a measure of the vulnerability to the magnitude of an earthquake, with separate functions being developed for each structure type.

2.2.1 Seismic vulnerability classification of building typologies

The purpose of building classification is to examine multiple buildings at once by placing them into categories based on their shared characteristics (and, by extension, their assumed seismic responses).

The difficulty that lies at the heart of classifying buildings lies in determining which structures can be considered equivalent to one another. Which aspects of the structures should be considered while classifying them into categories? The literature addresses classification in a variety of ways [31], and hence, several taxonomies and classification schemes have emerged. This section introduces some of the most widely used taxonomies and classification schemes, focusing

on the qualities they employ to inform classification. Stone [32] has provided detailed descriptions of the many types of construction that go into the various taxonomies.

The European Macro-Seismic Scale (EMS-98) [33] was created to categorize typical building types in Europe. It introduces categories for buildings according to their major structural material, with some additional categories for design level, Lateral load Resisting System (LLRS), reinforcing level, and/or floor material. The different categories presented in EMS-98 are depicted in table 2-1. EMS-98 is currently the subject of an effort that will make it more relevant on a worldwide scale [34].

The Hazard-US (HAZUS) initiative classifies the building stock based on seismic design standards, building height, and the fundamental structural system. When the number of storeys is considered, the sixteen building types developed for the US building stock increase to 36, which are divided into three categories: low-rise for structures with three to four storeys, mid-rise for structures with five to seven storeys, and high-rise for structures with eight to twenty storeys. Above twenty storeys, the use of classification is not recommended in favor of a more individualized, specific assessment. Including pre-code, low-code, moderate-code, and high-code engineering design levels expands the taxonomy to 132 distinct typologies [28]. Despite the fact that it was designed exclusively for the United States, HAZUS has seen widespread use across the globe, both with and without special regional modifications (for instance, in Canada [35], Venezuela [36], and in India [37]. It has also been used internationally to validate the findings of other SVAs [38], [39]. The 2013 UNISDR [40] is a significant adaption of a worldwide risk assessment research in which the authors employed the HAZUS building classification system and added classes were deemed essential to cover global building types [41]. This results in twenty-one structural kinds, which is five more than the initial HAZUS taxonomy required for international use. The groups are then subdivided into categories according on height and design level, much like HAZUS does as well, with a few minor differences in the heights and design levels considered. These are fully described by Stone [32].

The PAGER system [42] classifies worldwide building typologies using sixteen primary construction types that increase to eighty-seven sub-categories when more precise descriptions of structures are given, such as information on the type of diaphragms, construction methods, etc. The relatively extensive PAGER classes table can be found in Stone’s [32].

Another framework created to include many building typologies around the world is the Global Earthquake Model (GEM) building taxonomy. GEM was designed to be a categorization system that is collapsible (i.e., adaptable to all levels of building data detail), detailed, differentiates between different degrees of seismic performance, extensible, internationally applicable, and usability [31]. The GEM method has three tiers to classify datasets with varying levels of specificity and can be found in the work done by Stone [32]. Level 1 GEM data types are the most fundamental features of a structure that can be used for categorization. Level 1 information contained construction details such as the building's material, LLRS, height, age, general occupancy, location, shape (square, rectangular, etc.), roof pitch, flooring, and footings. Building classification methods used by GEM are similar to those used by the Syner-G project, which has a European focus [43].

The RESIS-II building categorization system was created with the express purpose of being utilized in Central American countries [44]. As with GAR-13, the system began with HAZUS structural categories but with fewer typologies that account for variances in height. For any structural typology, the design level is not taken into account in keeping with the level of building regulation in the area. Additional structural types have also been included to accommodate additional architectural typologies that are typical of Central America but are not seen in the United States. The resultant twenty-four classifications are provided by Stone in his work [32].

2.2.2 Seismic Vulnerability Evaluation Methods

For planning strategies and addressing the earthquake emergency management for risk analysis, researchers have worked previously on many methods for determining the vulnerability of the structures and a territorial scale evaluation was carried out for the European region and they classified them into two major groups:

1. Empirical Assessment Methods and
2. Analytical Assessment Methods.

Analytical approaches rely on mechanical models, while empirical methods rely on post-earthquake damage[45].

2.2.2.1 Empirical Assessment Methods

Empirical techniques rely on data from previous earthquakes to establish correlations between a selection variable and earthquake severity, such as damage or economic loss, with the presumption that the past will repeat itself. Aleatory uncertainties, like those caused by natural changes in ground shaking or building reactions, are taken into account automatically, which is a significant benefit. However, the broader applicability of results can be limited by a lack of data for 1) bigger, less common earthquakes, 2) similar engineering contexts, and 3) similar seismological and shallow geological contexts [46]. Empirical techniques are also unable to take into account variations in engineering and tectonic contexts, as well as unique structural elements and building strengthening [47]. Following are the several simplified seismic risk assessment;

1. P25 Scoring Method [48]
2. Vulnerability index methods
   2.1. Group of National Defense against Earthquake (GNDT) approach
   2.2. European Macro-Seismic (EMS) approach (RISK-UE) [29]
   2.3. Combined GNDT and macro-seismic approaches
3. Rapid Visual screening assessment methods [49]

2.2.2.1.1 P25 Scoring Method

The method is essentially based on monitoring, listing, and ranking the most critical structural elements that influence a building's seismic reaction one after another in regard to their relative significance. The fundamental idea behind the P25 preliminary assessment method was initially introduced by Bal [50] in 2006 and 2007, and it was then refined, developed, and calibrated as part of a research effort that was funded by TUBITAK (the Turkish Scientific and Technical Research Council). This method uses a combination of seven indices, including scores for the existence of short columns, soft floors, frame discontinuity, and pounding potential, as well as estimates of stiffness based on wall and column measurements (adjusted for height) and soil quality.

2.2.2.1.2 Vulnerability Index Methods

The precision of these indirect methods exceeds that of the macroseismic method, but it does necessitate the evaluation of a variety of typological and structural traits or susceptibility

factors that affect the building's seismic reaction. The disadvantage is that it requires more time and effort. The following are other categories for these techniques.

2.2.2.1.2.1 GNDT approach

This approach requires the gathering of a significant amount of potentially damaging survey information as well as data. A thorough assessment of each of the fundamental aspects that were influencing and governing structural building vulnerability is going to be developed as a result of the field survey, which has as its primary objective of this understanding. For instance, the type of footing, the sort and quality of the materials, and the elevation arrangements in the plan. Eleven parameters were considered, and each was given a qualifying coefficient (either Ki or Cvi) that corresponded to one of the four hazard categories (A, B, C, and D). Each parameter evaluated a particular structural characteristic that is connected to the reaction of the building to seismic loads. The parameters were then weighted based on their relative relevance, starting with the least important vulnerability parameters and working our way up. Values for the weights were determined at through the combined efforts of experts. This comprehensive data was coupled with coefficients to produce the vulnerability index (Iv), which classified building damage in response to earthquake.

2.2.2.1.2.2 European Macro-Seismic (EMS) approach (RISK-UE)

The RISK-UE program is another approach that was established for the purpose of evaluating the vulnerability in Europe. This initiative has received financing and assistance from the European Union (EU). Integrating a standardized approach to evaluating seismic risk across European countries has been the focus of this research. That, alongside the psychological, financial, and political fallout from the earthquakes in Turkey, Athens, and Greece, is on account of Europe's failure to construct a unified global infrastructure [45]. As a result of this, the vulnerability index method, also known as VIM, has been implemented as a form of vulnerability assessment after having been developed and tested in seven cities across Europe with great success [30].

This strategy is based on the classification of building typologies into six vulnerability classes (A to F), ranging from the most vulnerable to the least vulnerable. These structures can be grouped into one of four broad typologies:

a) masonry,

b) reinforced concrete,
c) steel, or
d) timber.

Additionally, it divided the degree of damage into five degrees, marked by the letters D1, D2, D3, D4, and D5, ranging from minor damaged to completely collapsed. The EMS-98 scale is intended to be used in the future to clarify the vision and definitions of several typology frameworks for European cities. It was developed as a methodology for the RISK-UE project and consider both old and current building types in the areas it studies [29]. Using the attributes of the building's typology, this method calculates a vulnerability score for a single structure or a group of buildings with similar structural characteristics. This index ranges from 0 (the least vulnerable) to 1 (the most vulnerable).

The macro-seismic framework provides the evaluation of vulnerability for various ensemble sizes of structures, ranging from a single structure to a large group of buildings. The vulnerability/susceptibility of a building to earthquakes is evaluated using a vulnerability index (V) and a ductility index (Q), with consideration given to the unique kind of building and its construction specifics (i.e., construction materials, lateral forces resisting systems, etc.). For identifying physical damages to structural and nonstructural components, the macro-seismic methodology employed in EMS-98 is based on building typology classifications, separated into six vulnerability classes (A to F), ranging from most vulnerable to least vulnerable. As illustrated in Table 2-1, the EMS-98 assigns several vulnerability classes to building structures based on their building construction materials and lateral force-resisting system. The severity of structural damages, on the other hand, is assessed from minor to full collapses using a five-level scale (D1 to D5) [33]. Based on the assessment of historical earthquake structural damages, an implicit Damage Probability Matrix (DPM) is built using descriptive language ("Few", "Many", "Most") to relate the degree of damage to earthquake intensities for various vulnerability classes, as presented in Table 2-2.

Table 2-1 Vulnerability classification for various constructions (EMS-98) [33]

Construction Materials	Lateral Force Resisting System	Range of Vulnerability Class	Most Likely Vulnerability Class
Masonry	Rubble stone, fieldstone	A	A
	Adobe (earth brick)	A-B	A
	Simple Stone	A-B	B
	Massive Stone	B-D	C
	Unreinforced manufactured stone units	A-C	B
	Unreinforced, with RC floors	B-D	C
	Reinforced or confined	C-E	D
Reinforced Concrete (RC)	Frame without ERD	A-D	C
	Frame with moderate level of ERD	B-E	D
	Frame with high level of ERD	C-F	E
	Walls without ERD	B-D	C
	Walls with moderate level of ERD	C-E	D
	Walls with high level of ERD	D-F	E
Steel	Steel structures	C-F	E
Wood	Timber structures	B-E	D

Table 2-2 Damage levels for different classes of vulnerability (EMS-98).

Intensity/ Damage level	D1 negligible to slight	D2 moderate	D3 substantial to heavy	D4 very heavy	D5 destruction
5	Few A/B				
6	Many A/B, Few C	Few A/B			
7		Many B, Few C	Many A, Few B	Few A	
8		Many C, Few D	Many B, Few C	Many A, Few B	Few A
9		Many D, Few E	Many C, Few D	Many B, Few C	Many A, Few B
10		Many E, Few F	Many D, Few E	Many C, Few D	Most A, Many B, Few C
11		Many F	Many E, Few F	Most C, Many D, Few E	Most B, Many C, Few D
12					Most D/E/F

In the context of the RISK-UE project, the implicit DPM was translated into numerical quantities as a development of the EMS-98 by fusing fuzzy set theory [29]. Using fuzzy set theory, the language terms "few," "many," and "most" were transformed into quantitative counterparts on a scale of one (1) to hundred (100) as shown in figure 2-3.

Membership function	χ=0	χ=1	χ=1	χ=0
Sub-class	++	+	-	--
Few	20	10	0	0
Many	60	50	20	10
Most	100	100	60	50

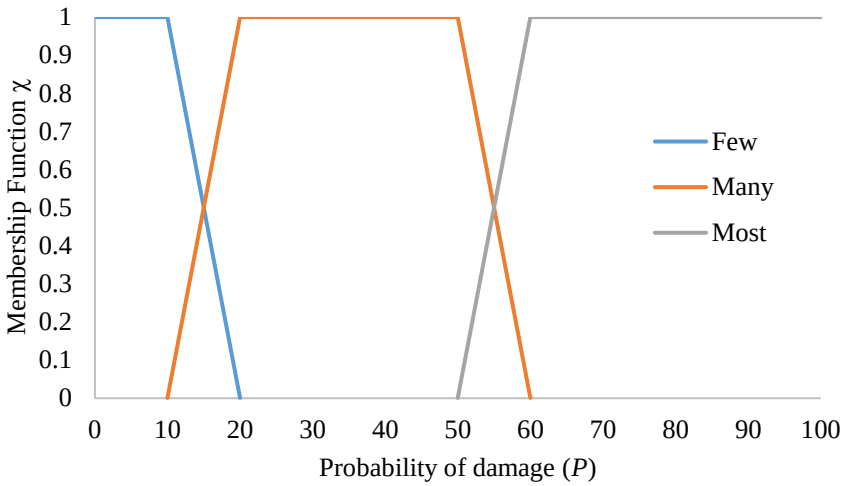

Figure 2-3 Membership function x

For the likelihood at each damage level, a binomial density function was introduced. For calculating each damage grade probability, a binomial function was introduced as given in equation 2-2.

$$p(k) = \frac{5!}{k!\,(5-k)!}\left(\frac{\mu_D}{5}\right)^k\left(1-\frac{\mu_D}{5}\right)^{5-k} \qquad \text{Equation 2-2}$$

where k represents the level of damage, from 1 (D1) to 5 (D5) and the mean damage value is μD.

Each vulnerability class is given four (4) potential sub-classes (++, +, -, --) for the density function for a certain earthquake intensity and damage level. As can be seen in Figure 2-3, the membership function provides a mapping between the corresponding damage probability (p) for the four (4) potential sub-classes and the descriptive language. Using the values presented in Figure 2-3, one may then convert this likelihood of damage (p) to the DPM, which can be found in Table 2-2.

Table 2-3 displays, for instance, the probability of harm (p) that is linked to vulnerability class B. The DPM displays "Few" for damage level 1 (D1) for intensity level 5. For each of the four potential subclasses (++, +, -, --), the appropriate probability of damage (p) at D1 can be calculated as 20%, 10%, 0%, and 0%, respectively. The DPM indicates "Many" for D1 and "Few" for D2 at intensity level 5. In this instance, the associated probability of damage (p) is assumed to be 20% for sub-class (-) and 10% for sub-class (--) at D1, and 20% for sub-class (++) and 10% for sub-class (+) at D2. For other intensities, you can use similar calculations to find the value k and probability p(k) for each outcome.

[51]**Table 2-3 Damage probability for Class B**

Intensity	DPM	Sub-class ++			Sub-class +			Sub-class -			Sub-class --		
		p (k)	Damage level (k)	μ_D	p (k)	Damage level (k)	μ_D	p (k)	Damage level (k)	μ_D	p (k)	Damage level (k)	μ_D
5	Few D1	20	D1	0.2	10	D1	0.1	0	D1	0.0	0	D1	0.0
6	Many D1, Few D2	20	D2	1.0	10	D2	0.6	20	D1	0.2	10	D1	0.1
7	Many D2, Few D3	20	D4	1.8	10	D4	1.3	20	D3	1.0	10	D3	0.6
8	Many D3, Few D4	20	D5	2.7	10	D5	2.2	20	D4	1.8	10	D4	1.3
9	Many D4, Few D5	20	D5	3.6	10	D5	3.2	20	D5	2.7	10	D5	2.2
10	Many D5	60	D5	4.5	50	D5	4.4	20	D5	3.6	10	D5	3.2

2.2.2.2 Analytical Assessment Methods

Analytical methods evaluate the response of a building under earthquake loading by simulating its behavior [52]. To a greater or lesser extent, structural models can be idealized, but they will always incorporate assumptions that can lead to significant disparities in outcomes [47]. There is considerable room for variation in analytical modeling due to the wide variety of possible modeling approaches, sources of information, and methods for tagging outputs with attributes. More assumptions are made in simpler models, but they are easier to design and solve; more

computer work and technical expertise are required in more complex models, resulting in more accurate results. In general, it may be divided into two categories:

1. Non-Linear static analysis (NLSA)/Pushover analysis (POA)
2. Non-Linear Time History Analysis (NLTHA)

2.2.2.2.1 Non-Linear static analysis (NLSA)/Pushover analysis (POA)

Non-linear static analysis' widespread adoption in seismic engineering can be attributed to the relative simplicity of the method. It has become an active engineering tool for evaluating the safety of structures against earthquake-induced collapse. The "Coefficient Method" was employed to determine target displacement for the first time when this approach was presented in FEMA 273 [53], and later it was modified in FEMA 356 [54]. The pushover analysis, which produces the well-known "Capacity Curve," is a type of non-linear static analysis. The ultimate objective of this method is to determine the dynamic attributes of the structure, such as its stiffness, strength, and ductility, under seismic loading.

To undertake a non-linear static analysis, commonly known as the POA procedure, the structure must be modeled in such a way that the non-linear force and displacement performance of its structural elements are taken into account. Then, a relationship between displacement and base shear (D vs. V) would be derived by submitting the structure to increasing lateral forces monotonically until the model's displacement reached or exceeded the allowable displacement that reflected a predetermined level of structural damage. The target displacement is defined as the permitted displacement. In the event that the slope of the curve turns negative, a global failure may occur. From this procedure, the inelastic response behavior for an analogous single degree of freedom may be established (SDOF). In order for this method to work, it requires reducing a system with multiple degrees of freedom (MDOF) to a system with a single MDOF. This transition, however, would only be exact if the structure vibrated in a single mode with a constant changing shape over time.

2.2.2.2.2 Non-Linear Time History Analysis (NLTHA)

This method is the most accurate and precise approach to evaluate a structure's or infrastructure's seismic performance. Recent advances in computer methodologies have allowed for the creation of tools like incremental dynamic analysis (IDA), which is an enhanced and

expanded version of the NLTHA methodology that can be used to assess the dynamic behavior of structures exposed to seismic vibrations. It was first suggested in 1977 by Bertero [55], and in the years that followed, a number of researchers and investigators devoted a significant amount of time and energy to examining it (Bazzurro [56], [57], Vamvatsikos and Cornell [58], Yun et al. [59]).

Furthermore, in 2000, it was certified by FEMA as a means of investigating the possibility of a global collapse. The application of incremental dynamic analyses has been of great help in recent years to the investigation of the overall behavior of structures, beginning with the stage of elastic response and continuing through the phases of yielding and non-linear response, all the way up to the stage where the structure becomes unstable. Additionally, IDA provided a clear picture of how a structure would behave in the event of a seismic event. In order to develop an incremental dynamic analysis (IDA), it is customarily necessary to collect a series of ground motion records using the NLTHA. In this particular instance, establishing the structural performance involved selecting the degree to which the ground motion was experienced. This could be accomplished by progressively increasing the seismic intensity until the global collapse capacity of the structure is reached. Graphing the ground motion intensity (IM) against a structural response parameter (EDP) is one way to illustrate the IDA result.

The main advantages of this method are that it can accurately describe a wide range of nonlinear material behavior, irregularities in structures with nonlinear geometry, how buildings behave when hit, and higher mode effects in high rise buildings. Nonetheless, this analysis has limitations, such as the need for a complex platform to construct the analytical model, the need for time to finish the analysis, and the need for a large quantity of ground motions needed to complete the study [45].

2.3 Seismicity in Almaty

We are aware that earthquakes occur on faults. In the waters, earthquakes are confined to small regions, frequently on single faults that define the boundary of the Earth's plates. In contrast, earthquakes within continents, notably in the Central Asia region, are dispersed over hundreds of kilometers on intricate networks of thousands of faults that move less regularly than one another. In light of this, it is considerably more challenging to locate these faults and comprehend the seismic hazard. On the continents, it can be thousands of years between earthquakes along the same fault. Before the 2003 earthquake in Bam, Iran, there was no documented or archaeological

evidence of any major earthquakes in the past 2,000 years. The last significant earthquake in Kazakhstan, which largely damaged Almaty, occurred in 1911, more than a century ago.

The absence of recent earthquakes often leads to the erroneous conclusion that a territory is not influenced by earthquakes. Nonetheless, as these examples demonstrate, there is still a major earthquake risk in Iran, the Tien Shan region, and throughout Central Asia due to the hundreds of active fault lines in the area that could trigger an earthquake at any moment. Due to a lack of investigation or because the faults' subtle or concealed effects on the terrain made them difficult to detect, many of the recent and destructive earthquakes in the innards of continents have occurred on previously unknown faults. It is challenging to discover and examine faults that never reach the Earth's surface, which is common in areas where convergent activity is forming mountains. One example is the mountain-front fault, which is thought to have caused the Verney (Almaty) earthquake of 1887 of magnitude 7.3.

Furthermore, large earthquakes don't necessarily occur on prominent faults that are visible from afar. The Chilik earthquake of 1889 occurred in Kazakhstan on a fault that had likely been immobile for thousands of years prior. With so many such faults, predicting which will create a large earthquake is extremely difficult. Moreover, a ruptured fault can be tens of kilometers away from the epicenter of an earthquake before damage is done. To accurately estimate risk, investigations of faults must span wide geographic areas.

Almaty has been damaged by powerful earthquakes multiple times in the last 150 years. The city sits on a significant seismically active fault zone in the northern Tien Shan Mountain range called Almaty fault or Tien Shan fault. While the Almaty Fault itself is hidden beneath layers of mezozoic and cainozoic strata, the strong seismicity in the area is evidence of its activity. Figure depicts the map of Kazakhstan's significant, well-known, and active faults [60]. Almaty is in danger because it is on the northern range of Zailijsky Alatau, which is the northernmost ridge of Tien Shan. Almaty is also at risk because weaker earthquakes can cause debris flows. It is necessary to increase the quantification of the seismic danger for areas with a population of over one and half million people [61].

The earthquakes having magnitude greater than 4 and less than from 250 BC to 2018 are depicted in figure 2-4 on a map of south-eastern Kazakhstan. The rectangle depicts the area surrounding Almaty city[45].

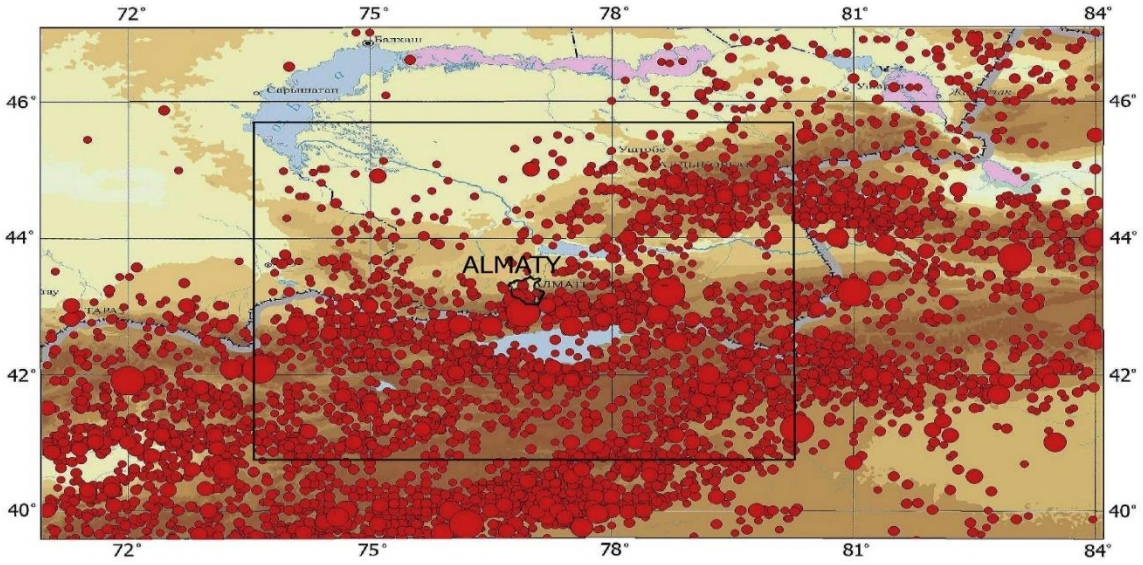

Figure 2-4 Earthquakes database from 250 BC to 2018 with seismicity 4≥Mw≥8[61]

The PGA increases rather evenly to the south and east from 0.31 g at the city's northwest boundary to 0.62 g at the hilly region's southeasterly border, assuming a return period of 475 years (Figure 2-5 on the left). The city's most highly populated area is located between 0.4 and 0.52 g with design basis earthquake PGA value of 0.487 with return period of 475 years. Figure 2-5 (right) shows that the increase in PGA continues to move south-eastward on the map for a return period of 2475 years, but its nature varies greatly since large, rare earthquakes dominate the risk in the

high mountains. The area of the city that is most densely populated lies within the bounds of 0.6 to 0.9 g with maximum considered earthquake PGA value of 0.7305 with return period of 2475 years.

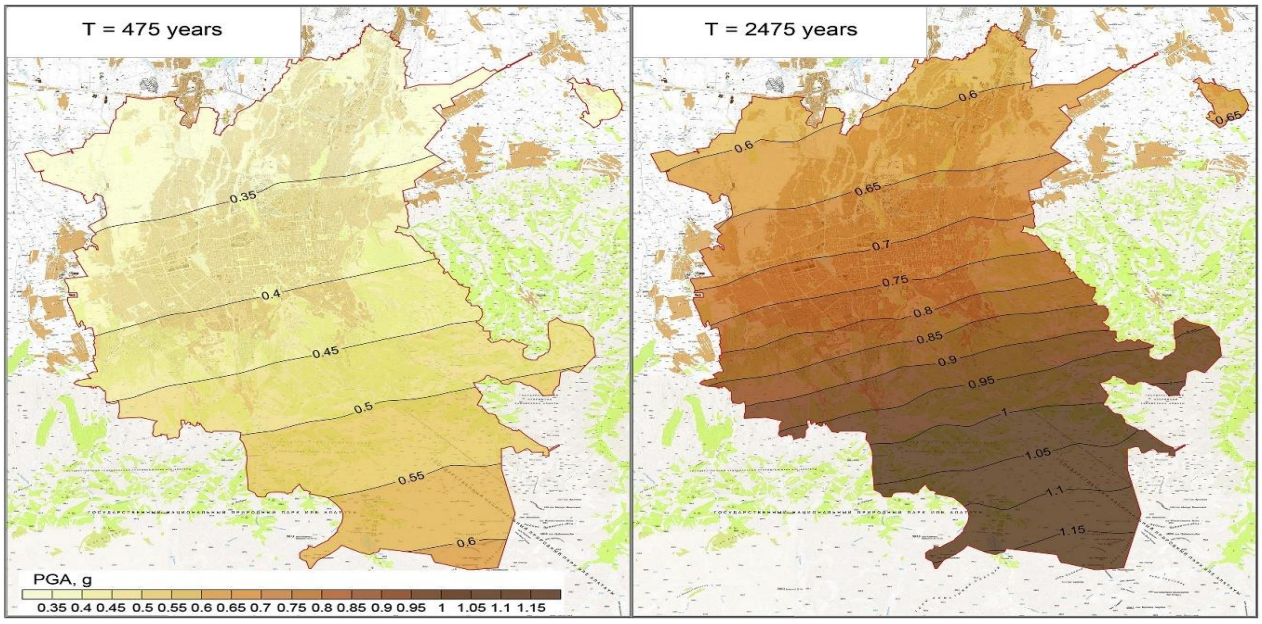

Figure 2-5 Seismic hazard maps of Almaty city, expressed in terms of the PGA and with return periods of 475 years (on the left) and 2475 years, respectively (right)[61]

Other than Almaty fault there are other faults are also present in the study area such as Zaili fault, diagonal fault and Boroldai fault as shown in Figure 2-6. Figure also shows a seismic micro-zoning map for the city of Almaty, displaying PGA for both a 10% chance of exceeding it within the next half-century (left) and a 2% chance of doing so (right). The primary tectonic faults in the city are indicated by gray strips.

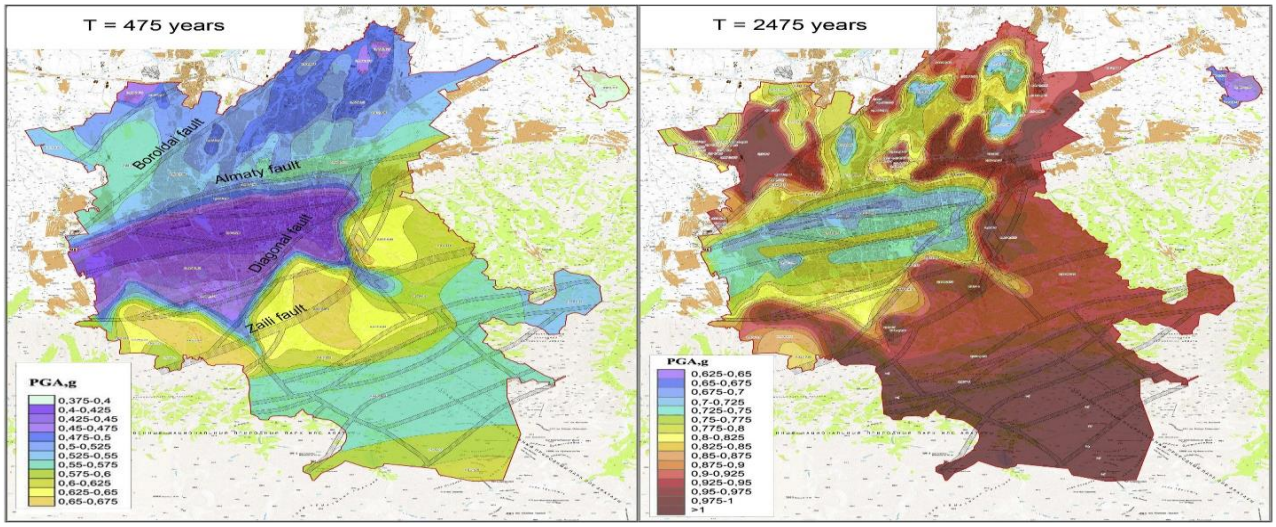

Figure 2-6 Microzonation map of Almaty in terms of PGA

Chapter 3 - Empirical Evaluations

3.1 Categorization of the buildings in Almaty

3.1.1 Residential Buildings

Approximately 8171 high-rise apartment complexes were built during the Soviet era (between the 1960s and the 1990s), according to data collected by the government agency (KazNIISA). The materials used in their construction, as well as their lateral force-resisting systems and ductility capacities, were taken into consideration while classifying these buildings. Masonry, reinforced concrete, precast concrete, wood, and steel are among the building materials. A bearing wall, wall panels, an emulated moment frame, a moment frame, and a shear wall make up the lateral force-resisting system. In addition, the building was classified as having a ductility capacity that was somewhere between medium and low, taking into account the construction materials, the year it was built, and the design code requirement. In Figure 3-1, we see the total number of buildings together with their breakdown into several types. The majority of the buildings were constructed by using precast and reinforced concrete. There are also a sizable number of brick and wood structures.

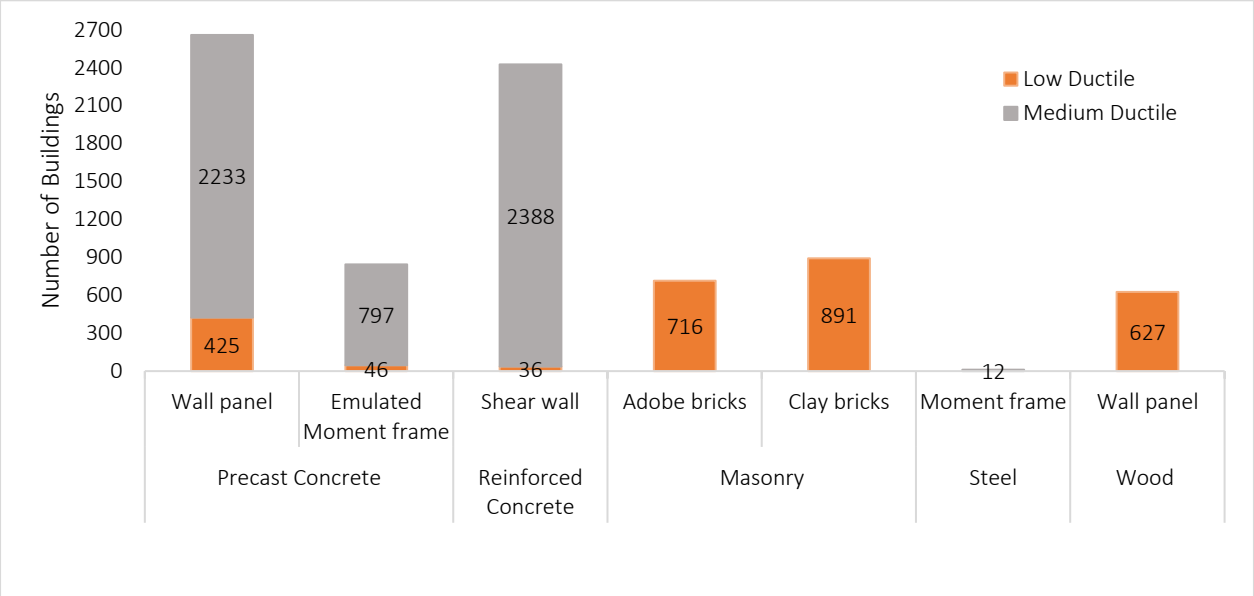

Figure 3-1 Categorization of Residential Buildings

3.1.2 Industrial Buildings

There are approximately 5890 industrial buildings that were constructed from 1950 to 2000. Similar to residential buildings these buildings were also categorized based on the construction material, lateral force resisting system and ductility etc. The distribution of the total number of buildings across the various categories is depicted in Figure 3-2. Precast and reinforced concrete were used in the construction of the vast majority of buildings. There are also a sizable number of brick and wood structures.

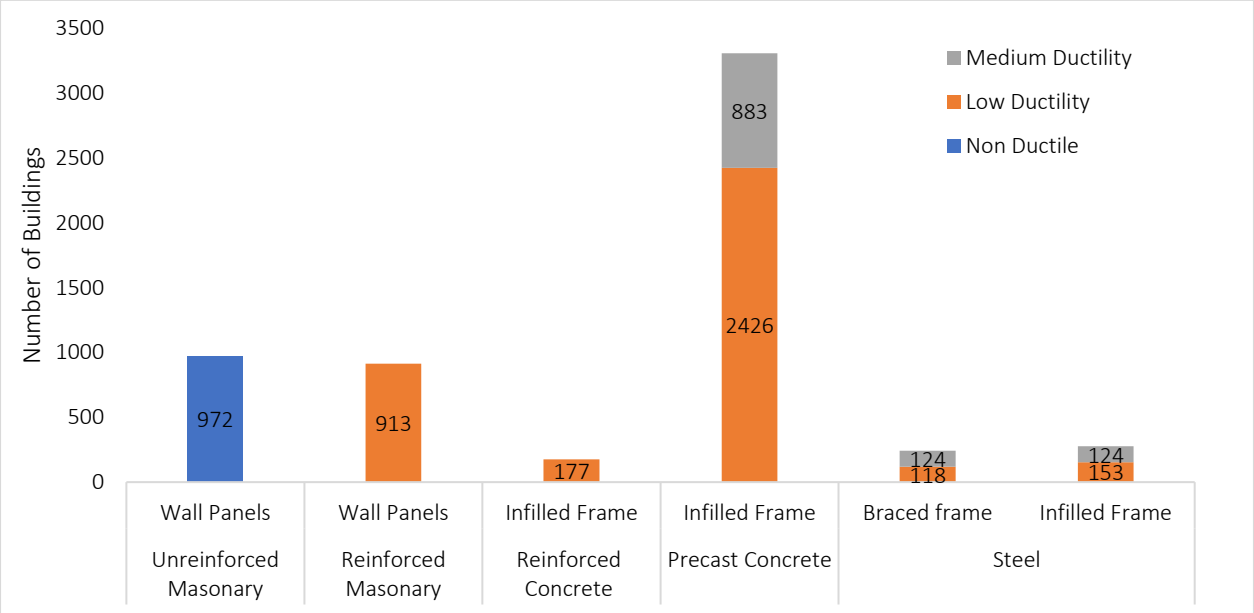

Figure 3-2 Categorization of Industrial Buildings

3.1.3 Commercial Buildings

There are approximately 17759 industrial buildings constructed from 1950 to 2000. Similar to residential and industrial buildings these buildings were also categorized based on the construction material, lateral force resisting system and ductility etc. The distribution of the total number of buildings across the various categories is depicted in Figure 3-3. Like industrial buildings, most of the buildings were constructed using reinforced concrete. Masonry structures also have significant numbers in the commercial buildings.

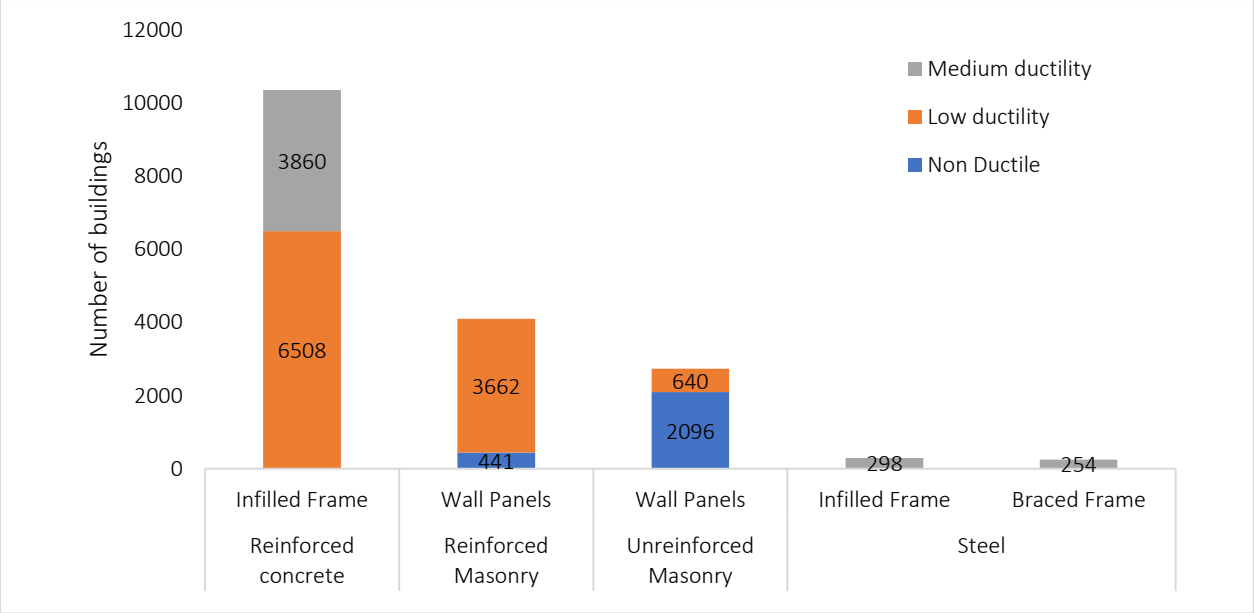

Figure 3-3 Categorization of Commercial Buildings

3.2 Vulnerability and Ductility Index

It is possible to determine the mean damage value (μD) for each vulnerability class at a variety of intensities and probable sub-classes as shown in figure 3-4 by plugging the values of k and p(k) into Equation 2-2. Following this approach, the mean damage value (μD) can only be calculated at discrete points. An empirical equation given in EMS-98 [33] is utilized for a continuous evaluation to relate intensity of earthquake (I) and the mean damage value (μD) utilizing the vulnerability (V) and ductility index (Q).

$$\mu_D = 2.5[1 + \tanh\left(\frac{I + 6.25V - 13.1}{Q}\right)] \qquad \text{Equation 3-1}$$

This study uses curve-fitting to match the mean damage-intensity curves obtained from Equation 3-1 to the discrete points shown in figure 3-4. For each sub-class vulnerability (V) index and ductility index (Q) can be calibrated using the curve-fitting method. For the curve fitting, it was controlled that the R square values exceed 0.95. The vulnerability index (V) is then derived from the mean values of the vulnerability sub-classes for each vulnerability class. Table 3-1 displays the determined vulnerability (V) and ductility (Q) index values after curve fitting.

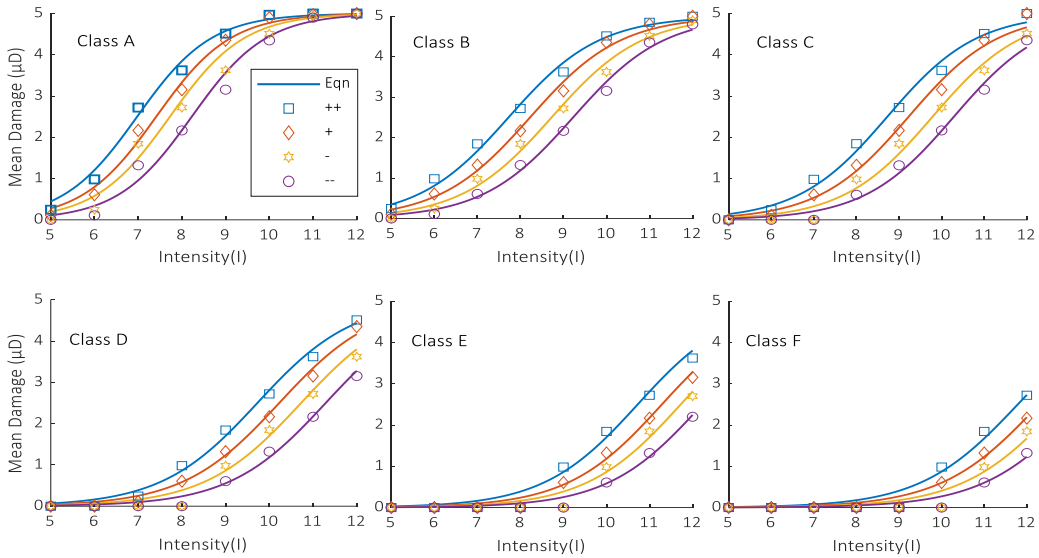

Figure 3-4 Earthquake Intensity versus mean damage of each class

Table 3-1 Vulnerability and Ductility Index values for each class

Vulnerability Index (V)	Vulnerability Class					
	A	B	C	D	E	F
Sub-class ++	0.98	0.86	0.7	0.54	0.38	0.21
Sub-class +	0.91	0.78	0.62	0.46	0.29	0.13
Sub-class -	0.86	0.7	0.53	0.38	0.22	0.05
Sub-class --	0.78	0.62	0.45	0.29	0.14	-0.03
Average	0.88	0.74	0.58	0.42	0.26	0.1
Ductility Index (Q)	1.7	2.1	2.1	2.2	2.2	2.3

3.3 Mapping of building categories to the EMS-98 grades

The next stage is to map these residential buildings to the EMS-98 vulnerability class and sub-class based on the information gathered about them. Table 3-2 to 3-4 displays the relationship between Almaty's residential, industrial, and commercial buildings and the EMS-98 scale. First, the buildings were matched to structure types in the EMS-98 based on their building materials, systems for resisting lateral forces, and capacity to deform. The following method is utilized for the mapping of the EMS-98 in order to account for the fact that many vulnerability classes are associated with each type of structure, as indicated in Table 2-1 .

Due to the fact that each type of structure in the EMS-98 has a variety of vulnerability classes, as stated in Table 2-1, the following mapping process is utilized:

1. The EMS-98 scale places masonry and wood at the top due to the limited ductility of these materials in the absence of structural seismic details.
2. Structures made of concrete that had a low ductility were given a higher vulnerability rating within the range.
3. At the middle of the spectrum, where the ductility of reinforced concrete and steel is moderate, these buildings are categorized as medium-vulnerable.
4. Structures consisting of precast wall panels with emulated moment frames that had a medium level of ductility were categorized as having a high to medium level of vulnerability.

After assigning the vulnerability class/sub-class to the residential building, the associated vulnerability (V) index and ductility (Q) index for the building categories can be computed using Table 3-1.

Table 3-2 Mapping of Almaty's residential buildings to EMS-98 scale (modified from [62]**).**

Residential buildings in Almaty	Construction Materials	Precast Concrete				Reinforced concrete		Unreinforced Masonry		Steel	Wood
	Lateral Force Resisting Systems	Wall Panels		Emulated Moment Frames		Shear Walls		Adobe Walls	Brick Walls	Moment Frames	Wall Panels
	Ductility	Low	Medium	Low	Medium	Low	Medium	Low	Low	Medium	Low
EMS-98 scale	Type of Structures	Wall without ERD	Wall with moderate level of ERD	Frame without ERD	Frame with moderate level of ERD	Wall without ERD	Wall with moderate level of ERD	Adobe (earthquake brick)	Unreinforced with RC floors	Steel structures	Timber structures
	Vulnerability Class Ranges	B-D	C-E	A-D	B-E	B-D	C-E	A-B	B-D	C-F	B-E
Mapping	Assigned Vulnerability Class	B+	C++	B	C+	B-	D++	A++	B++	D+	B++
	V	0.78	0.7	0.74	0.62	0.7	0.54	0.98	0.86	0.46	0.86
	Q	2.1	2.1	2.1	2.1	2.1	2.2	1.7	2.1	2.2	2.1

Table 3-3 Mapping of Almaty's industrial buildings to EMS-98 scale.

Industrial buildings in Almaty			EMS-98 scale		Mapping		
Construction Materials	Lateral Force Resisting Systems	Ductility	Type of Structures	Vulnerability Class Ranges	Assigned Vulnerability Class	V	Q
Reinforced concrete	Infilled Frame	Low	Frame with moderate level of ERD	B-E	B	0.74	2.1
Precast Concrete		Low			B+	0.78	2.1
		Medium			C+	0.62	2.1
Reinforced masonry	Wall Panels	Low	Reinforced or Confined	C-E	C	0.575	2.1
Unreinforced masonry		None	Unreinforced with RC floors	B-D	B	0.74	2.1
Steel	Braced frame	Low	Steel structures	C-F	C-	0.53	2.1
		Medium			D-	0.38	2.2
	Infilled Frame	Low			C+	0.62	2.1
		Medium			D	0.415	2.2

Table 3-4 Mapping of Almaty's commercial buildings to EMS-98 scale.

Commercial buildings in Almaty			EMS-98 scale		Mapping		
Construction Materials	Lateral Force Resisting Systems	Ductility	Type of Structures	Vulnerability Class Ranges	Assigned Vulnerability Class	V	Q
Reinforced concrete	Infilled Frame	Low	Frame with moderate level of ERD	B-E	B	0.74	2.1
		Medium			C+	0.62	2.1
Reinforced Masonry	Wall Panels	None	Reinforced or Confined	C-E	C++	0.7	2.1
		Low			C	0.575	2.1
Unreinforced Masonry	Wall Panels	None	Unreinforced with RC floors	B-D	B	0.74	2.1
		Low			B-	0.7	2.1
Steel	Infilled Frame	Medium	Steel structures	C-F	D	0.415	2.2
	Braced Frame				D-	0.38	2.2

3.4 Development of Vulnerability Curves

After obtaining the vulnerability (V) and ductility (Q) indices for each group of the different building categories in Almaty, the mean damage (μD) can be calculated using Eqns. 3-1. Figure 3-5 to 3-7 displays the relationship between the mean damage (μD) and earthquake intensity (I) for various groups of residential, industrial and commercial buildings respectively. With an increase in earthquake intensity, the vulnerability class/sub-class and vulnerability index predict that masonry and wood buildings will sustain the greatest mean damage value, followed by precast and reinforced concrete structures. The mean damage values are lowest for steel buildings.

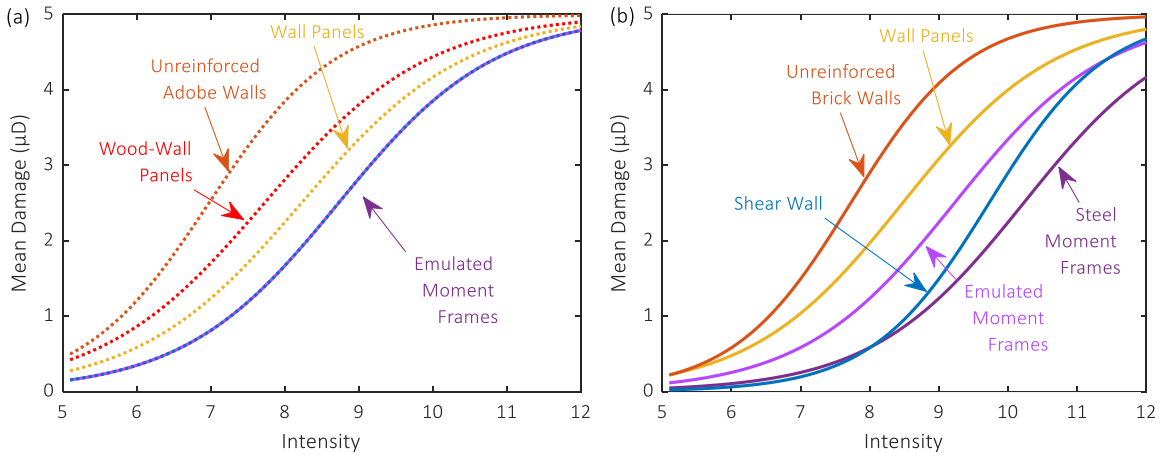

Figure 3-5 Mean damage vs. intensity for different groups of residential buildings: (a) low ductility; (b) medium ductility

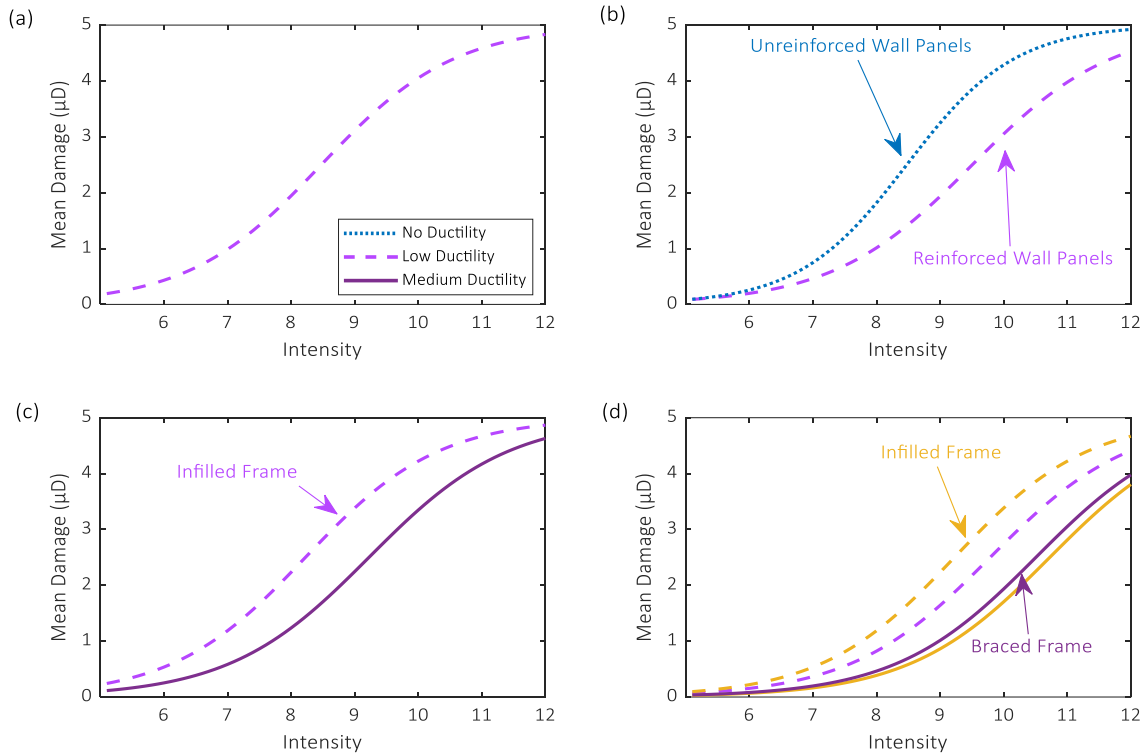

Figure 3-6 Mean damage vs. intensity for different groups of industrial buildings: (a) reinforced concrete infilled wall; (b) masonry; (c) precast concrete; (d) steel.

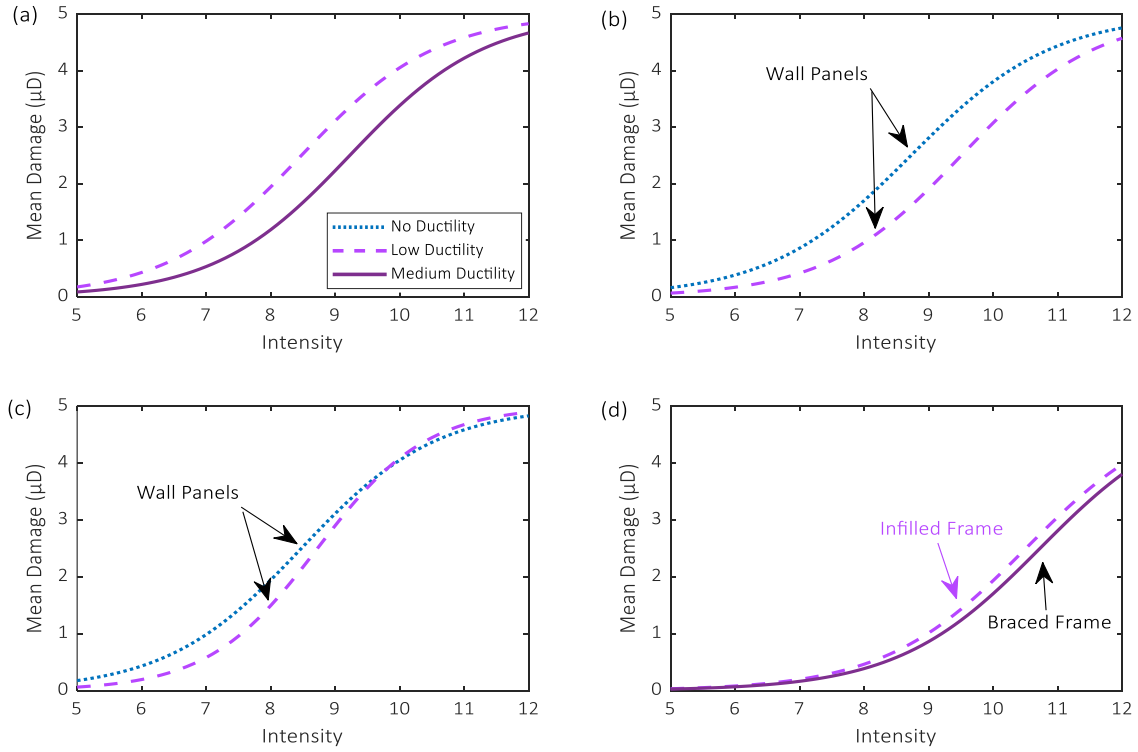

Figure 3-7 Mean damage vs. intensity for different groups of commercial buildings: (a) reinforced concrete infilled wall; (b) reinforced masonry; (c) unreinforced masonry; (d) steel.

Though Figure 3-5 to 3-7, mean damage curves depict the damage at various earthquake intensities, it is still vital to determine which intensity level accurately represents potential earthquakes in the Almaty area. Kazakhstan's seismic design code [63] has mapped the peak ground acceleration in its region at two earthquake levels: design basis earthquake (DBE) with a return period of 475 years and maximum considered earthquake (MCE) with a return period of 2475 years. As a result, it is essential to evaluate the buildings' vulnerability to earthquakes on each of these two levels. Consequently, the earthquake intensity level must be linked to the peak ground acceleration (PGA) demand, as the PGA for the DBE and MCE levels can be found in the Almaty region's design code. This research utilizes an empirical equation derived by Masi et al. [51] to establish the following link (equation 3-1) between earthquake intensity and peak ground acceleration:

$$PGA = e^{\left(\frac{I-6.32}{0.48}\right)} \text{ if } I \leq 5;\ PGA = e^{\left(\frac{I-9.82}{1.72}\right)} \text{ if } I > 5 \qquad \text{Equation 3-2}$$

The relationship between the mean damage (μD) and the PGA can be determined by resolving I in equation 3-1 and entering the result into equation 2-3. Figure 3-8 to figure 3-10 depicts this link for several types of buildings categories based on construction material for residential, industrial, and commercial. In these figures, the vertical dashed and dashed-dot trend lines show the DBE (with a return period of 475 years) and MCE (with a return period of 2475 years) PGAs in the Almaty area. Figure 3-8 to 3-10 depicts the estimated mean damage (μD) at two earthquake levels in the Almaty region, namely the Design Basis Earthquake (DBE) and the Maximum Considering Earthquake (MCE). The intersections of the mean damage curves with the vertical trend lines are used to determine the μD values at the respective earthquake levels and are depicted in Figure 3-11 to 3-13. This method permits a direct evaluation of the projected mean damage at DBE and MCE earthquakes in the Almaty region.

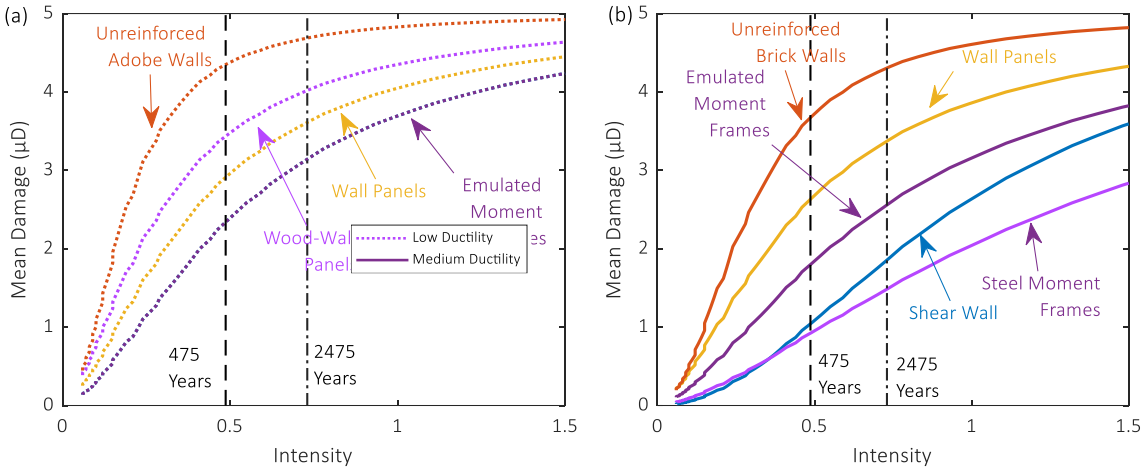

Figure 3-8 Mean damage vs. PGA for different groups of residential buildings: (a) low ductility: (b) medium ductility

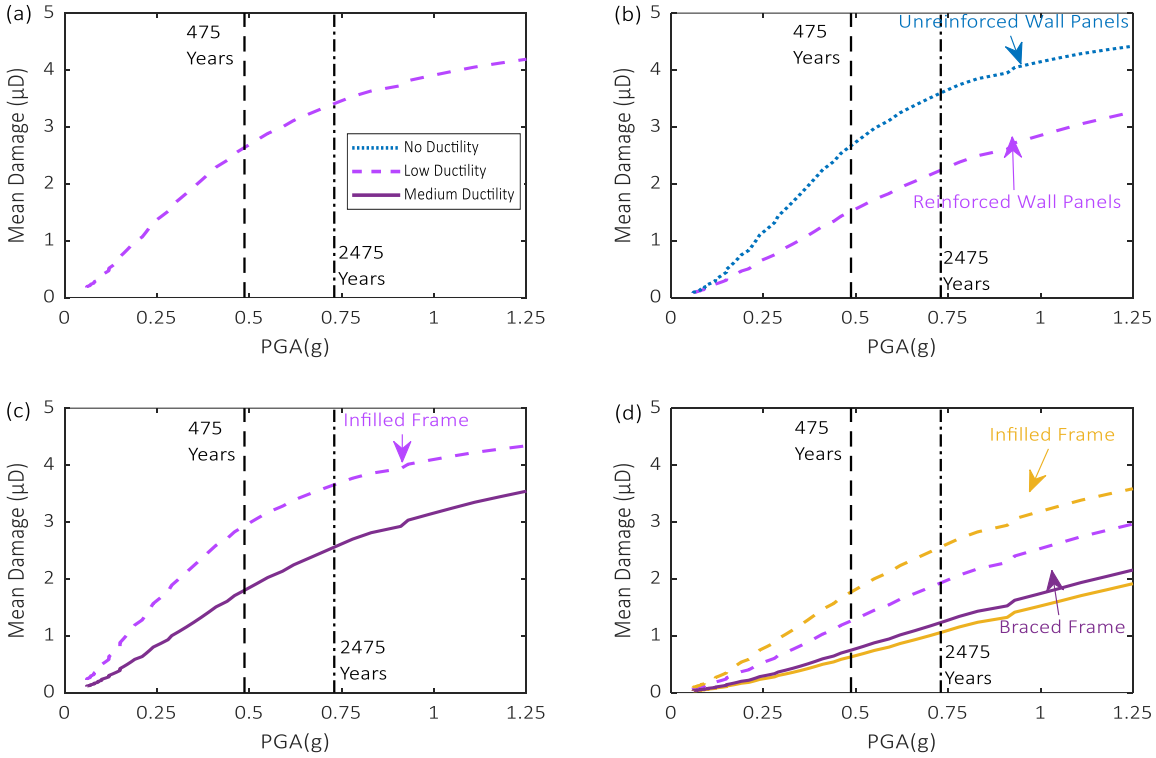

Figure 3-9 Mean damage vs. PGA for different groups of industrial buildings: (a) reinforced concrete; (b) masonry; (c) precast concrete; (d) steel.

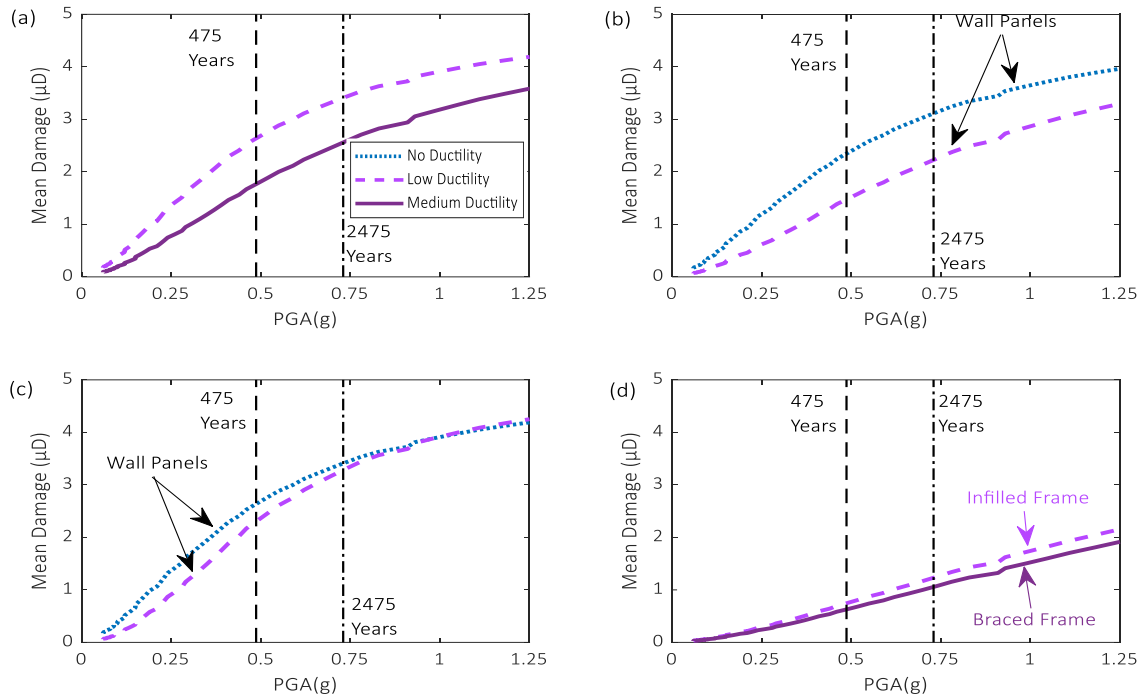

Figure 3-10 Mean damage vs. PGA for different groups of commercial buildings: (a) reinforced concrete; (b) reinforced masonry; (c) unreinforced masonry; (d) steel.

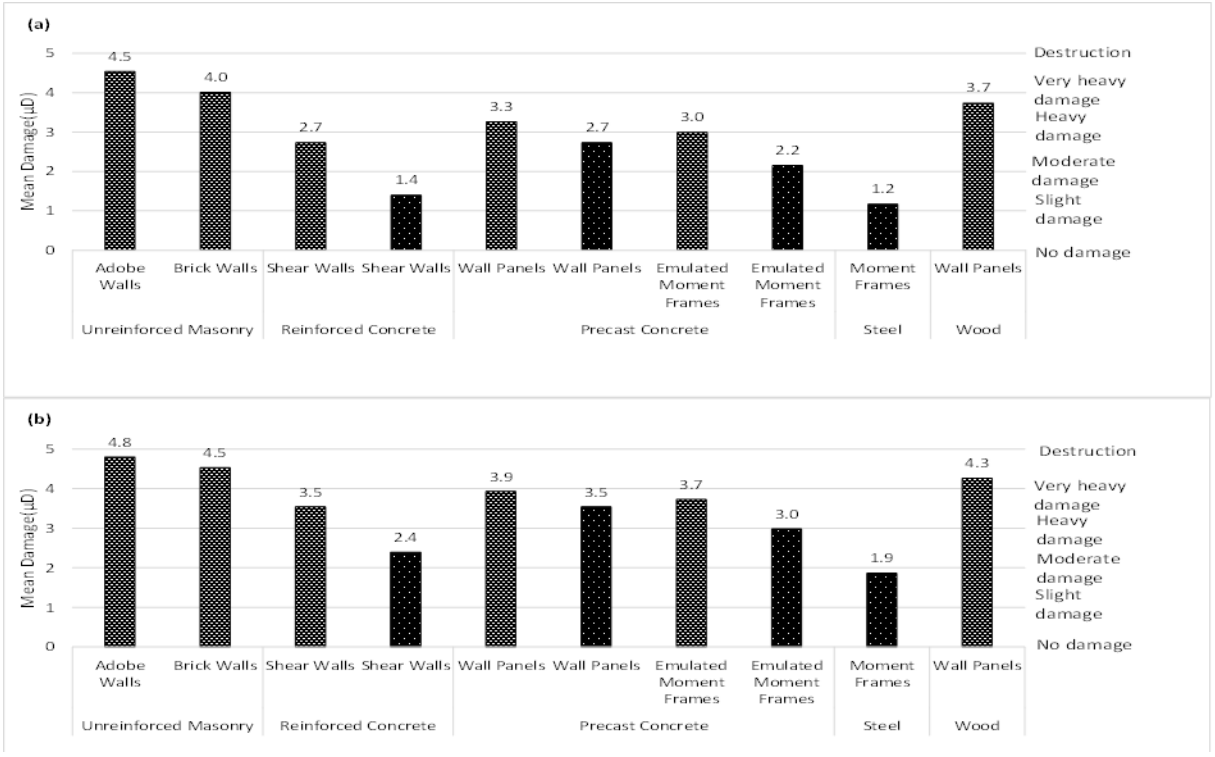

Figure 3-11 Mean damage for distinct types of residential structures at: (a) DBE (475 years return period); (b) MCE (return period of 2475 years).

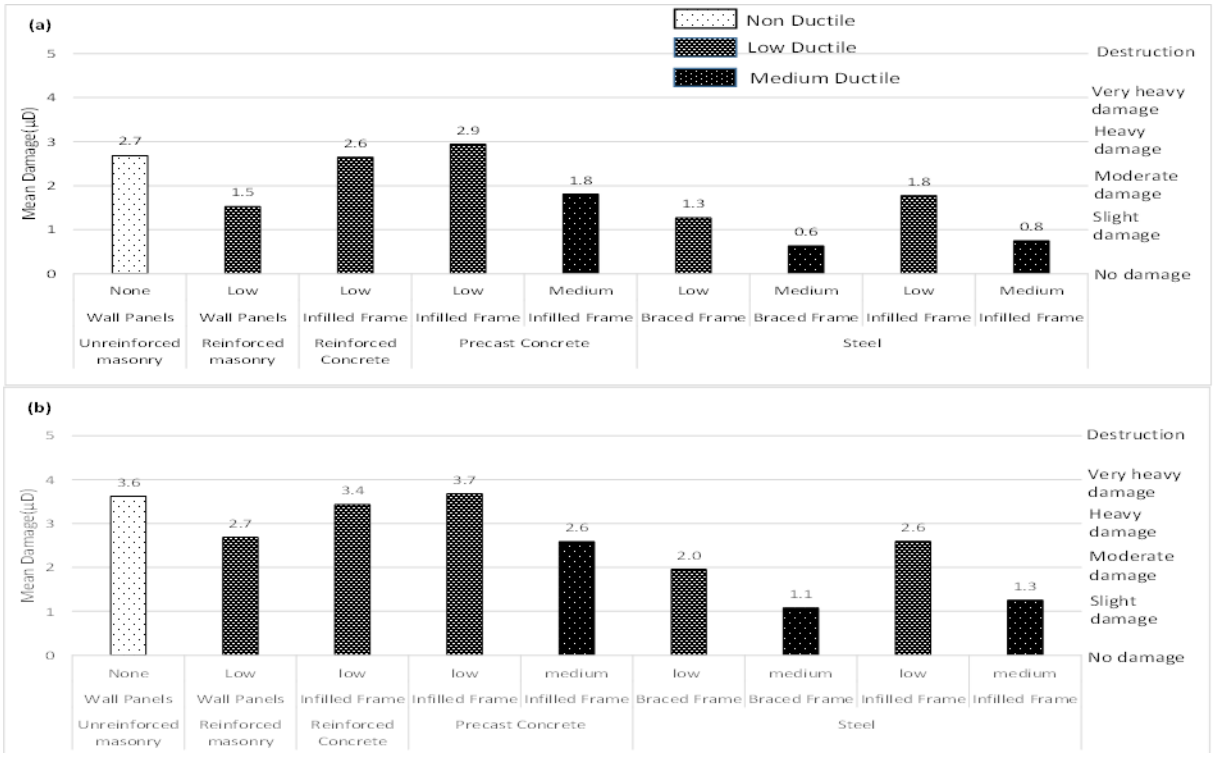

Figure 3-12 Mean damage for distinct types of industrial structures at: (a) DBE (475 years return period); (b) MCE (return period of 2475 years).

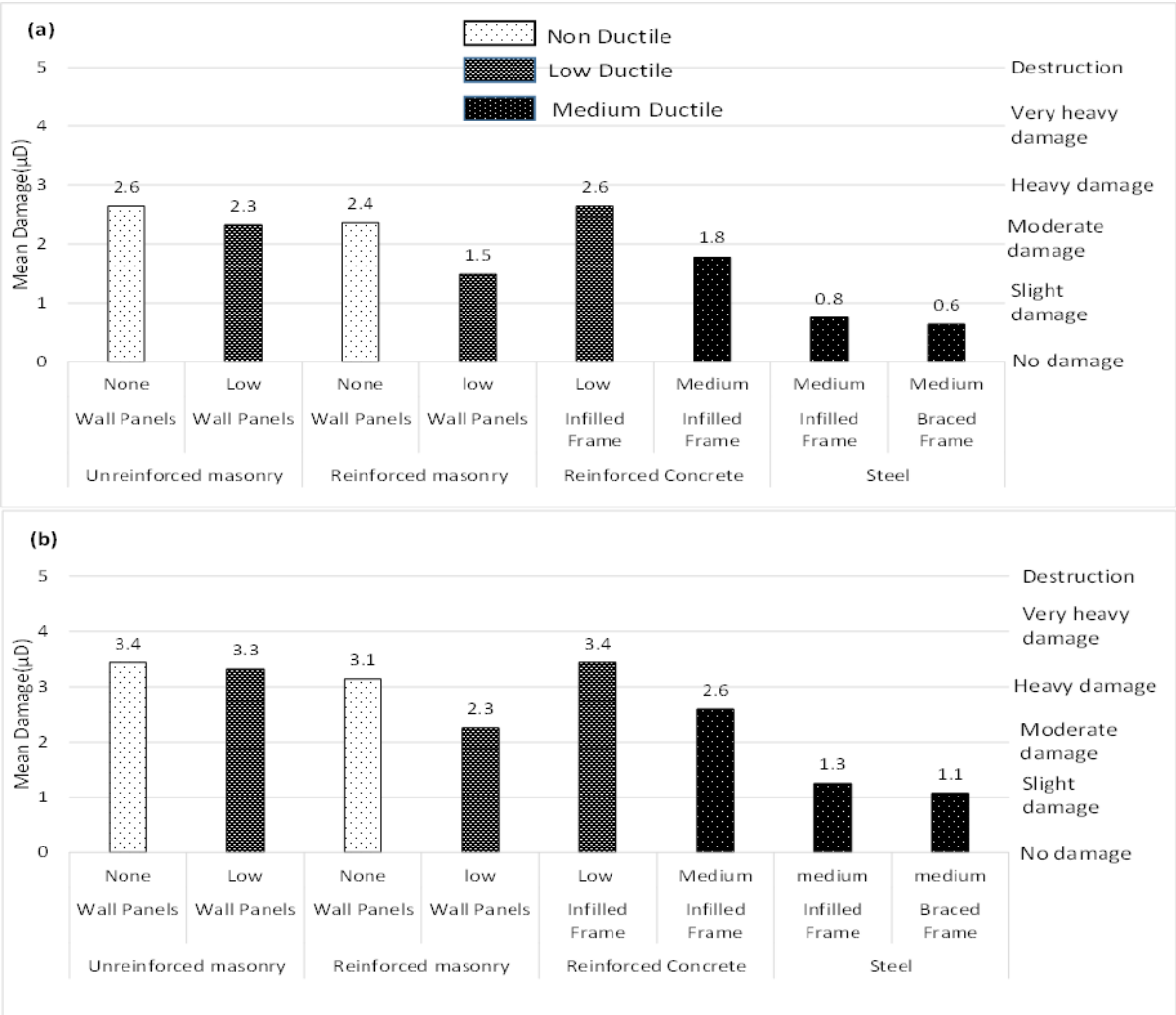

Figure 3-13 Mean damage for distinct types of commercial structures at: (a) DBE (475 years return period); (b) MCE (return period of 2475 years).

After determining the mean damage to building structures, it is worthwhile to determine the probability of damage. By plugging in the average amount of damage sustained by each building category into Equation 2-2 will give you the probability of the damage occurring at each of the damage levels. Given that μD is proportional to PGA, we may calculate an individual building group's damage probability given its PGA. Figure 3-14 to 3-16 provides an illustration of the likelihood of damage (p) vs. PGA for two types of buildings: (a) masonry with brick walls, and (b) reinforced concrete shear wall, both of which have poor ductility. In Figure 3-14 to 3-16, the vertical dashed and dashed-dot trend lines represent the DBE and MCE PGAs in the Almaty area, respectively. The likelihood of severe damage is maximized at high PGA, as shown in Figure 3-14 to 3-16, while the likelihood of minor damage is maximized at low PGAs.

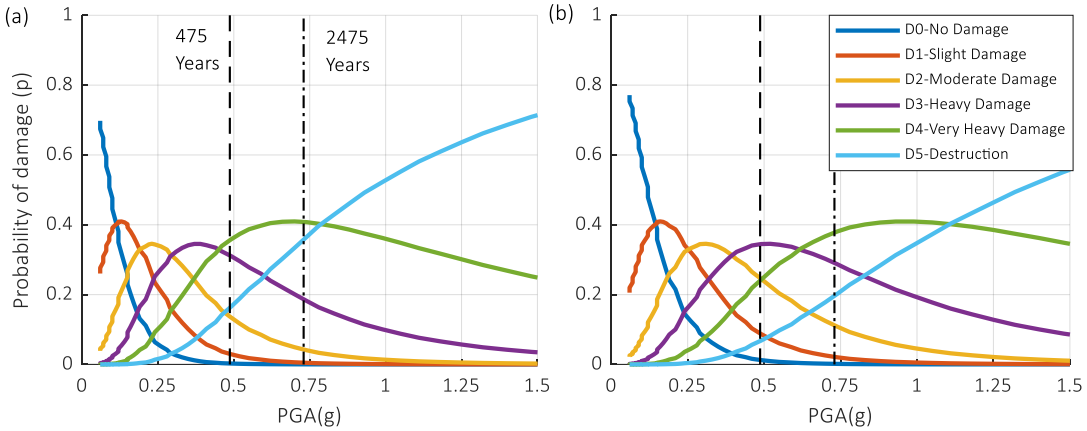

Figure 3-14 Probability of the damage (p) vs. PGA for residential buildings: (a) masonry brick walls with low ductility; (b) precast concrete wall panels with low ductility.

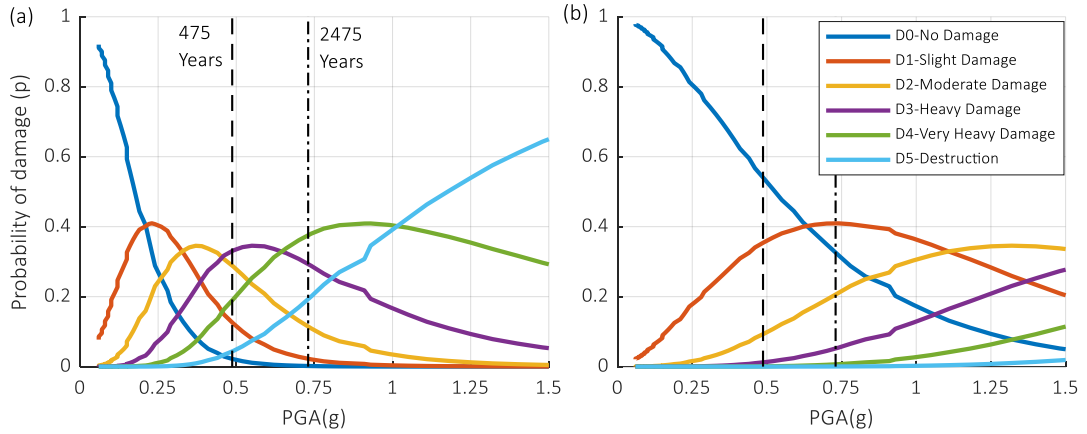

Figure 3-15 Probability of the damage (p) vs. PGA for industrial buildings: (a) reinforced concrete infilled frame with low ductility; (b) steel braced frame with medium ductility.

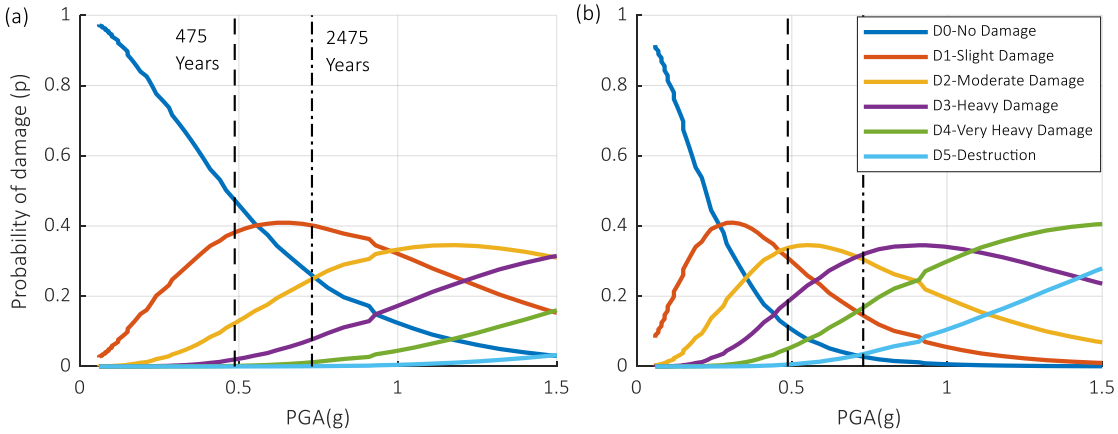

Figure 3-16 Probability of the damage (p) vs. PGA for commercial buildings: (a) unreinforced masonry wall panels with no ductility; (b) reinforced infilled frame with medium ductility.

We may determine the likelihood of damage for either of the two earthquake intensities by examining the points at which the probability curves for each level connect with the vertical trendlines (Figure 3-14 to 3-16). Identical computations may be done to different categories of structures. Damage probabilities for several categories of Almaty residential, industrial and commercial buildings subjected to direct evaluation at DBE and MCE earthquake intensities are shown in Figure 3-17 to 3-19. As shown in Figure 3-17, masonry and wood buildings have a high probability of destruction under DBE (over 20%) and MCE (over 40%). To withstand future major earthquakes, these buildings must be strengthened.

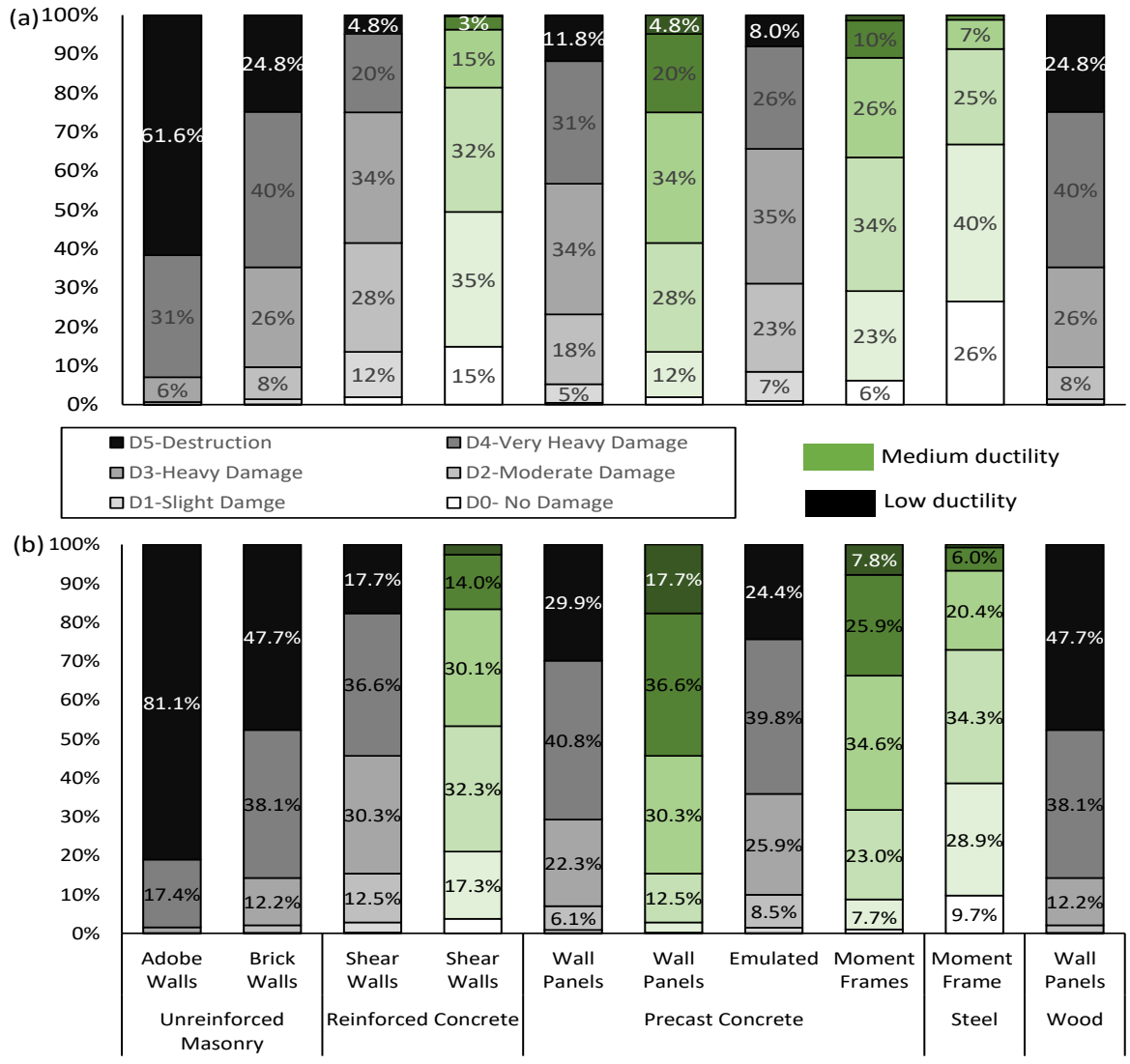

Figure 3-17 Residential buildings damage probabilities at (a) DBE (return period of 475 years) and (b) MCE (return period of 2475 years).

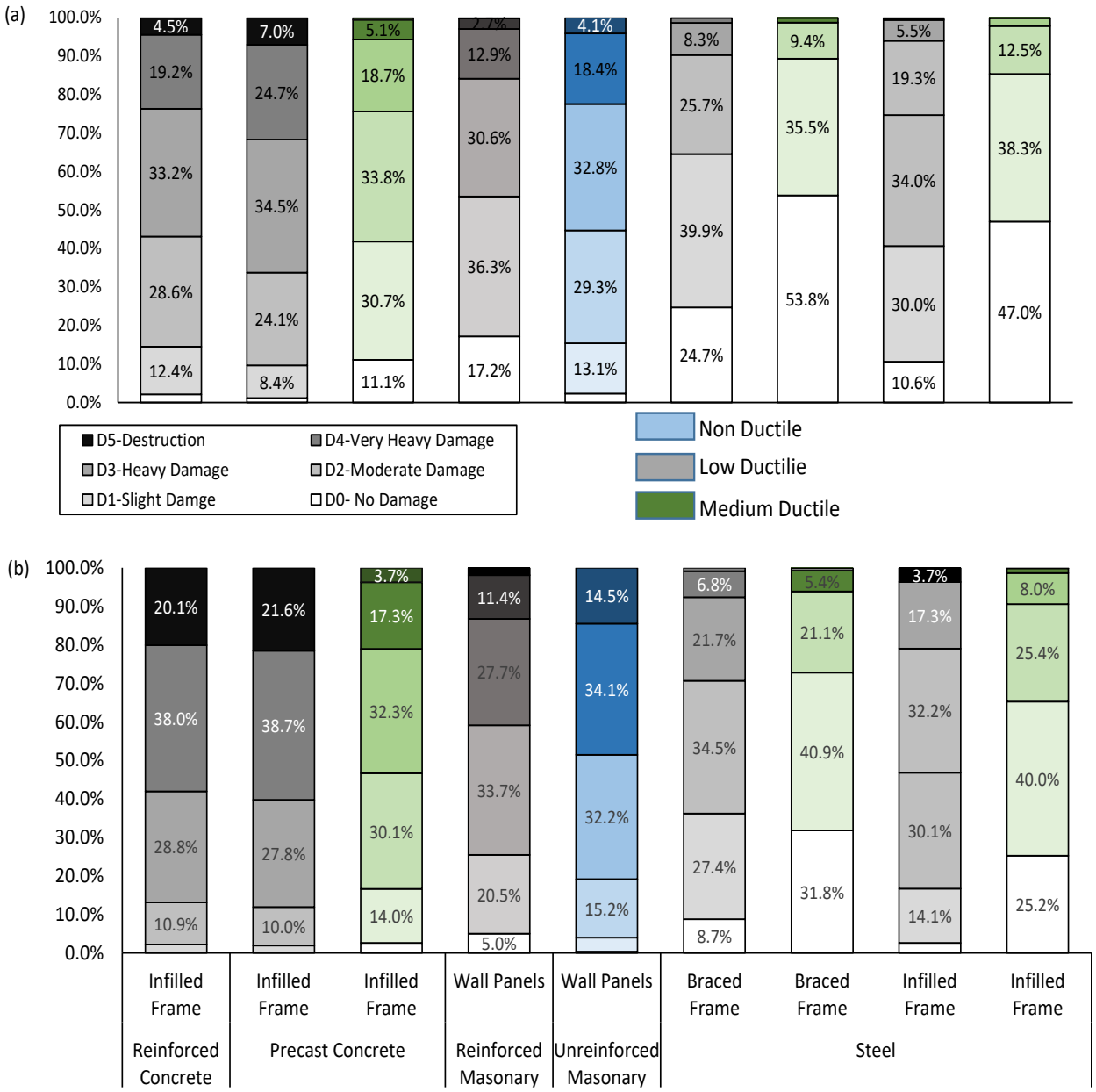

Figure 3-18 Industrial buildings damage probabilities at (a) DBE (return period of 475 years) and (b) MCE (return period of 2475 years).

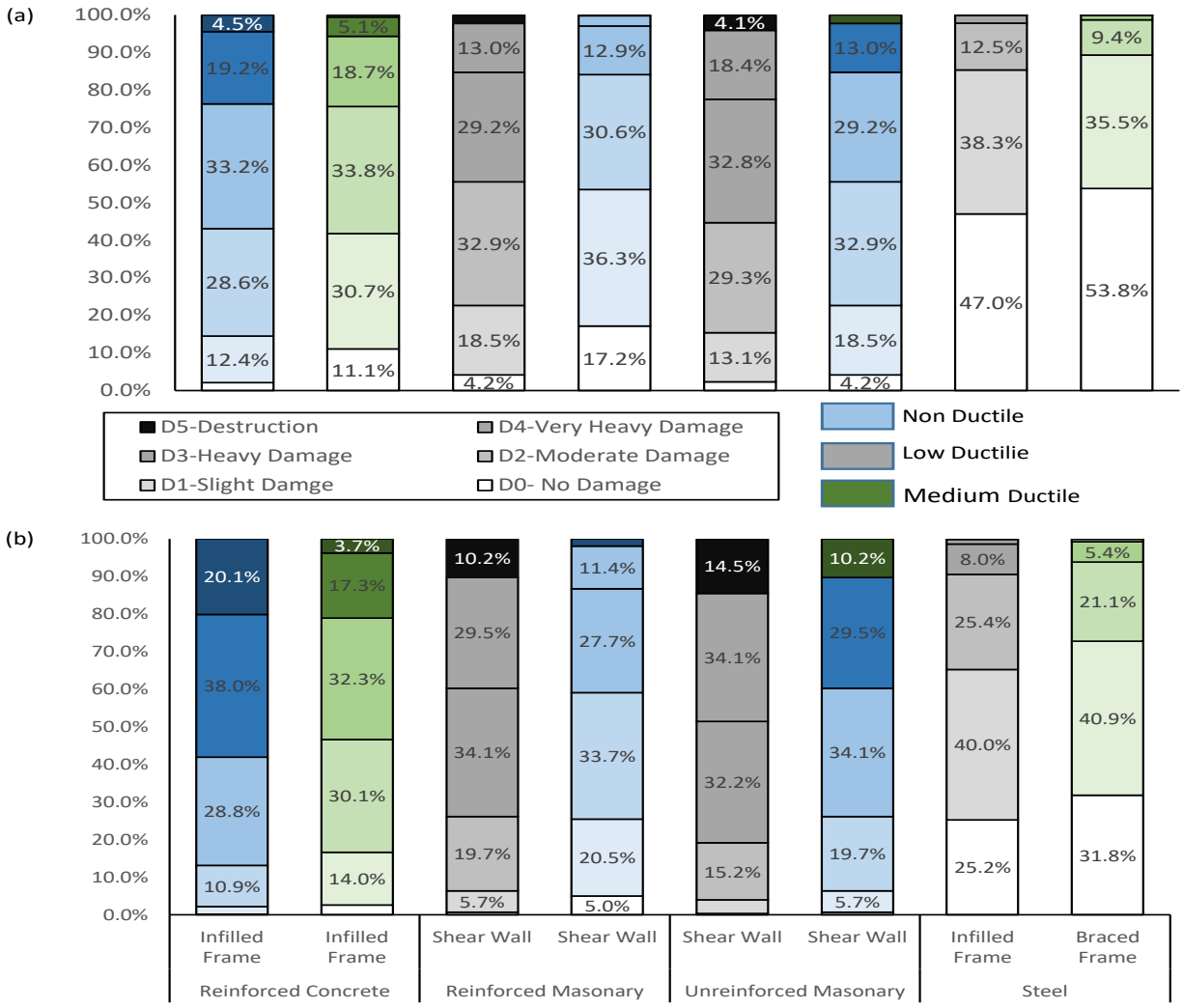

Figure 3-19 Commercial buildings damage probabilities at (a) DBE (return period of 475 years) and (b) MCE (return period of 2475 years).

3.5 Recommendations

Following the EMS-98 scale, a micro-seismic assessment methodology was adopted to qualitatively evaluate residential, industrial and commercial buildings constructed with a wide variety of materials. These structures were initially classified based on the construction materials they were made of, as well as the lateral force-resisting systems and ductility capacities they featured. Each was then assigned a vulnerability class and sub-class according to EMS-98. For different earthquake intensities and PGA, the estimated mean damage as well as the probability of the damage at each level was calculated. Mean damages and probability of each damage grade

were calculated for both the DBE (for return period 475 years) and MCE (for return period of 2475 years), under the expected earthquakes. These evaluation outcomes can be utilized by government decision-makers for future seismic disaster mitigation. One can draw the following conclusions:

1. Unreinforced masonry and concrete with low ductility were used for the construction of the majority of the residential buildings in Almaty in the Soviet Union era, while most of the industrial buildings were made of precast concrete. Similarly for the commercial buildings the majority were constructed using reinforced concrete.

2. For residential buildings, unreinforced masonry, and wood structures, both DBE and MCE predict a high likelihood of total destruction. Nevertheless, the danger of destruction is substantial, exceeding 20% under DBE and 40% under MCE. As a result, depending on the results of subsequent financial evaluations, it is proposed that these buildings be extensively strengthened or demolished. DBE and MCE both predict moderate to high levels of predicted mean damage for low ductility reinforced and precast concrete buildings. Between 60% and 70%, the probability of harm is also dominant.

3. For industrial buildings unreinforced masonry, reinforced concrete, and precast concrete with low ductility structures, both DBE and MCE predict a high likelihood of heavy to very heavy damage. Nonetheless, the risk of heavy damage is high, topping 18% in DBE and 34% in MCE. Similarly steel with low ductility predict moderate level of damage.

4. For commercial buildings unreinforced masonry with no ductility and reinforced concrete with low ductility structures, both DBE and MCE predict a high likelihood of moderate to heavy damage. Nonetheless, the risk of moderate damage is high, topping 30% in DBE and 30% in MCE. Similarly reinforced concrete with medium ductility predicts moderate level of damage.

Chapter 4 - Analytical Evaluations

4.1 Identify Prototype RC Buildings

For the analytical assessment, two (2) pre-cast concrete emulated moment frame buildings were selected, constructed in Almaty from 1970s to 1990s where each building represents one decade. More information about the prototype buildings is given in the sections below.

4.1.1 VT Series

This type of construction of residential buildings (Figure 4-1) was carried out in Almaty from 1970 to 1980. The building is five-storeys with a basement, rectangular in plan with dimensions in the outermost axes with dimensions of 20.0 x 12 m. The bearing structures are transverse frames with two spans of 6.0 m. The transverse frames are connected by the longitudinal beams of the longitudinal frames with spans of 4.0 m, made in the plane of the slabs. The plan view of the building is shown in figure 4-2.

Figure 4-1 Building View VT Series

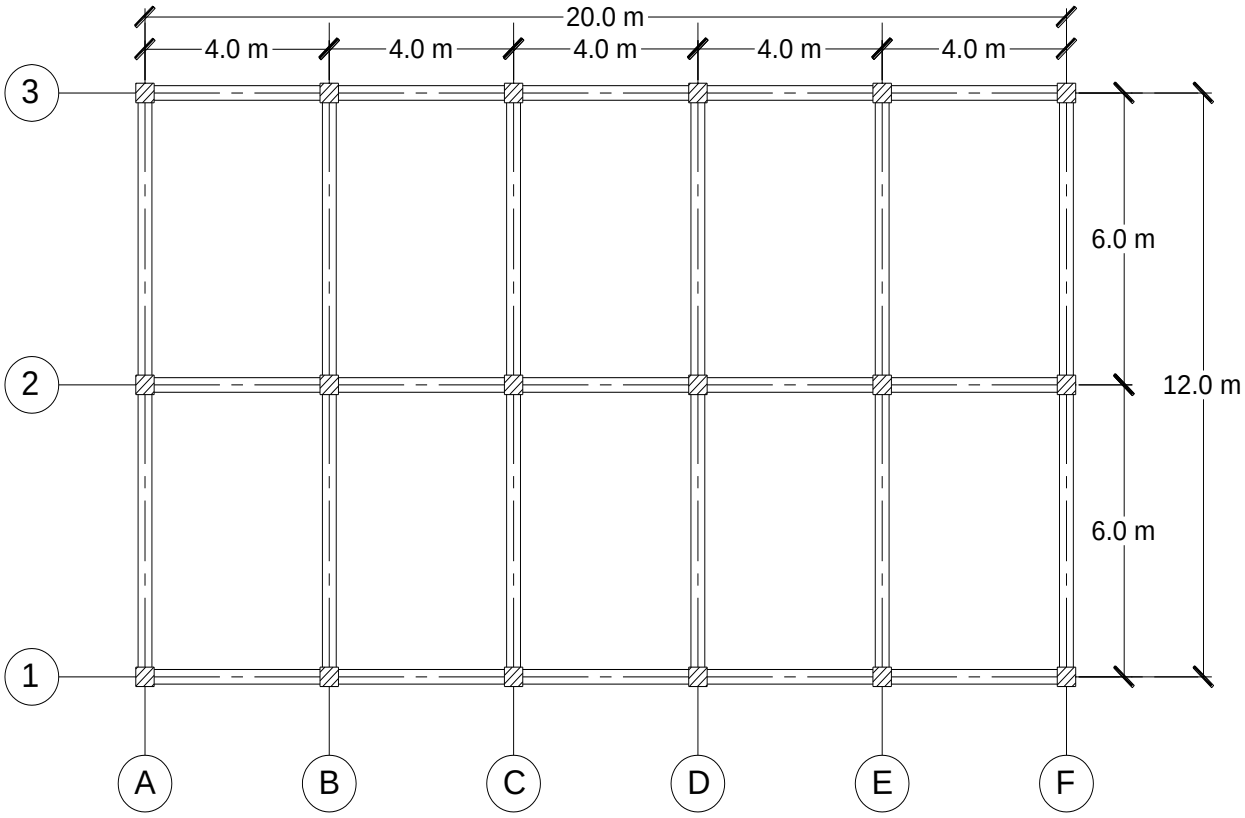

Figure 4-2 Plan view of VT series

The building is 15 meters tall, with a standard story height of 3 meters, measured from the average level of the earth surface to the roof. The building's elevation view is depicted in Figure 4-3.

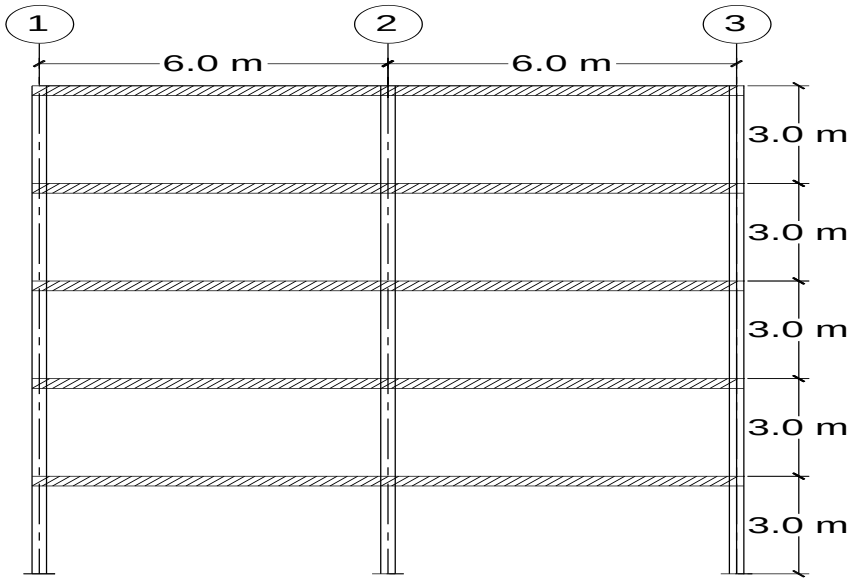

Figure 4-3 Elevation view of VT series

4.1.1.1 Cross-section Size

The columns were made of monolithic reinforced concrete with cross-sectional dimensions of 400x400 mm while the dimensions of the sections of the transverse beams were 350x500 (h) mm, and of longitudinal beams were 300x400 (h) mm. Cross section details of the columns and beams are given in the figure 4-4.

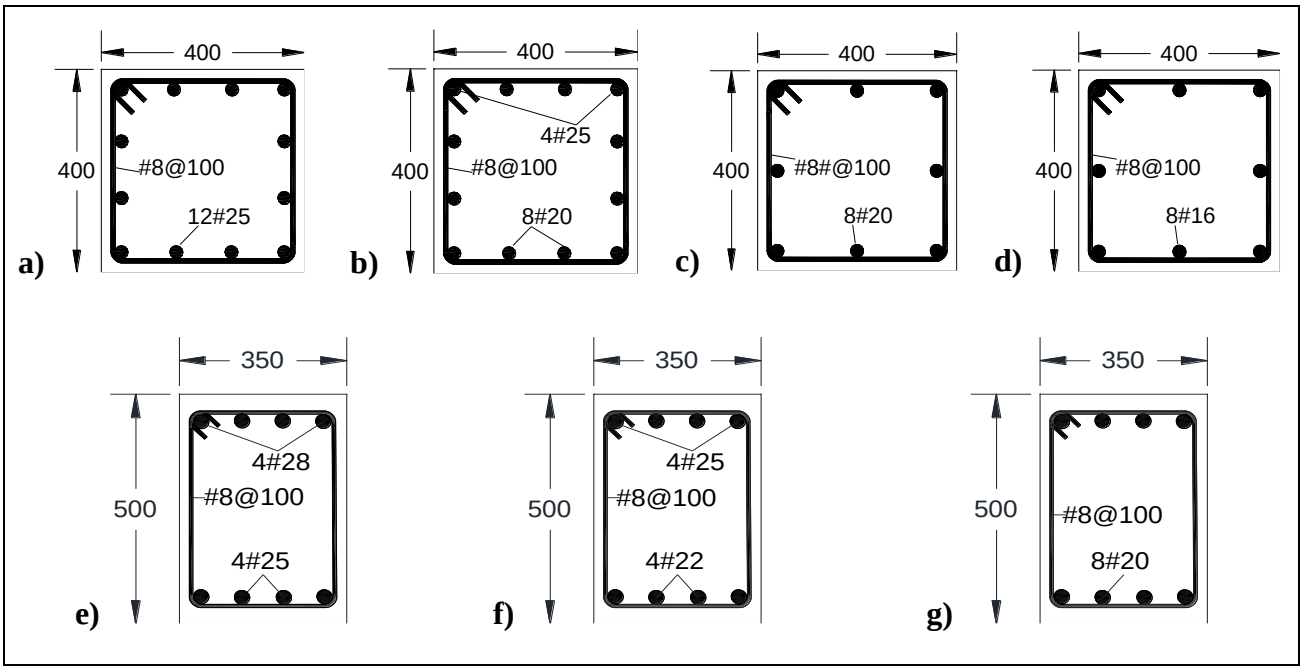

Figure 4-4 Cross Section Details of VP Series (all units are in mm) a) Column of 1st floor b) Column of 2nd floor c) Column of 3rd floor d) Column of 4th and 5th floor e) Beam 1st floor f) Beam of 2nd and 3rd floor and g) Beam of 4th and 5th floor.

4.1.1.2 Reinforcement Details

The columns of the first floor were reinforced on each face with four bars Ø25 of class A-III; and stirrups of 8 mm reinforcing bars of class A-III with the spacing of 100. The columns of the second floor were reinforced in the corners with bar Ø25 of class A-III on each face with two bars Ø20 of class A-III; and stirrups of Ø8 mm reinforcing bars of class A-III with spacing of 100 mm. The columns of the third floor were reinforced on each face with three bars Ø20 of class A-III; and stirrups of 8 mm reinforcing bars of class A-III with the spacing of 100. The columns of the fourth and fifth floor were reinforced on each face with three bars Ø16 of class A-III; and stirrups of 8 mm reinforcing bars of class A-III with the spacing of 100.

Transverse beams of the first floor were reinforced by two Ø28 mm bars of class A-III and two Ø25 mm bars of class A-III. The transverse frame beams of the second and third floors were reinforced by two Ø25 mm A-III bars and two Ø22 mm A-III bars. The transverse frame beams of the fourth and fifth floors were reinforced by four A-III class Ø20 mm bars; the stirrups were made of A-III class Ø8 mm reinforcing bars with the spacing in the supporting zone of about 100 mm.

4.1.1.3 Compressive Strength

The compressive strength of concrete used for building the columns and beams was about 30.5 MPa and 25.7 MPa respectively. Grade A-III steel was used for reinforcement with yield strength of 390 MPa and ultimate strength of 590 MPa.

4.1.1.4 Nominal Strengths

Strong column-weak beam (SCWB) refers to the requirement that the node's column end's and beam's actual flexural capacities, Mb and Mc, satisfy the following Mc > Mb. Columns are made stronger so that they can withstand vertical loads and the beams can withstand horizontal loads like wind or seismic forces. As is well knowledge, if a high-rise building's beam fails, it only affects that particular floor. However, if a structure's column fails, the entire building will collapse. Therefore, a strong column, weak beam design is required. Heavy earthquakes cannot cause a building to collapse, but faulty design can.

This method is useful for protecting the columns from brittle failure mechanisms including shear and torsion. ACI 318 recommends a SCWB ratio of 1.2. Based on the geometry shown in figure 4-4 and material characteristics provided in section 4.1.1.3, nominal shear, and moment strengths for both the columns and beams are calculated and provided in Table 4-1. These nominal values are a cautious approximation of the member's capacity to resist shear and bending moment are determined using equation 4-1 and 4-2 respectively as per ACI 318 [64] design codes.

$$V_n = V_c + V_s \qquad \text{Equation 4-1}$$

Where as

$$V_c = 0.17 * \ \lambda * \sqrt{f'_c} * b_w d$$

$$V_{s,min} = \left(\frac{A_{v,min}}{s}\right) \varphi * d * f_{yt}$$

$$M_n = A_s f_y (d - \frac{a}{2})$$ Equation 4-2

Table 4-1 Nominal Shear and Moment Strength of VT series buildings

	Floor Level	Nominal Shear Vn (KN)	Nominal Moment Mnc (KN-m)		Floor Level	Nominal Shear Vn (KN)	Nominal Moment Mnb (KN-m)	ΣMnc (KN-m)	ΣMnb (KN-m)	ΣMnc/ ΣMnb	Strong Column weak Beam
Column	1st	297.25	541.66	Beams	1st	261.98	368.66	995.32	659.64	1.51	Satisfied
	2nd	297.25	453.66		2nd	261.98	290.98	768.38	581.96	1.32	Satisfied
	3rd	297.25	314.72		3rd	261.98	290.98	533.46	501.80	1.06	Not Satisfied
	4th	297.25	218.74		4th	261.98	210.82	381.06	421.63	0.90	Not Satisfied
	5th	297.25	162.32		5th	261.98	210.82	324.64	421.63	0.77	Not Satisfied

Table 4-1 also depicts that the structural elements of the first three floors satisfy the strong column weak beam criteria showing that the beam will fail before the columns as beam failure generally results in partial failure of structure while that of 4^{th} and 5^{th} floor are not satisfying this criterion showing the possibility of failure of columns before beams which will ultimately leads to the failure of whole structure.

4.1.2 VP Series

This type of construction of residential buildings (Figure 4-5) was carried out in Almaty from 1980 to 1990. The building is five-storeys with a basement and technical floor, rectangular in plan with dimensions in the outermost axes with dimensions of 54.0 x 14.8 m. The bearing structures are transverse frames with two spans of 3.6 m. The transverse frames are connected by the longitudinal beams of the longitudinal frames with spans of 5.4 m, made in the plane of the slabs. The plan view of the building is shown in the figure 4-6.

Figure 4-5 Building View of VP Series

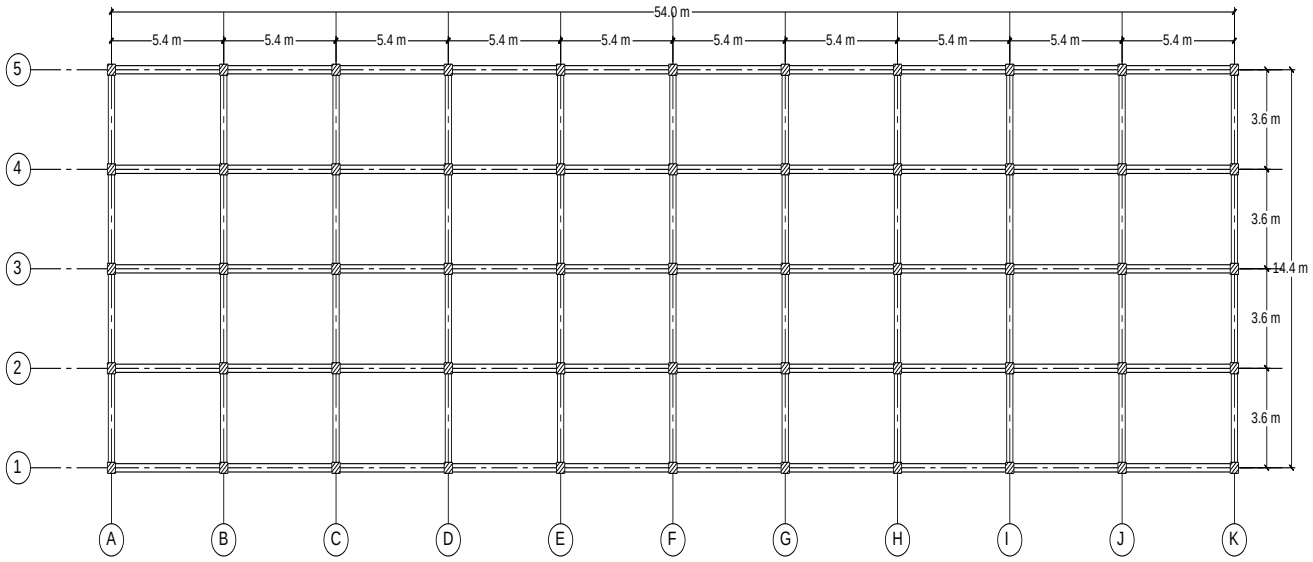

Figure 4-6 Plan view of VP series

The building is 17.5 meters tall from the ground up, with an average floor height of 3.0 meters on the first through fifth floors and a height of 2.15 meters on the technical floor. Figure 4-7 depicts the building's elevation view.

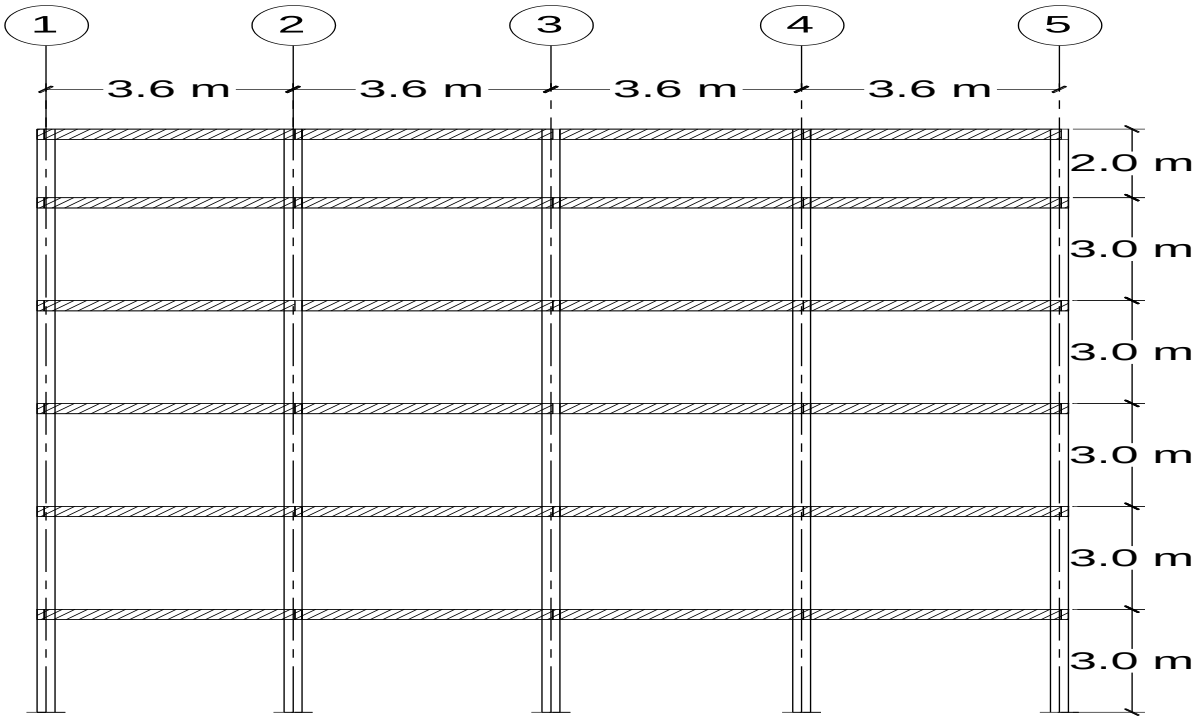

Figure 4-7 Elevation view of VP series

4.1.2.1 Cross-section Size

The cross-sectional dimensions of the columns were 400x400 mm, while the dimensions of the sections of the transverse beams were 350x500 (h) mm. The columns were composed of monolithic reinforced concrete. Figure 4-8 shows the cross sectional details of the columns and beams in detail.

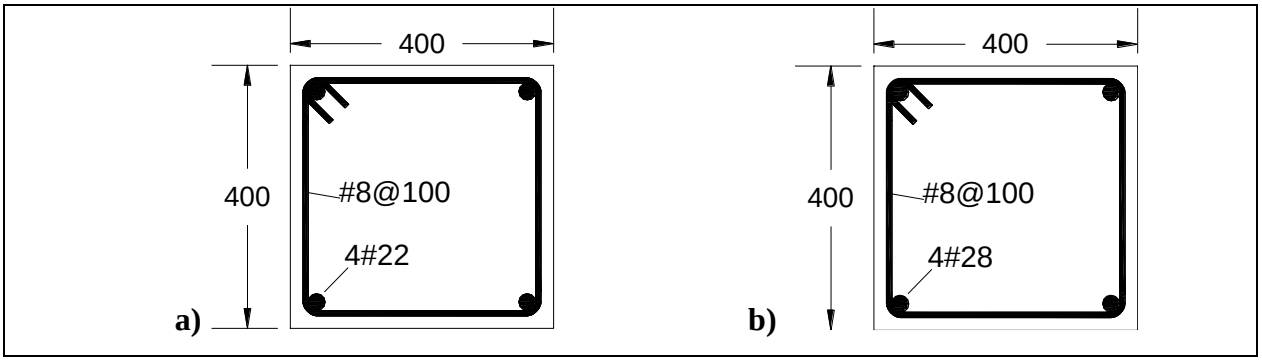

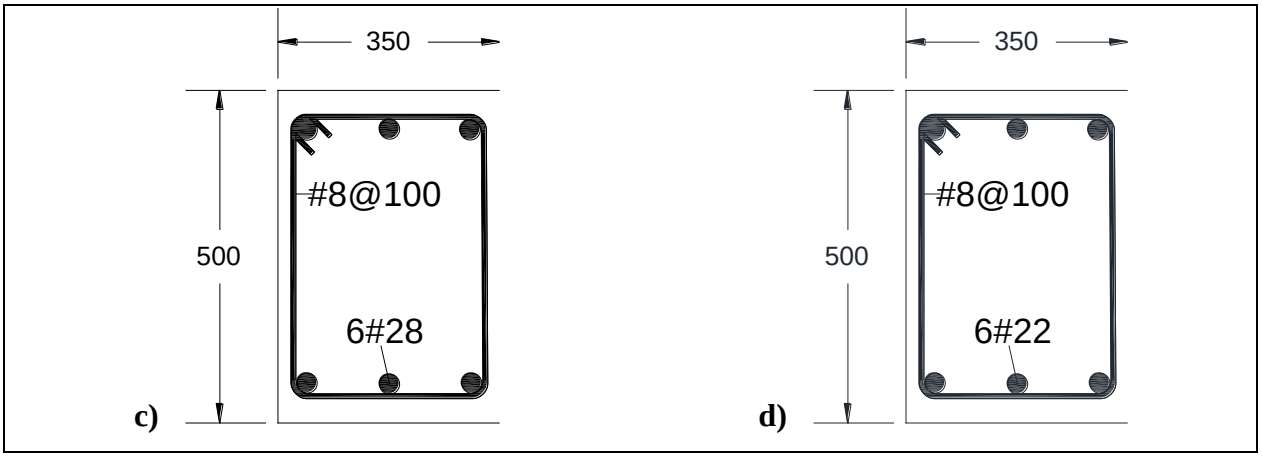

Figure 4-8 Cross Section Details of VP Series (all units are in mm) a) Column of 1st to 5th floor b) Column of the technical floor c) Beam 1st of 5th floor and d) Beam technical floor.

4.1.2.2 Reinforcement Details

The columns of the first to fifth floor were reinforced on each face with on each face by two bars Ø28 of class A-III; and stirrups of 8 mm reinforcing bars of class A-III with the spacing of 100 while the columns of the technical floor were reinforced on each face with two bars Ø22 of class A-III; stirrups of Ø8 mm reinforcing bars of class A-III with step 100 mm.

Transverse beams of the first to fifth floor were reinforced by three Ø28 mm bars of class A-III; the stirrups were made of A-III class Ø8 mm reinforcing bars with the spacing in the supporting zone of about 100 mm. The transverse frame beams of the technical floor were reinforced by three Ø22 mm A-III bars; the stirrups were made of A-III class Ø8 mm reinforcing bars with the spacing in the supporting zone of about 100 mm.

4.1.2.3 Compressive Strength

The compressive strength of concrete used for building the columns and beams was about 23 MPa and 27 MPa respectively. Grade A-III steel was used for reinforcement with yield strength of 390 MPa and ultimate strength of 590 MPa.

4.1.2.4 Nominal Strengths

When designing with a strong column weak beam strategy, the columns are made to be stronger than the beams so that they can withstand vertical loads and the beams can withstand horizontal loads like wind or seismic forces. This method is useful for protecting the columns from

brittle failure mechanisms including shear and torsion. ACI 318 recommends a SCWB ratio of 1.2. Based on the geometry shown in figure 4-4 and material characteristics provided in section 4.1.2.3, nominal shear, and moment strengths for both the columns and beams are calculated and provided in Table 4-2. These nominal values are a cautious approximation of the member's capacity to resist shear and bending and are determined using equation 4-1 and 4-2 as per ACI 318 [64] design codes.

Table 4-2 Nominal Shear and Moment Strength of VP series buildings

	Floor Level	Nominal Shear Vn (KN)	Nominal Moment Mn_c (KN-m)		Floor Level	Nominal Shear Vn (KN)	Nominal Moment Mn_b (KN-m)	ΣMn_c	ΣMn_b	$\Sigma Mn_c/\Sigma Mnb$	Strong Column weak Beam
Columns	1st	286.35	420.01	Beams	1st	264.12	308.51	804.73	617.02	1.30	Satisfied
	2nd	286.35	384.71		2nd	264.12	308.51	730.58	617.02	1.18	Not Satisfied
	3rd	286.35	345.86		3rd	264.12	308.51	649.40	617.02	1.05	Not Satisfied
	4th	286.35	303.54		4th	264.12	308.51	561.46	617.02	0.91	Not Satisfied
	5th	286.35	257.92		5th	264.12	308.51	386.10	500.24	0.77	Not Satisfied
	Technical	286.35	128.17		Technical	264.12	191.73	256.35	383.47	0.67	Not Satisfied

Table 4-2 also depicts that the structural elements of the first three floors satisfy the strong column weak beam criteria showing that the beam will fail before the columns and beam failure generally results in partial failure of structure while that of 4^{th}, 5^{th} and 6^{th} floor are not satisfying this criterion showing the possibility of failure of columns before beams which will ultimately leads to the failure of whole structure.

4.2 Model development

Though many analytical modeling methods have been published, only a few of these models have been incorporated into the commercial and open-source computational tools available to the engineering and scientific communities at large. One of the computing platforms that is most frequently used in the discipline of structural and seismic engineering is called OpenSees, or the Open System for Earthquake Engineering Simulation [65]. The free and open source OpenSees software can be used to do nonlinear analyses of structural components and systems that are susceptible to seismic ground vibrations. OpenSees offers a variety of features, including model elements, material models, various solution methodologies, and so on.

It is necessary to identify the physical characteristics of the steel and concrete reinforcement used in the moment frame. This contains the materials' elastic modulus, yield strength, and ultimate strength as shown in table 4-3 and table 4-4. Furthermore the stress strain curve of concrete for VP series beams and steel is depicted in figure 4-9 and figure 4-10 respectively. Following the definition of the geometry, material properties, and hinge properties, the model is loaded with data and boundary conditions to simulate how the moment frame will behave under various loading conditions. Furthermore, gravity loads, and P-delta effects were also considered to obtain an accurate and realistic response behavior of the structures during seismic event.

Table 4-3 Properties of Concrete

Building Series	Element	Compressive Strength (MPa)	Compressive Strain at Peak Strength	Elastic Modulus (MPa)
VP Series	Columns	23	0.002	23000
	Beams	27	0.002	27000
VT Series	Column	30.5	0.002	30500
	Beams	25.7	0.002	25700

Table 4-4 Mechanical Properties of A-III Steel

Yield Stress (MPa)	Elastic Modulus (MPa)	Fracture Strength (MPa)	Strain Hardening Ratio
390	200000	590	0.01

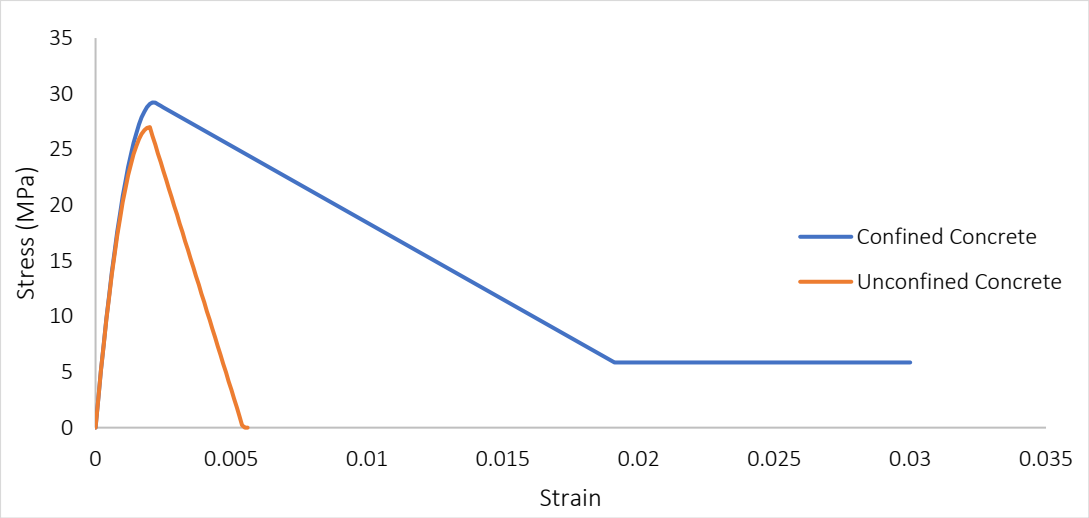

Figure 4-9 Stress Strain Curve of Concrete of VP series

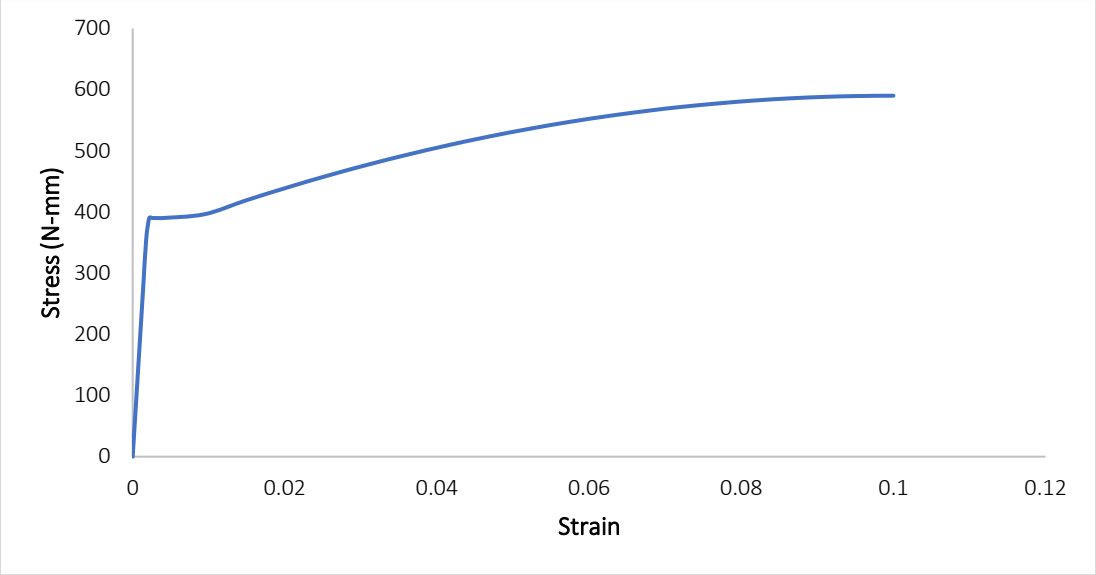

Figure 4-10 Stress Strain Curve of Steel

The model incorporates all elements of the structure, including the fundamental vertical plane elements (moment frames), gravity system columns, and floor system perimeter beams. Element type beams with hinges were used to model these structural members. Further the columns were modeled using the fiber sections. The beam's curvature characteristic is calculated with the help of the XTRACT (a section analysis program) using Kent Park concrete model. Figure 4-11 displays the two-dimensional FEM model of the VP series. Furthermore 2% damping is selected for both buildings with fixed boundary conditions. Similarly, eigen value of 1st and 3rd mode were considered for the calculation of Rayleigh damping. Understanding a moment frame's behavior is crucial to building a structure to withstand these stresses. To precisely replicate the behavior of a reinforced concrete moment frame, the element type of beam with hinges is extensively utilized. Hinge connections are used to represent joint connections between beams and columns, simulating their rotational motion. The "plastic hinge integration" method allows the user to choose the lengths of the plastic hinges at the element ends which determines the positions and weights of the element integration points. The length of the plastic hinges used in our study are calculated based on the equation 4-3 provided by Park [66].

$$L_p = 0.5H \qquad \text{Equation 4-3}$$

Where H is the depth of the section.

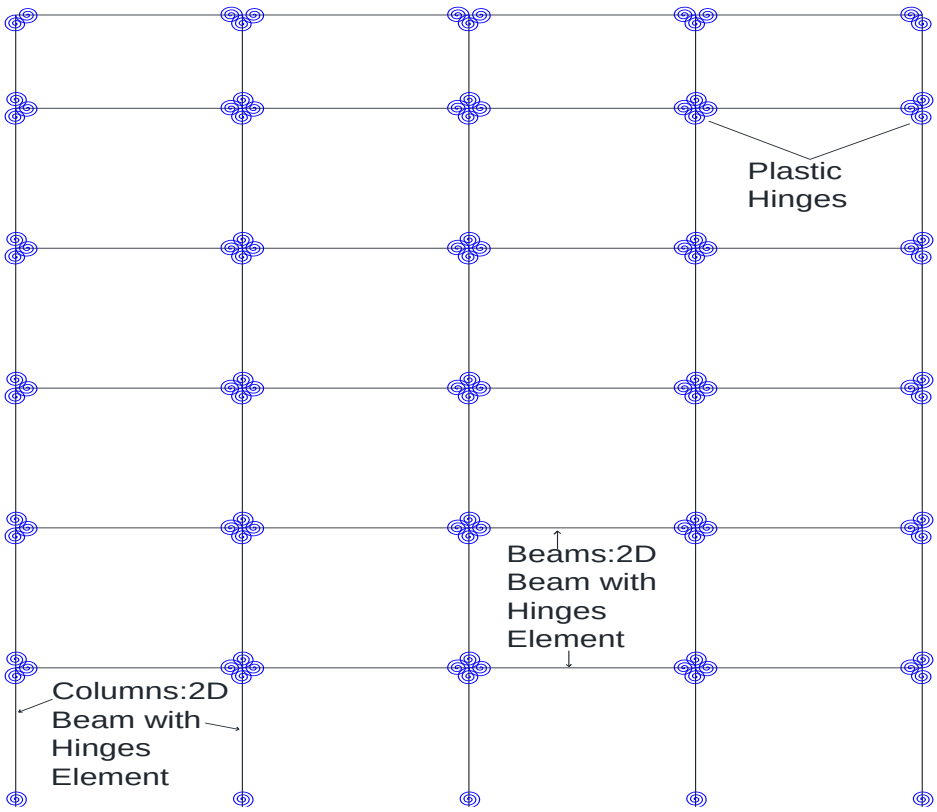

Figure 4-11 Two-dimensional model of the VP Series

4.3 Ground motions input

The ground motions input used for this study is taken from the FEMA-P695 FF ground motion set. Twenty-two records are included in the FEMA-P695 FF GM collection (44 individual components). They are all typical of high magnitude events having magnitude between 6.4 to 7.7, observed at locations at least 10 kilometers away from the rapture fault. It includes ground motions caused by shallow crustal earthquakes, which can have either strike-slip or reverse (thrust) causes and occur within around 30 km of the surface. The PEER NGA database contains recordings that are part of this collection of ground motions [67].

For this study we have selected the eight (8) records (sixteen individual components, shown in table 4-5, having reverse (thrust) or reverse oblique fault type from the FEMA-P695 FF GM set as it pertains to study area, in Almaty. This knowledge is essential for selecting a ground motion model that effectively captures the distinctive features of the research area's reverse fault system.

Table 4-5 Selected Ground Motions [67]

ID PEER	Event	Magnitude	Year	Record	EQ	Fault Type	Duration (Sec)	dt(Time Increment)
9	Chi-Chi Taiwan	7.6	1999	CHY100	EQ1	Reverse	90	0.005
10	Chi-Chi Taiwan	7.6	1999	CHY101	EQ2	Reverse	90	0.005
11	Friuli Italy	6.5	1976	Tolmezzo	EQ3	Reverse	36.345	0.005
12	Friuli Italy	6.5	1976	Tolmezzo	EQ4	Reverse	36.345	0.005
13	Chi-Chi Taiwan	7.6	1999	TCU045	EQ5	Reverse	46.1	0.005
14	Chi-Chi Taiwan	7.6	1999	TCU045	EQ6	Reverse	46.1	0.005
25	San Fernando	6.6	1971	LA - Hollywood Stor FF	EQ7	Reverse	79.45	0.01
26	San Fernando	6.6	1971	LA - Hollywood Stor FF	EQ8	Reverse	79.45	0.01
31	Loma Prieta	6.9	1989	Capitola	EQ9	Reverse Oblique	39.995	0.005
32	Loma Prieta	6.9	1989	Capitola	EQ10	Reverse Oblique	39.995	0.005
33	Loma Prieta	6.9	1989	Gilroy Array #3	EQ11	Reverse Oblique	39.985	0.005
34	Loma Prieta	6.9	1989	Gilroy Array #3	EQ12	Reverse Oblique	39.985	0.005
41	Northridge	6.9	1994	Beverly Hills - 14145 Mulhol	EQ13	Reverse	29.99	0.01
42	Northridge	6.9	1994	Beverly Hills - 14145 Mulhol	EQ14	Reverse	29.99	0.01
43	Northridge	6.9	1994	Canyon Country - W Lost Cany	EQ15	Reverse	19.99	0.01
44	Northridge	6.9	1994	Canyon Country - W Lost Cany	EQ16	Reverse	19.99	0.01

Figure 4-12 shows the spectrum of the selected ground motions with period from 0.1 to 4 seconds.

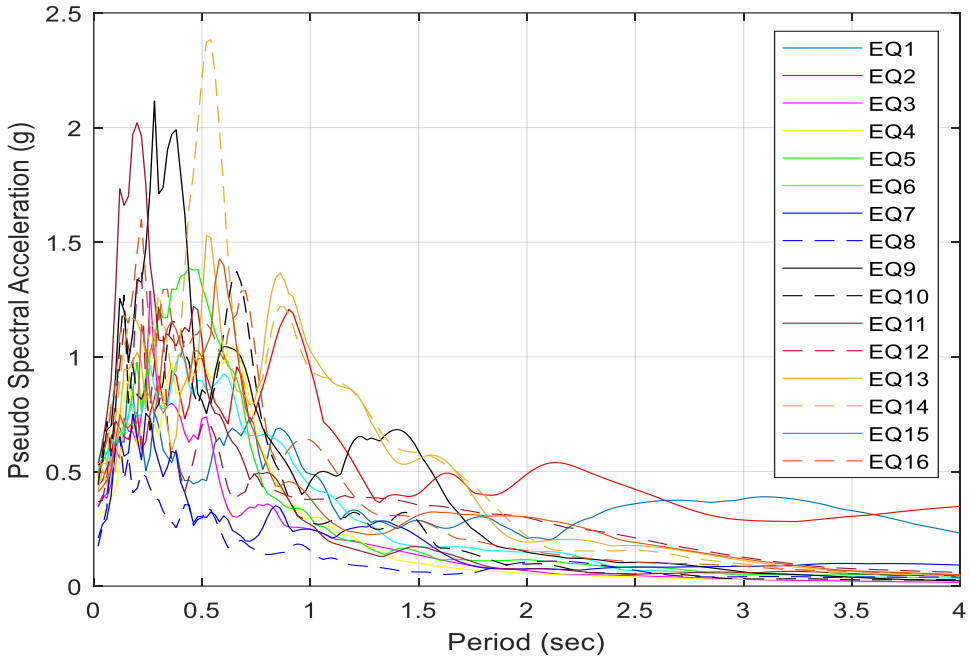

Figure 4-12 Ground motion's spectrum with period [0.1-4.0] seconds

4.4 Design Response Spectrum of Almaty

The design response spectrum of Almaty city is shown in figure 4-11 with return period of both 475 and 475 earthquakes. Furthermore, the period of both VP series and VT series are also illustrated in figure 4-13.

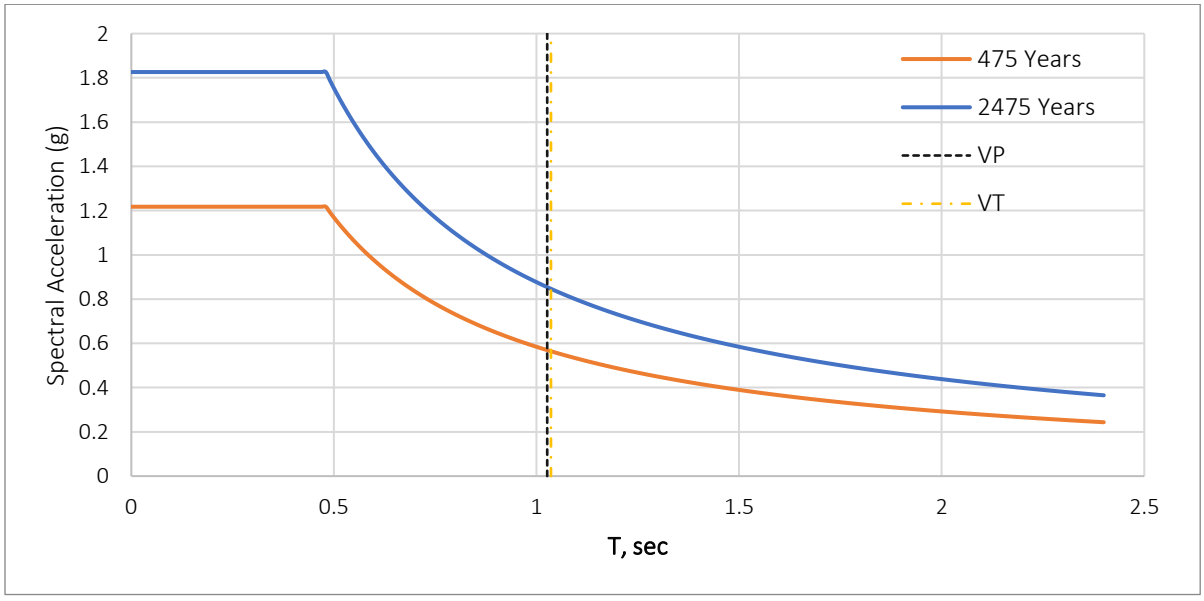

Figure 4-13 Design response spectrum of Almaty, Kazakhstan

4.5 Pushover Analyses

Pushover analysis is a static methodology that use a simple nonlinear method to evaluate seismic structural deformations. During earthquakes, buildings reorganize themselves. When one part of a structure gives way or fails, the dynamic forces that are acting on the building are redistributed to the other parts of the structure. Pushover analysis has been included in several new retrofit seismic design guidelines and is widely used to determine an existing building's seismic resistance [68]. It can also aid performance-based earthquake-resistant building design.

Pushover analysis is utilized in this study to assess how well the buildings perform in both the longitudinal (the direction running along lengthwise of building) and transverse (perpendicular to the longitudinal) directions to determine which way is weaker for the building. The results for both buildings are shown in figure 4-14. This figure illustrates that both buildings are stronger in the longitudinal direction. Based on this analysis the performance behavior of both buildings was evaluated in the transverse direction and results are presented in the sections ahead.

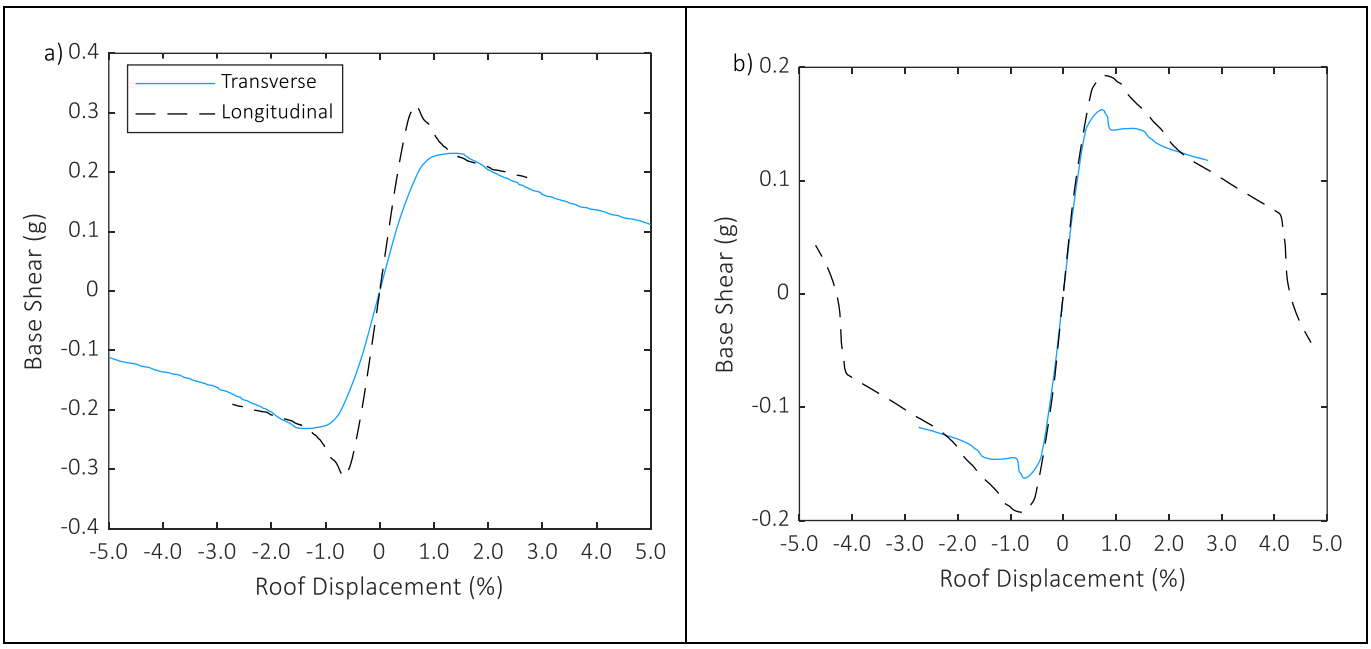

Figure 4-14 Pushover Analysis a) VT series b) VP series

4.6 General results

This section contains the general results such as hysteresis plot, hinge plots, plastic hinge formation and plastic rotation in both beams and columns. All these plots are plotted for earthquake 3.

4.6.1 Hysteresis Plot

The gravitational force acting on the members of the frame is comparatively weak when the value of Spectral acceleration (Sa(g)) is low. Because of this, lateral loads like seismic or wind forces only cause slight deformations in the frame. The deformation is predominantly elastic, meaning that if the lateral load is removed, the frame will revert to its original shape. The hysteresis loop for this behavior is smaller and less noticeable. On the other hand, if the value of g is increased, then the gravitational force that is acting on the components of the frame will be significantly increased. Significant deformations occur in the frame as a result of the increased axial load and bending moment on the members, leading the frame to exhibit both elastic and inelastic behavior. The early loading and unloading cycles exhibit elastic behavior, but succeeding cycles exhibit inelastic behavior. As a result, the hysteresis loop widens and becomes more prominent, with a bigger disparity between the loading and unloading branches. The hysteresis plot for both VT and VP series building is depicted in figure 4-15 and 4-16 at different values of g for EQ3.

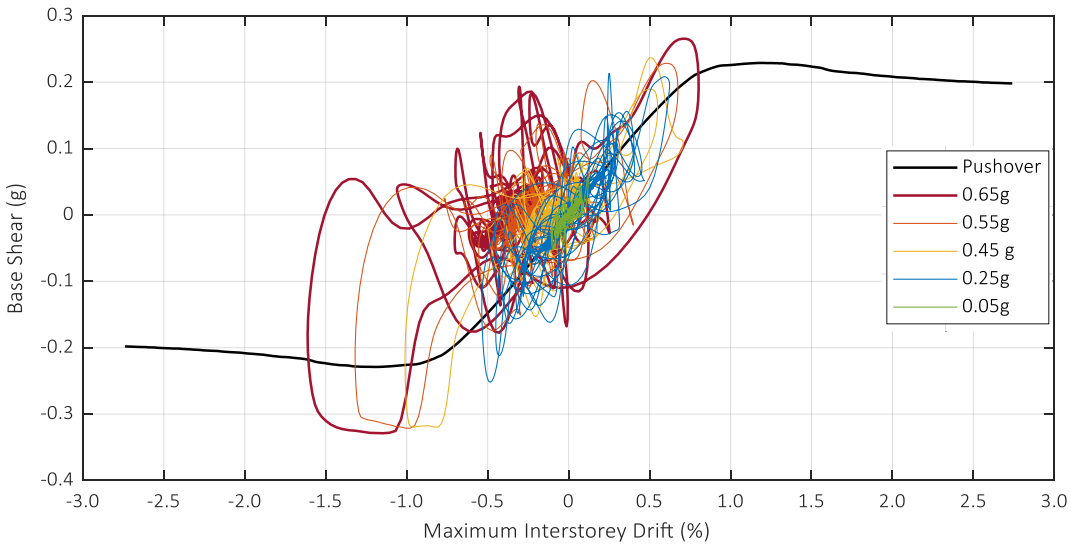

Figure 4-15 Hysteresis Plot of VT series at various values of Sa(g)

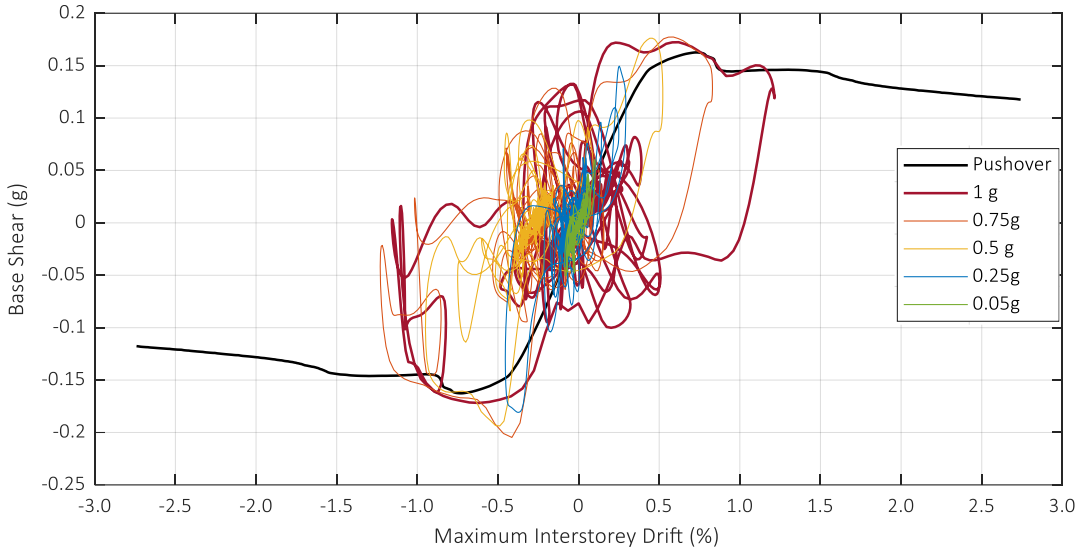

Figure 4-16 Hysteresis Plot of VP series at various values of Sa(g)

From the figure 4-15 and 4-16 it can be seen that by increasing the value of g the hysteresis loop starts to widen up and becomes more important. It can also be seen that at Sa value of 1.0 the hysteresis plot is exhibiting more base shear than the pushover cover because the graph plotted for different value of g is between the maximum inter-storey drift and base shear while for pushover curve it is between the roof drift versus the base shear.

4.6.2 Plastic Hinges Formation

At the completion of the nonlinear analysis, the positions of plastic hinges are illustrated in figure 4-17 and figure 4-18 where the degree of plastic rotation is indicated by the different sizes of the circle. For both columns and beams, plastic rotations were calculated in accordance with the plastic rotations of the members at the ends while the elastic rotation part were subtracted from to it depict better formation of plastic hinges under different values of spectral acceleration. In cases of intense seismic activity, columns within a building structure may behave nonlinearly and even experience a weak story mechanism, as seen in figure 4-17 (b). Notably, this tendency is even stronger when the SCWB ratios of all joints get close to one (1), which could mean that the connections among structural elements could be weak. The occurrence of such events could result in significant deformation and, ultimately, collapse of the concerned columns, especially if they are exposed to seismic forces that are greater than those allowed for during the design phase of the building. According to the findings of Lee's [69] research, the potential for hinges in normal

columns is greater at the bottom end of the joints than it is at the top. This result is consistent with what Lee's investigation revealed. This is due to the fact that beam-to-column connections have higher concentrated moments at the base. This phenomenon might be influenced by several different factors, including the frequency response of earthquake data and the consequences of higher mode earthquakes. Conversely, plastic hinges may form at the top end of column if the column's cross-section is changed. This increases the likelihood of plastic hinge creation at both ends of a story's columns.

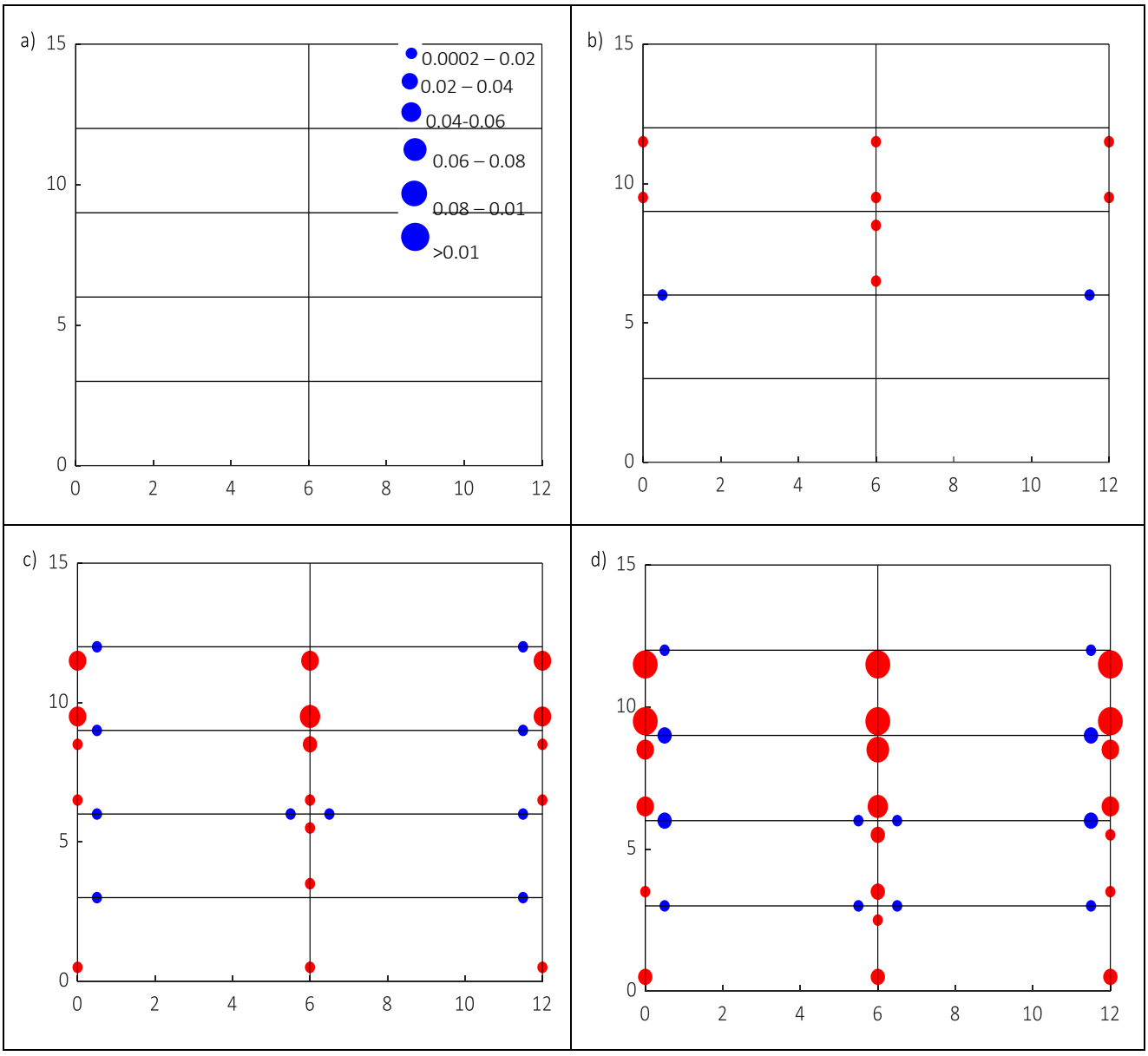

Figure 4-17 Plastic Hinge Formation of VT Series at a) 0.15 g; b) 0.25 g; c) 0.5 g; and d) 1.0 g

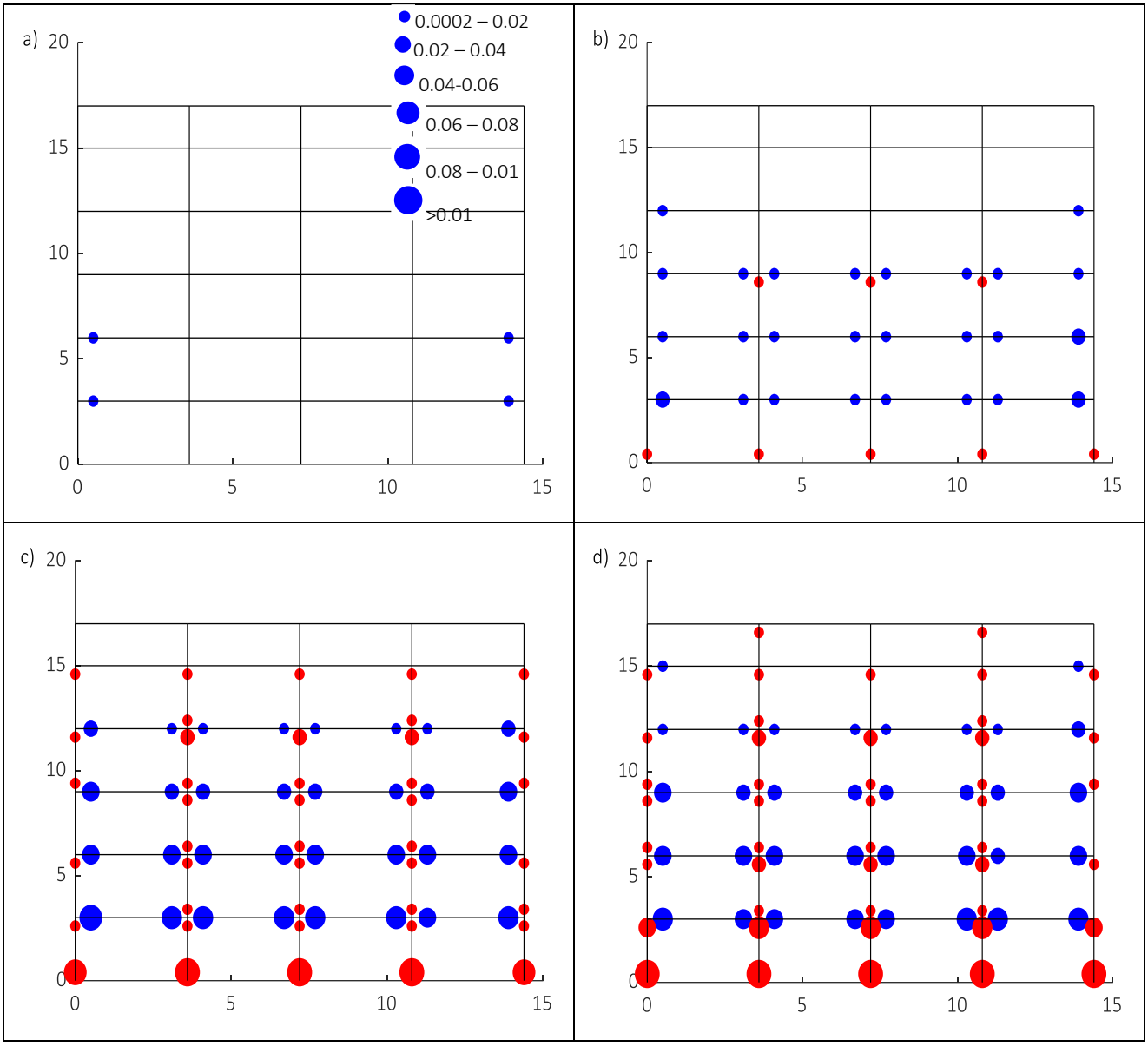

Figure 4-18 Plastic Hinge Formation of VP Series at a) 0.15 g; b) 0.25 g; c) 0.5 g; and d) 1.0 g

4.6.3 Plastic Rotation in Beams and Columns

Plastic hinges' idealized force-rotation/deformation relationship is shown in Figure 4-19 where P represents the primary elements or components, and S represents the secondary elements or components. This idealized curve can be represented as linear from its origin (point A) to its yield point (point B), then as linear with reduced stiffness from point B to its ultimate point (point C), and finally as linear with abruptly reduced lateral load capacity (point D). After the final linear

behavior, there will be a further reduction in stiffness leading up to point E, which will ultimately result in a loss of capacity at point E.

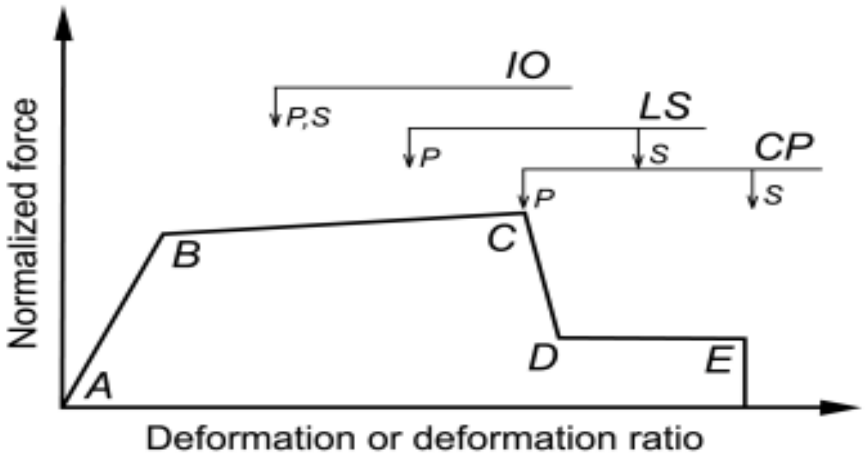

Figure 4-19 Relationship between force and deformation for concrete materials

In accordance with the FEMA 356 [17] recommendation, the acceptance criteria for various performance limits such as immediate occupancy (IO), life safety (LS), and collapse prevention (CP) of reinforced concrete frame elements is calculated and presented in table 4-6.

Table 4-6 Plastic Rotation Values for RC columns and beams

Building Series	Element	IO	LS	CP
VT Series	Column	0.0043	0.014	0.018
	Beam	0.010	0.020	0.025
VP Series	Column	0.0038	0.013	0.017
	Beam	0.010	0.020	0.025

Note that these limits apply to RC elements that failed due to flexural forces, and that brittle/shear failure does not occur before these plastic rotational limits have been exceeded. Figure 4-20 and 4-21 illustrate the plastic rotation for both beams and columns of both buildings. Furthermore figure 4-20 depicts that at g value of 0.75 the maximum rotation in columns at storey at 2nd, 3rd and 4th is greater than the performance limit of collapse prevention which indicates the failures of columns of these stories. Also, the columns at 3rd storey have the maximum value which

also indicates that the columns at 3rd storey are least strong as compared to other stories as can be seen in figure 4-4. Similarly for beams at g value of 0.75, the beams of 1st and 2nd storey exhibit maximum rotation more than the performance limit of collapse prevention showing the failure of beams at these stories.

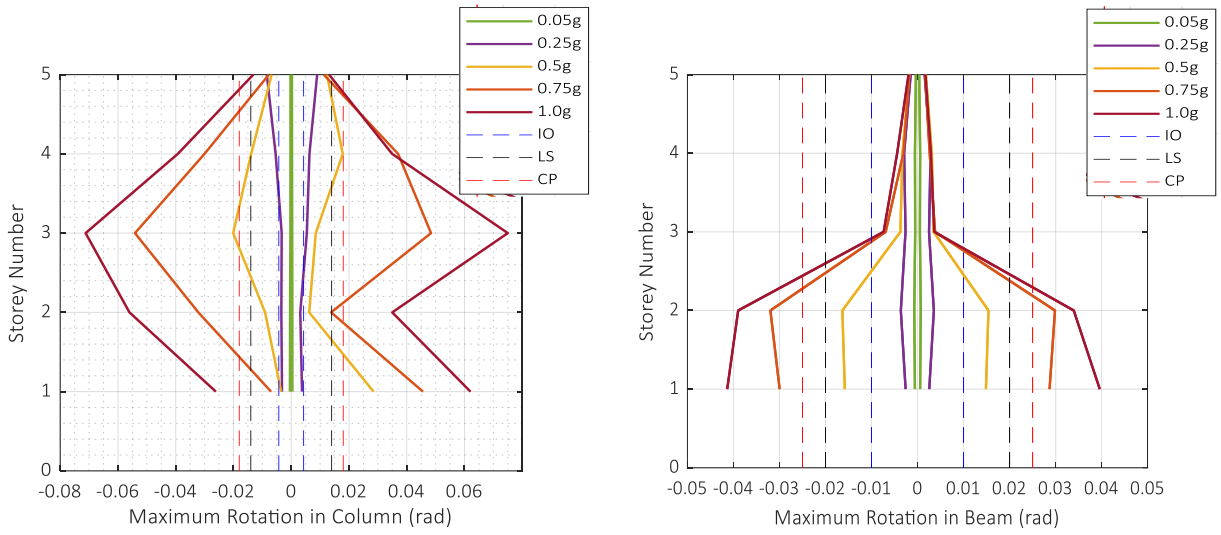

Figure 4-20 Maximum rotation on each storey of VT series

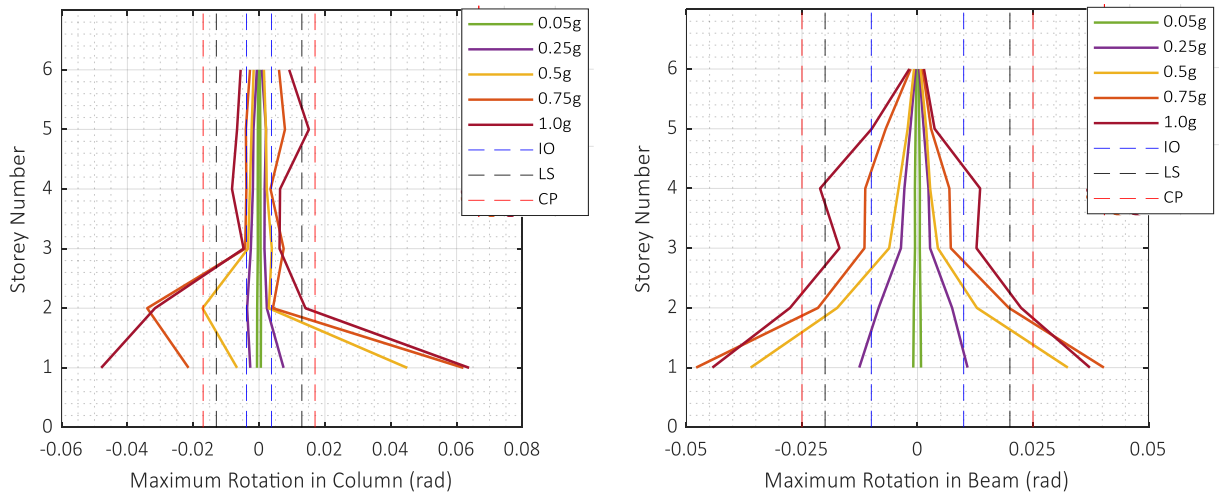

Figure 4-21 Maximum rotation on each storey of VP series

4.6.4 Maximum Inter-storey Drift

In displacement-based engineering, the maximum Inter-storey drift ratio (MIDR) is thought to be one of the most important criteria for judging the performance of existing structural systems during a seismic event. Because of the potential for Inter-storey drift to cause structural damage,

functional loss, and even collapse, it is important to account for drift when designing and evaluating buildings. For this purpose, the maximum Inter-storey drift for both buildings are calculated and shown in figure 4-22 and 4-23 for VT and VP series respectively. It can be seen in figure 4-22 that the 4th floor has the maximum Inter-storey drift showing the soft storey mechanism as it can be seen in the figure 4-3 where the reinforcement details are provided. Also, it can be seen that as by increasing the value of g the Inter-storey drift is also increased. Furthermore, both the buildings show the possibility of collapse at g value of 0.75 and higher. It should also be kept in mind that this value is very close to PGA value of 0.7305g with return period of 2475 years for the city of Almaty.

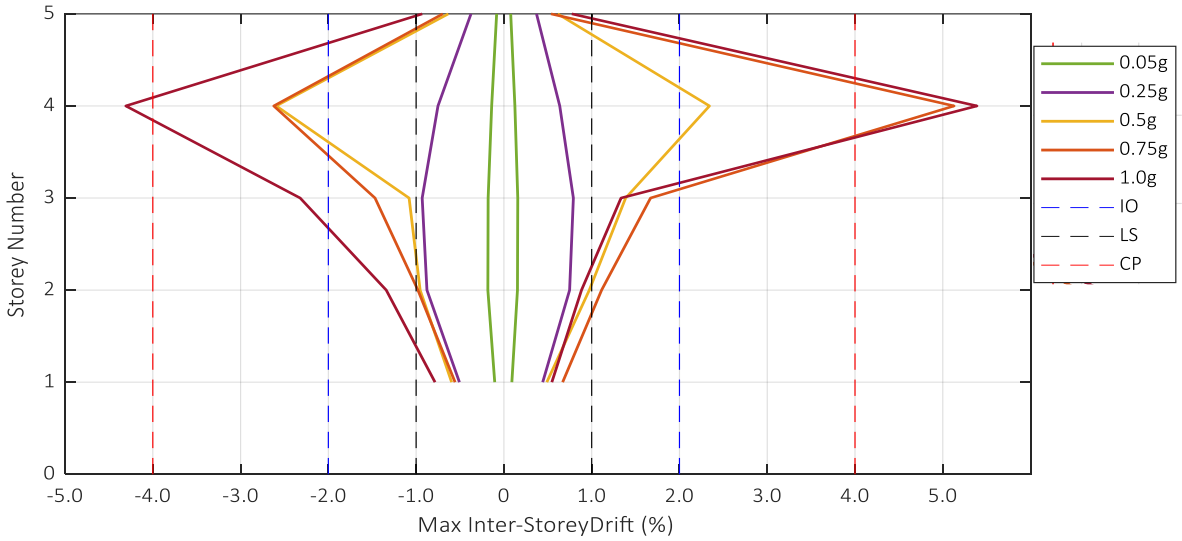

Figure 4-22 Maximum Inter-storey Drift of each Floor of VT series

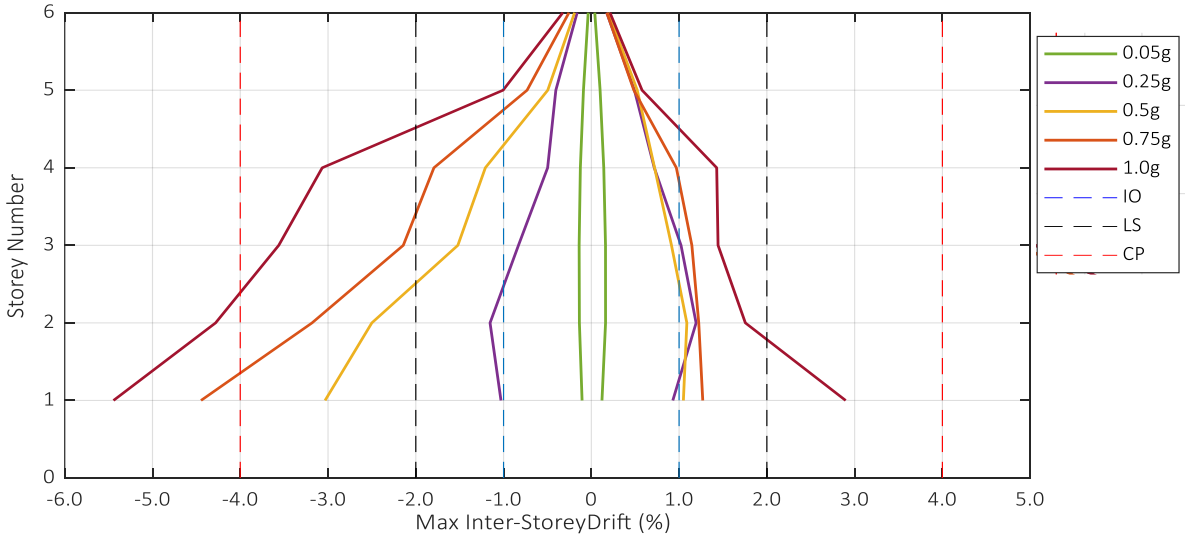

Figure 4-23 Maximum Inter-storey Drift of each Floor of VP series

4.6.5 Shear Strength Failure

Figure 4-24 and 4-25 shows that V_{max}/V_n values of structural elements of both VT and VP series respectively. It can be seen in both the figures that none of the structural elements have shear failure when subjected to different ground motions.

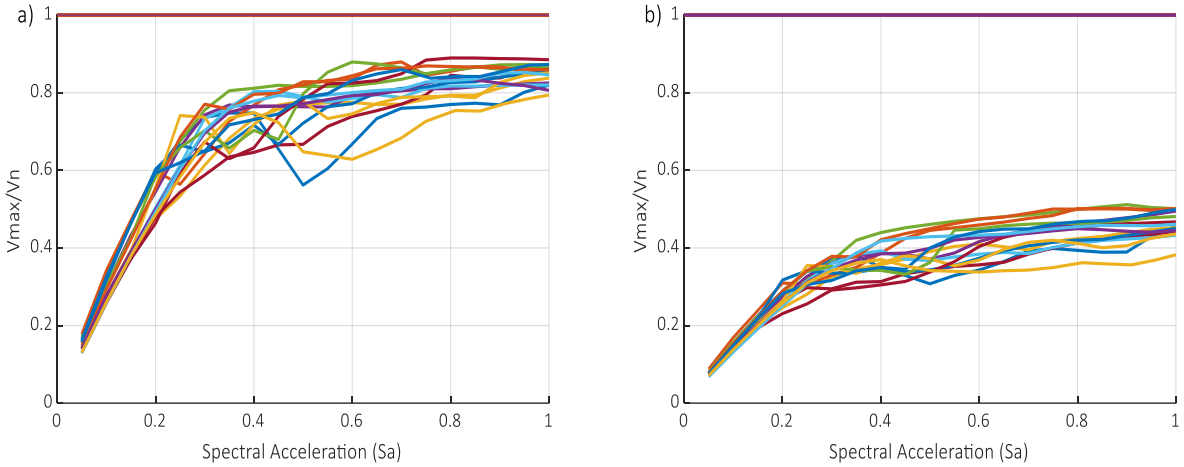

Figure 4-24 Vmax/Vn of VT series buildings a) columns b) beams

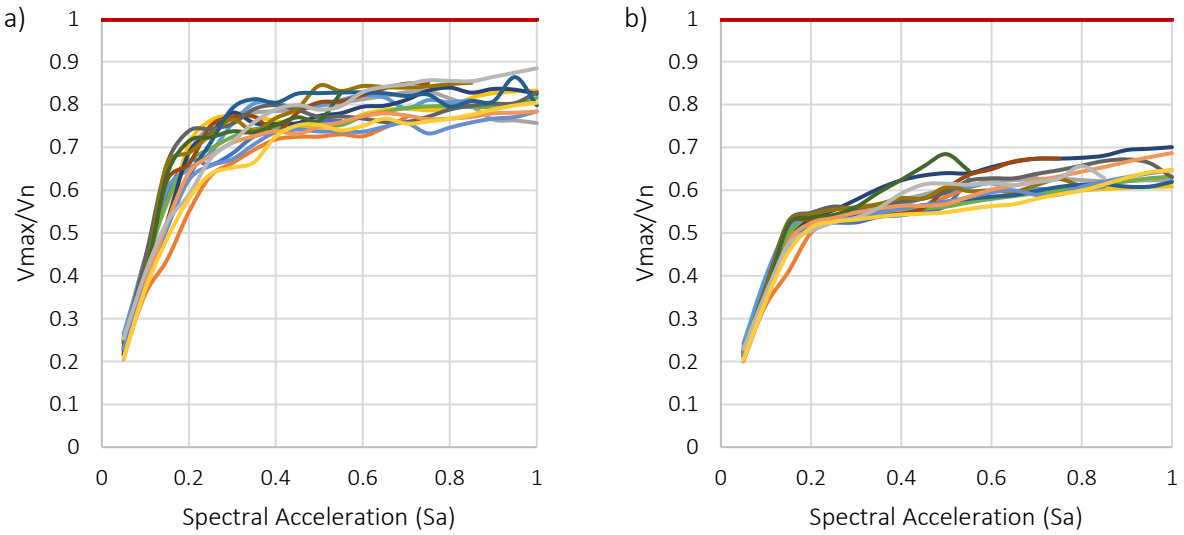

Figure 4-25 Vmax/Vn of VP series buildings a) columns b) beams

4.7 Parametric results (Fragility curves)

The earthquake damage estimation problem is probabilistic due to the inherent uncertainty in earthquake occurrence. It has been demonstrated by Shome and Cornell [70] that for mid-rise buildings, ten to twenty ground motion records are typically adequate to offer sufficient precision

in the assessment of seismic demand. To simulate the unpredictable character of earthquakes, this study used a total of sixteen (16) different types of ground motions as shown in table. Figure 4-12 depicts the acceleration spectrum of the ground motions used for this study.

4.7.1 Damage Levels

This study considers IO, LS and CP to be fundamental damage levels whereas IO is equivalent to light or minor damage, LS is equivalent to moderate damage and CP is equivalent to severe damage. Recently published studies that were similar to this one accounted for varying degrees of damage and their associated bounds using various damage metrics. For example, Kircher [71] and Smyth [72] established four different damage levels for different building types: minor, moderate, major or severe, and collapse. As the damage metric, the maximum inter-story drift ratio was selected, and there is an assumed limit value for the inter-story drift ratio for each of the damage levels. The vast majority of the damage levels that were utilized in earlier investigations are linked to the expected limit values of the damage measure that was being investigated. Using an analytical method, it is very hard to find the limit values of the damage measure being considered. They are founded on the findings of a few experiments, engineering expertise, and knowledge gained from earlier earthquakes. As yielding and collapse are the two phenomena that can be calculated analytically with good precision [73], they are the only ones examined here.

4.7.2 Incremental Dynamic Analysis

Incremental dynamic analysis, also known as IDA, is a parametric analysis method that can be used to estimate how well a structure will perform in response to a number of different ground motions. Vamvatsikos and Cornell [74] provide an in-depth discussion of the methodology. As a result of multiple non-linear dynamic analyses, a curve of damage intensity vs damage magnitude is generated to illustrate the impact of scaled ground motions. Based on previous research, we estimate that the maximum inter-story drift ratio is the best predictor of damage, and we utilize a damped elastic spectral acceleration of 5% as the ground motion intensity measure for this study. The magnitude of each ground motion is correspondingly scaled in respect to the associated spectral acceleration based on the elastic fundamental period of each sample structure. A spectral acceleration increment of 0.05 g is selected so that an accurate representation of the structure's yield and its capacity to collapse may be obtained. The maximum inter-storey drift ratio and

spectral acceleration have a linear relationship up to the yield point. That point at which the curve departs from linearity due to spectral acceleration is known as the structure's yield capacity. When the structure has reached the point where it can no longer support its own weight, a rise in the intensity measure will effectively create an unlimited increase in the damage measure. Scaling up the ground motion and running repeated non-linear dynamic studies until dynamic instability occurs as a result of a non-converging run are used to determine the collapse capability of the structure. Immediate occupancy (IO[1]), life safety (LS[2]) and collapse prevention (CP[3]) were selected to analyze the performance behavior of the structures and drift values of one (1) percent, two (2) percent and four (4) percent are selected respectively as per FEMA 356 [75].

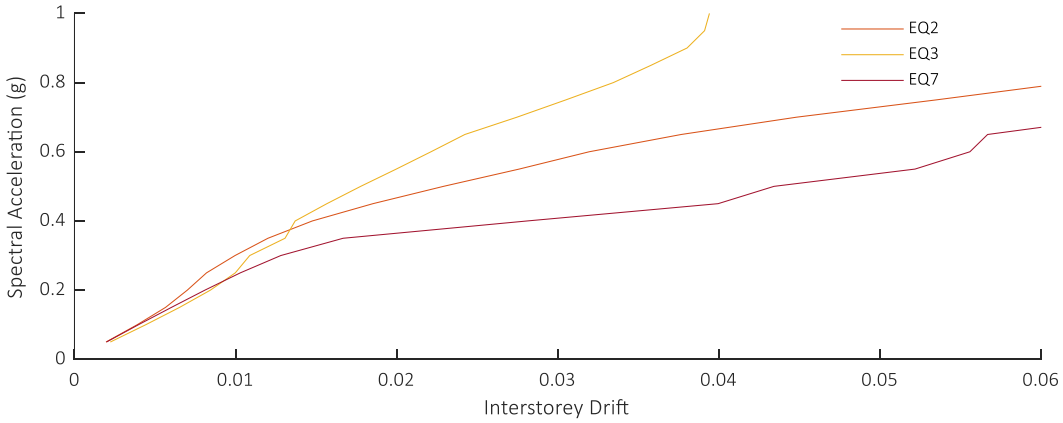

Figure 4-26 IDA Curve for VT series with different ground motions

4.7.3 Inter-storey Drift

The maximum Inter-storey drift ratio (MIDR) is considered to be among the most relevant criteria in displacement-based engineering for assessing the structural performance of existing structural systems during a seismic event. Drift is a significant factor in building design and assessment since significant Inter-storey drift can cause structural damage, functional loss, and

[1] Immediate Occupancy refers to the post-earthquake damage situation in which there has been minimal structural damage. Structural damage poses a low risk of serious injury, and although certain repairs may be necessary before reoccupation, they are usually not mandatory.

[2] Life Safety refers to the condition of a structure after an earthquake when there has been considerable structural damage but there is still some protection from either partial or complete structural collapse. Although there is a chance that someone will get hurt during the earthquake, there isn't a high likelihood that structural damage will result in a serious injury.

[3] Collapse prevention refers to the post-earthquake stage in which a building is on the edge of partial or complete collapse. Potentially serious injury risks arise due to falling debris from buildings. Because to the risk of more damage from aftershocks, the building is not yet safe for reoccupation.

even collapse. Regardless of where on the building's height the drift demand of the building structure under seismic event is essentially proportional to the maximum values of Inter-storey drift ratio (IDR). In this light, it is more convenient to express the drift need in the context of the maximum Inter-storey drift ratio rather than determining Inter-storey drift ratio for each floor. In the seismic event, If the maximum Inter-storey drift limit is exceeded, the structure may sustain considerable damage, which may put its structural integrity at risk. FEMA 356 [75] provides three performance levels for measuring the Inter-storey drift known as Immediate occupancy, life safety and collapse prevention and the corresponding performance limit values are provided in the table 4-7. Figure 4-27 and 4-28 depicts the maximum Inter-storey drift ratios for VT and VP series building respectively.

Table 4-7 Performance Limits for Inter-storey Drift as per FEMA 356

Sr. #	Performance Level	Performance Limit
1	Immediate Occupancy	1%
2	Life Safety	2%
3	Collapse Prevention	4%

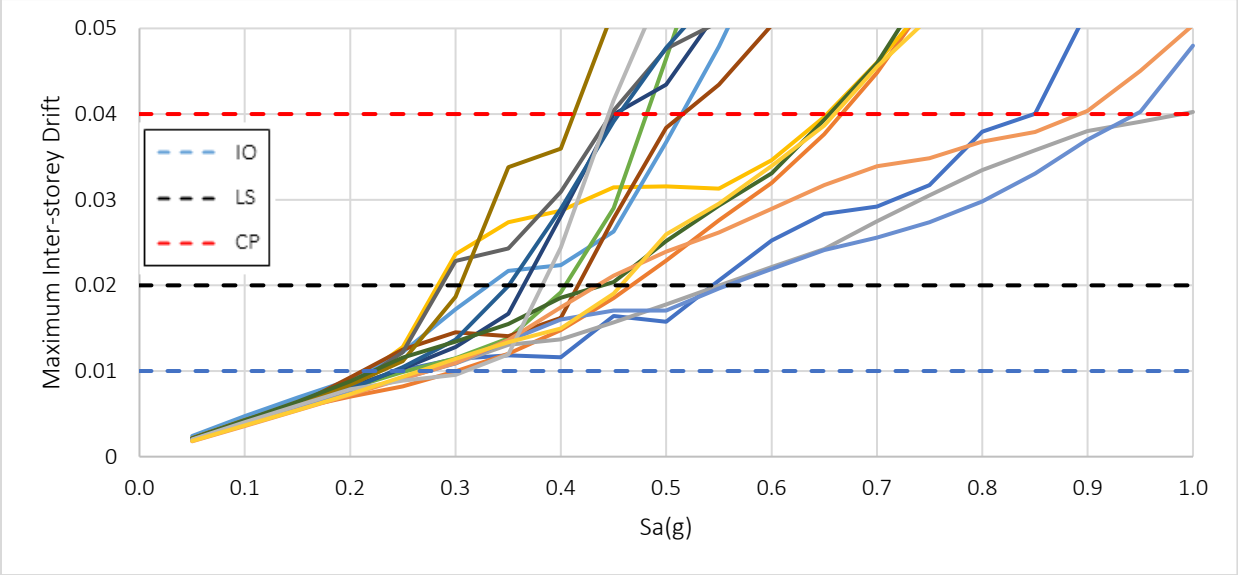

Figure 4-27 Maximum Inter-storey Drift of VT series

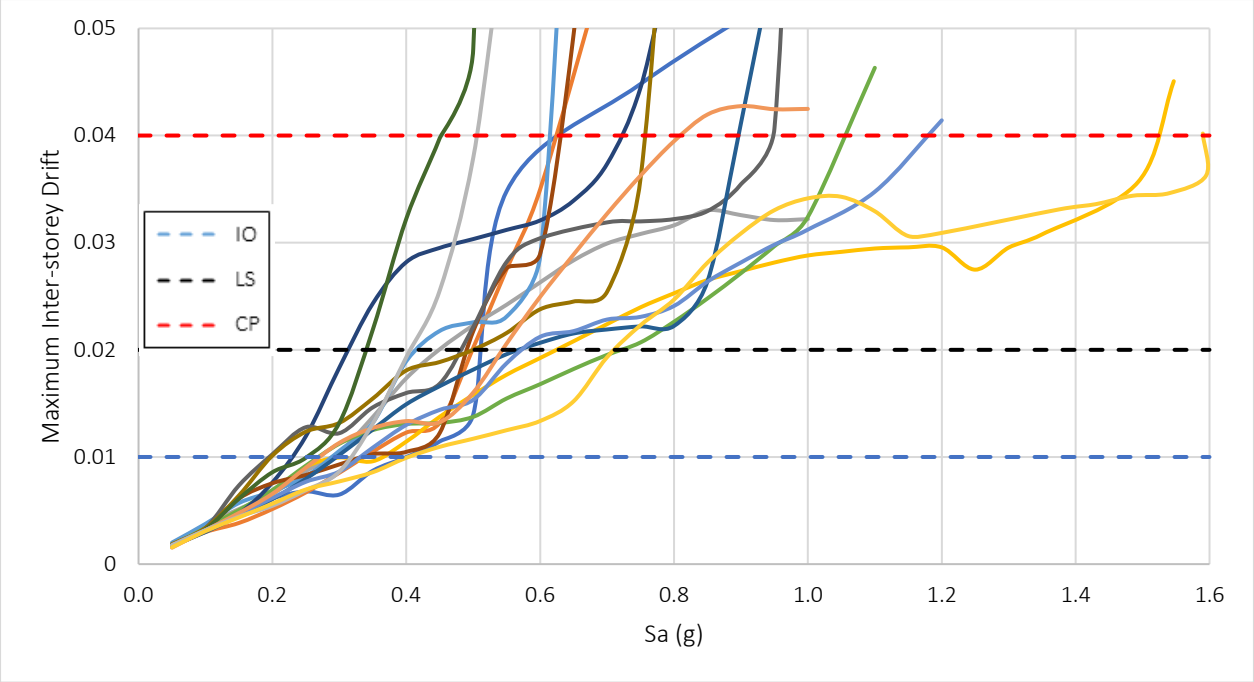

Figure 4-28 Maximum Inter-storey Drift of VP series

4.7.4 Plastic Rotation

Figure 4-29 to 4-30 depict the maximum plastic rotation behavior in the structural components of both VT and VP series respectively versus the spectral. The local behavior of columns and beams subjected to sixteen various ground motions at different performance levels of Immediate occupancy, life safety, and collapse prevention is depicted in these pictures, and the limits for these performance levels are presented in table 4-6.

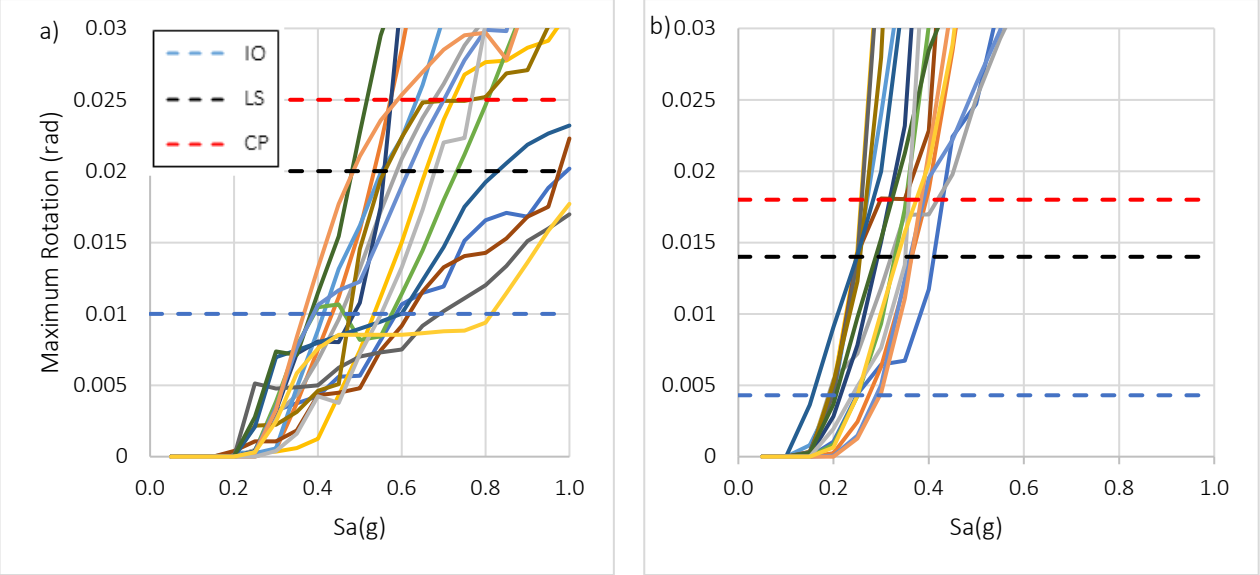

Figure 4-29 Maximum rotation in structural components of VT series a) beams b) columns

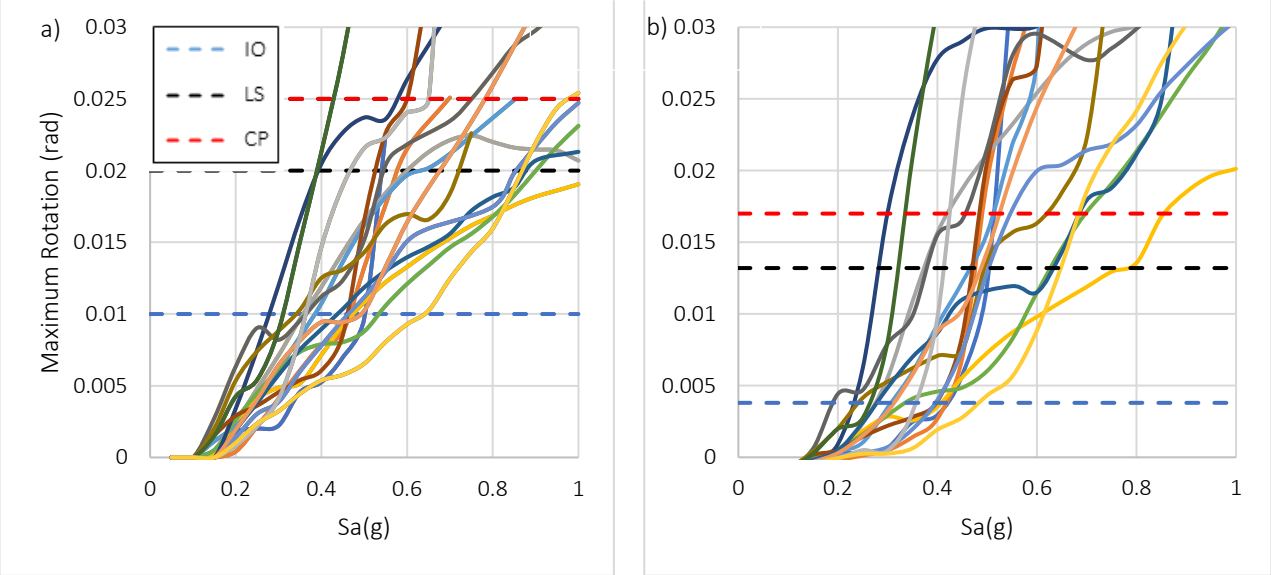

Figure 4-30 Maximum rotation in structural components of VP series a) beams b) columns

4.7.5 Fragility Curves

Fragility curve is a quantitative tool for assessing the vulnerability of buildings and structures to earthquake-caused damage. They illustrate the chance of structural damage as a function of the intensity of ground motion caused by an earthquake, which is assessed by the spectral acceleration (Sa). It is anticipated that fragility curves can be defined by using two-

parameter lognormal distribution functions. Using this premise as a foundation, the cumulative likelihood of damage equal to or greater than damage level D is given as equation 4-4

$$P(\leq D) = \phi(\frac{\ln X - \lambda}{\zeta}) \qquad \text{Equation 4-4}$$

Whereas:

Φ is the standard normal distribution,

X represents an index of ground motion with a lognormal distribution (e.g., Sa,),

and λ and ζ represents the mean and standard deviation of ln X respectively.

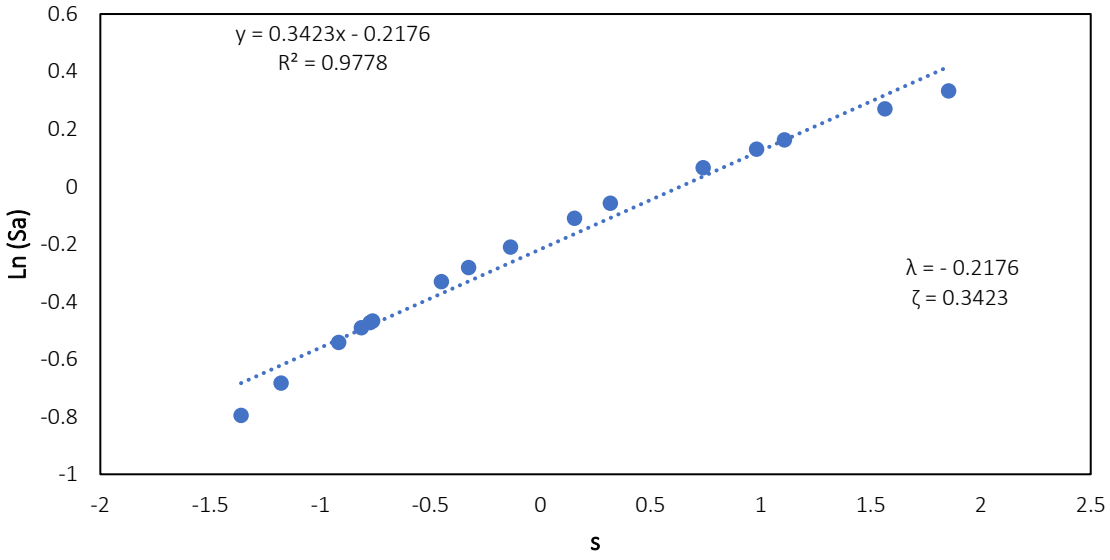

Figure 4-31 Lognormal plot of VP series for life safety

The mean and standard deviation of the ground motion index are calculated for each amount of damage, as illustrated in Figure 4-31, which depicts the lognormal plot of ln X and the corresponding standard normal variable. This method involves plotting ln X against the applicable standard normal variable on a lognormal scale, and then performing a linear regression analysis to calculate the mean and standard deviation of ln X for each damage level [76]. The relations between them are expressed in equation 4-5.

$$s = \frac{\ln X - \lambda}{\zeta} \qquad \text{Equation 4-5}$$

Where:

s represents the standard normal variable in the equation 4-5.

Figure 4-31 demonstrates the standard lognormal plot for the collapse prevention of VP series building structures.

4.7.5.1 Global Failure

Figure 4-32 and figure 4-33 exhibit the fragility curves for Immediate occupancy, life safety and collapse prevention of the VP and VT series, respectively as a global failure of the buildings using the maximum Inter-storey drift as evaluation criteria. Both VT and VP series buildings have 100% chances of sustaining minor or light damage for spectral acceleration with return period of 475 years and 2475 years. But it is worth noting that in figure 4-32, there are approximately 90% chances of sustaining moderate damage and 40 % chances of sustaining severe damage for any earthquake with return period of 475 years. Similarly, the chance of sustaining moderate damage is more than 90% at MCE while the chances of severe damage are more than 85%.

For VP series there are approximately more than 70% chances of sustaining moderate damage and more than 15% chances of sustaining severe damage for any earthquake with return period of 475 years. Similarly, the probability of sustaining moderate damage is more than 95% at MCE while the probability of severe damage is more than 50%.

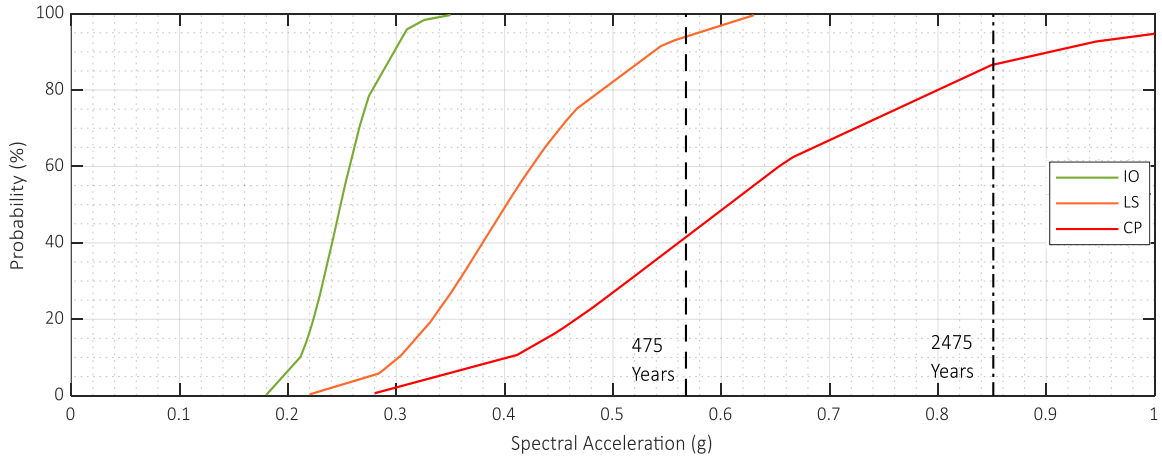

Figure 4-32 Fragility curves for VT series

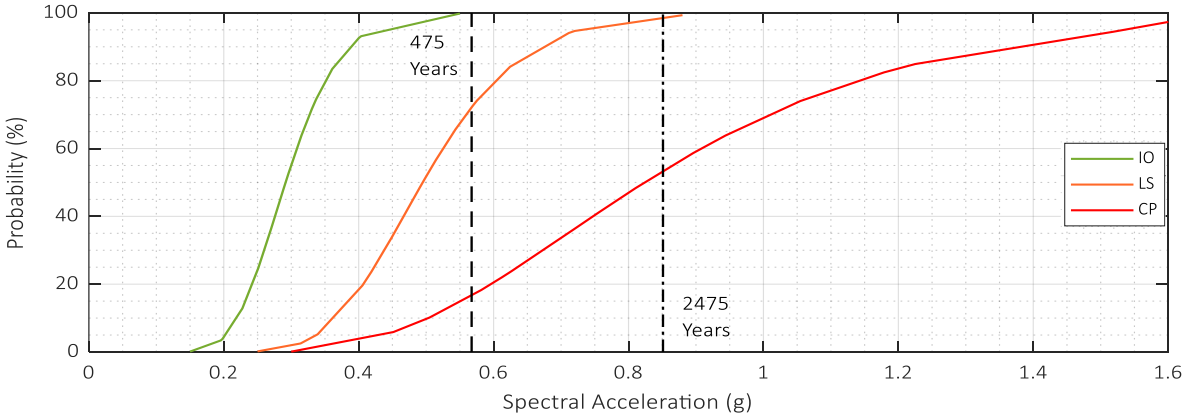

Figure 4-33 Fragility curves for VP series

Macro-seismic assessment of the residential building constructed using the reinforced concrete shows that these residential buildings will have moderate to high damage during an earthquake with return period of 475 and 2475 years respectively as shown in chapter 3 figure 3-8. Which suggests the need for analytical assessment of these buildings which is done in chapter 4 and fragility curves are developed and shown in figure 4-32 and 4-33. These figures also illustrate that the probability of moderate damage is more than 70% for both buildings at DBE but the probability of severe damage is less than 25 % buildings showing the accuracy of macroseismic assessment.

4.7.5.2 Local Failure of Structural Elements

Beside developing the fragility curves using maximum Inter-storey drift as an evaluation criterion for global failure the fragility curves for local failure of structure elements of columns and beams are also developed using plastic rotation as an evaluation criterion for both VT and VP series buildings and are shown in figure 4-34 and 4-35 respectively.

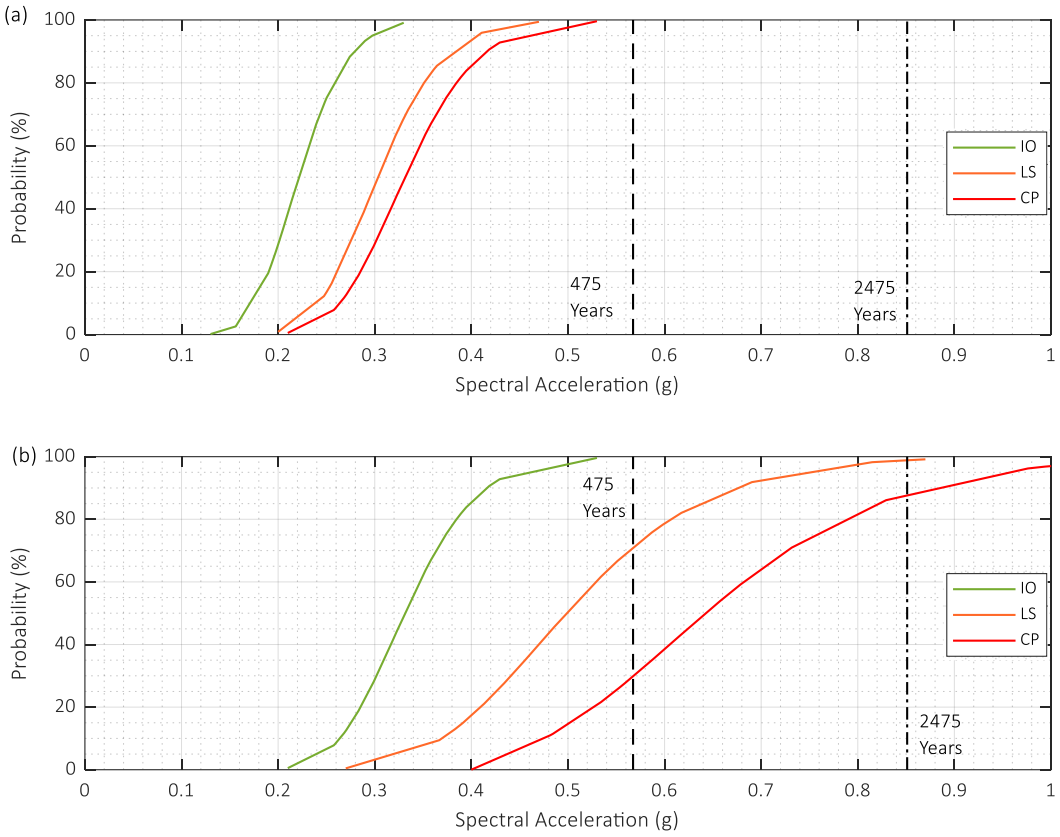

Figure 4-34 Fragility curve for Local failure of structural elements of VT series a) columns b) beams

It can be seen in figure 4-34 that columns have a 100 % probability of having light, moderate and severe damage during any seismic event with return period of both 475 and 2475 years while beams have a 100% probability of having light damage, more than 70% for moderate damage and more than 30% for severe damage at DBE. But this probability increases to approximately 100% for moderate damage and 85% for severe damage at MCE.

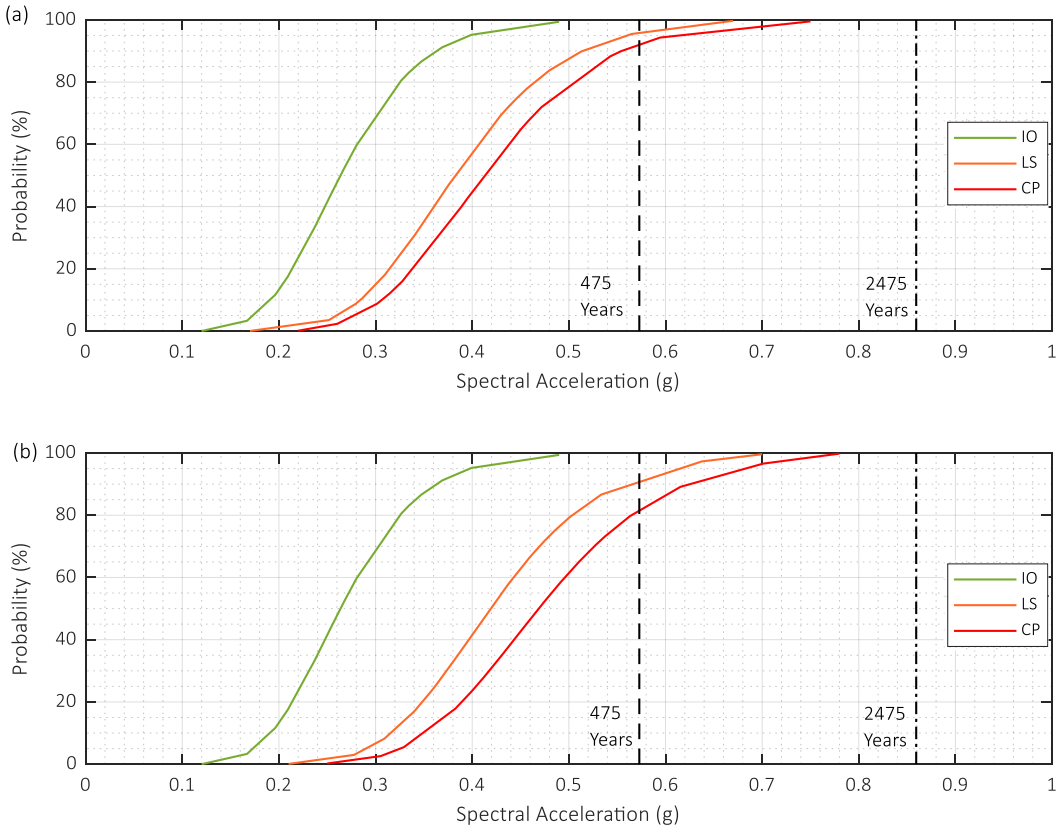

Figure 4-35 Fragility curve for Local failure of structural elements of VP series a) columns b) beams

From figure 4-35, It can see that both columns and beams have a probability of 100% of having light damage, 90% probability for moderate damage and 80% chances for severe damage at DBE. Similarly, this probability increases to 100% for all structural elements to have a severe damage showing that the building will collapse at MCE.

4.8 Recommendations

Probabilistic approaches for estimating structural damage are being developed due to the unpredictability of future earth motions. The fragility curve methodology is a useful way for assessing the structural damage caused by future earthquakes to certain types of structures. By conducting probabilistic seismic hazard calculations and nonlinear dynamic analyses of the structure, fragility curves are typically derived. At first the fault type of Almaty was figured out by studying previous literature. After Identifying the fault type in the Almaty region, the earthquakes data set was selected, and it made sure while selection that all the earthquakes should have the same fault type (Reverse fault) as in Almaty region. The selected ground motion intensity

is then fed into the structure's nonlinear dynamic analysis, simulating the structure's reaction to the ground motion.

The objective of the current study was to develop fragility curves for reinforced concrete moment frames that are typical of Almaty's contemporary building stock. The constructions were subjected to 16 different ground motion scenarios to produce the fragility curves, which were produced in terms of spectral acceleration (Sa). The performance levels of IO, LS, and CP are considered when evaluating a building's level of safety because these values can be established analytically with a respectable level of accuracy. Furthermore the performance level IO represents light/minor damage, LS is equivalent to moderate damage and CP is equivalent to severe damage. Fragility curves for both global and local failure of structural elements are developed whereas the maximum Inter-storey drift is considered as an evaluation criterion for global failure of structure elements while plastic rotation is considered as an evaluation criterion for local failure of structural elements. The outcomes of this study can be utilized by the local government authorities to devise future risk and seismic disaster mitigation to avoid human loss and casualties. Following outcomes can be drawn from the analytical assessment of this study:

1. For global failure, it has been found that the pre-cast concrete emulated moment frame buildings have 100% chances of having a light damage, more than 70% chances of having moderate damage and more than 20% chances of having a severe damage at DBE. Similarly at MCE, the probability of having moderate damage increase from 70 % to 100% and for severe damage it increases from 20% to 55%.
2. Similarly for local failure of structural elements of VT series, at performance level of immediate occupancy, both columns and beams have a 100% probability of having a light damage at both DBE and MCE. Similarly, the columns have a probability of 100% of having moderate damage while beams have a probability of 70% at DBE and 100% at MCE to sustain moderate damage. All stories still have a little bit of residual stiffness and strength. Since all the beams will suffer moderate damage making the structure beyond economical repair. The columns have the probability of having severe damage is 30% and 85% at DBE and MCE respectively. It can also be said that the building is near collapse, and it is better to abandon the structure at this level.

3. Furthermore, for local failure of structural elements of VP series, at performance level of immediate occupancy, both columns and beams again have 100% probability to have light damage at DBE and MCE. At performance level of life safety, both columns and beams have a probability of more than 90% to have moderate damage at DBE. Similarly at performance level of collapse prevention both columns and beams have a probability of more than 80% to sustain severe damage at DBE and building will collapse.

Based on the results it is recommended that the increase the strength of these structures where it is possible otherwise tear down or abandon these structures to avoid any casualties and human loss.

Chapter 5 - Conclusion

Seismic vulnerability assessment is a critical technique that determines the probability and extent of damage that a structure may sustain during an earthquake. Analytical and empirical approaches are two frequently employed techniques for this assessment. Both techniques are employed in this study to assess the seismic vulnerability of the structures.

The empirical approach uses statistical information from previous earthquakes to calculate the likelihood of structural damage. This approach takes into account elements including the seismic hazard, building type, lateral force resisting system and construction materials. A damage index, which represents the degree of damage that a building might sustain after an earthquake, is used to present the assessment results. In this study the macro-seismic assessment, one of the empirical approaches is used to assess the vulnerability of the structures constructed in the Soviet Union era. A macro-seismic assessment methodology was used to qualitatively analyze residential, commercial, and industrial structures made of a wide range of materials using the EMS-98 scale. These structures were initially categorized according to the materials used in their construction, as well as their lateral force-resisting systems and ductility capacities. Following that, a vulnerability class and sub-class were designated for each one in accordance with EMS-98. The estimated mean damage as well as the likelihood of damage at each level were computed for various earthquake intensities and PGA. Under the anticipated earthquakes, the mean damages and likelihood of each damage grade were estimated for both the DBE (for a return period of 475 years) and the MCE (for a return period of 2475 years).

Following the macro-seismic assessment of the buildings, the analytical approach is used to assess the seismic vulnerability of pre-cast concrete emulated moment frame structures. For this purpose, non-linear time history analyses, one of the analytical assessment approaches, is employed for the development of the fragility curves for performance levels of immediate occupancy, life safety and collapse prevention. The fragility curve method is helpful for estimating the potential seismic damage to specific building types in the future. Fragility curves are often created by doing nonlinear dynamic studies of the structure along with probabilistic seismic hazard estimations. Firstly, the fault type of Almaty city was found it. After figuring out the type of fault in the Almaty area, the earthquakes data set was chosen, and it was made sure that all the earthquakes had the same type of fault (Reverse fault) as the ones in the Almaty area. The chosen ground motion

intensity is then incorporated into the nonlinear dynamic analysis of the structure, modeling the response of the structure to the ground motion. After studying the performance behavior of the structure, the fragility curves were developed for both DBE and MCE.

5.1 Conclusion of Phase-I

Using the macro-seismic assessment study following results are drawn:

1. Both the DBE and the MCE suggest that there is a high risk of destruction of residential buildings, made of unreinforced masonry, and wood. Yet, there is a significant risk of damage, one that exceeds 20% under DBE and 40% under MCE. It is therefore proposed that these structures undergo substantial strengthening or demolition, with the decision being made based on the outcomes of following financial assessments. Both DBE and MCE predict that buildings made of reinforced and precast concrete with low ductility will have moderate to high levels of mean damage. The likelihood of damage is also between 60% and 70%.
2. For industrial and commercial buildings made of unreinforced masonry and concrete shows a high probability of moderate to very heavy damage for both DBE and MCE. The likelihood of heavy damage lies between 20% to 30%.

5.2 Conclusion of Phase-II

Following outcomes can be drawn from the analytical assessment of this study:

1. It has been determined that pre-cast concrete emulated moment frames have 100% probability of having light damage at both DBE and MCE in the occurrence of a global failure. While these buildings have probability of more than 70% to sustain moderate damage at DBE, however at MCE, this probability increases to 100%. Similarly, the probability of sustaining severe damage is more than 15 % at DBE, however at MCE, this probability increases to 50%.
2. In a similar way, for VT series buildings, the columns have 100% probability to sustain severe damage at DBE, but beams have a probability of about 70% of having moderate damage and 30% probability to sustain severe damage, but they will retain some of their original stiffness and strength for performance level of life safety. Similarly, at MCE beams have 100% probability to sustain moderate damage and

95% chances to sustain severe damage. From these results we can predict that the building will collapse if Almaty has an earthquake with a return period of 475 years in future.

3. For VP series buildings the chance of sustaining moderate damage is more than 85% while for severe damage the probability is more than 80% at DBE. These probabilities increase to 100% to sustain severe damage at MCE predicting the failure of the buildings. As it has been seen the failure of beam corresponds to the partial failure of the structures while that of columns corresponds to the full collapse of the structures.

No major disaster has happened in Almaty in the last century despite the facts that buildings have probabilities of sustain moderate and severe damages at DBE and MCE is because the city has not been hit by a major earthquake in the last century. But this might lead to misinterpretation, that it will not be hit by one in future, which will lead towards a major disaster. Nonetheless, these evaluation results can be used by government decision-makers to formulate policies to mitigate future seismic disasters to avoid such disaster.

5.3 Limitations and Future work

The analytical assessment is only employed to the pre-cast concrete emulated moment frame structures in this study. The seismic vulnerability assessment of other categories of the building structures should also be studied using analytical assessment in the future. Furthermore, this study mainly focused on the buildings constructed in the Soviet Union era, which leaves a room for studying the behavior of the buildings constructed after the Soviet Union era or recent infrastructure development.

Bibliography

[1] S. Glaister and R. Pinho, “Development of a simplified deformation-based method for seismic vulnerability assessment,” *Journal of Earthquake Engineering*, vol. 7, no. 1, pp. 107–140, 2003, doi: 10.1080/13632460309350475.

[2] B. Wei, G. Nie, G. Su, L. Sun, X. Bai, and W. Qi, “Risk assessment of people trapped in earthquake based on km grid: a case study of the 2014 Ludian earthquake, China,” *Geomatics, Natural Hazards and Risk*, vol. 8, no. 2, pp. 1289–1305, 2017, doi: 10.1080/19475705.2017.1318795.

[3] B. Wei, G. Su, and F. Liu, “Public response to earthquake disaster: A case study in Yushu Tibetan Autonomous Prefecture,” *Natural Hazards*, vol. 69, no. 1, pp. 441–458, 2013, doi: 10.1007/s11069-013-0710-2.

[4] J. E. Daniell, “The CATDAT Damaging Earthquakes Database - 2010 - The Year in Review : Damaging Earthquakes Database 2010 – The Year in Review James Daniell,” no. January 2011, 2014.

[5] D. N. Pane, M. EL Fikri, and H. M. Ritonga, “Postearthquake safety evaluation of buildings at doe facilities,” *J Chem Inf Model*, vol. 53, no. 9, pp. 1689–1699, 1989.

[6] A. Masi and M. Vona, “Vulnerability assessment of gravity-load designed RC buildings: Evaluation of seismic capacity through non-linear dynamic analyses,” *Eng Struct*, vol. 45, pp. 257–269, Dec. 2012, doi: 10.1016/j.engstruct.2012.06.043.

[7] N. v. Silacheva, U. K. Kulbayeva, and N. A. Kravchenko, “Probabilistic seismic hazard assessment of Kazakhstan and Almaty city in peak ground accelerations,” *Geod Geodyn*, vol. 9, no. 2, pp. 131–141, 2018, doi: 10.1016/j.geog.2017.11.002.

[8] A. Zhanabayeva *et al.*, “Comparative Analysis of Seismic Design Codes for Shallow Foundations Adhering to the Kazakhstani and European Approaches,” *Sustainability*, vol. 15, no. 1, p. 615, Dec. 2022, doi: 10.3390/su15010615.

[9] A. Zhanabayeva, S. Abdialim, A. Satyanaga, J. Kim, and S.-W. Moon, “Comparative analysis of international codes of practice for pile foundation design considering negative skin friction effect,” *International Journal of Geo-Engineering*, vol. 13, no. 1, p. 11, Dec. 2022, doi: 10.1186/s40703-022-00176-5.

[10] A. Shaldykova, S.-W. Moon, J. Kim, D. Lee, T. Ku, and A. Zhussupbekov, “Comparative Analysis of Kazakhstani and European Approaches for the Design of Shallow Foundations,” *Applied Sciences*, vol. 10, no. 8, p. 2920, Apr. 2020, doi: 10.3390/app10082920.

[11] A. Zhanabayeva, N. Sagidullina, J. Kim, A. Satyanaga, D. Lee, and S.-W. Moon, “Comparative Analysis of Kazakhstani and European Design Specifications: Raft

Foundation, Pile Foundation, and Piled Raft Foundation," *Applied Sciences*, vol. 11, no. 7, p. 3099, Mar. 2021, doi: 10.3390/app11073099.

[12] K. Anderson, G. Capannelli, E. Ginting, and K. Taniguchi, "Kazakhstan: Accelerating Economic Diversification," 2018.

[13] UNISDR, "Global Assessment Report on Disaster Risk Reduction. Geneva: UNISDR.," 2015.

[14] UNISDR, "Sendai Framework for Disaster Risk Reduction 2015. Geneva: UNISDR.," 2015.

[15] Thomas Tanner and Jun Rentschler, "Unlocking the 'Triple Dividend' of Resilience. London: ODI.," 2015.

[16] J. Daniell, F. Wenzel, and A. Schaefer, "The economic costs of natural disasters globally from 1900-2015: historical and normalised floods, storms, earthquakes, volcanoes, bushfires, drought and other disasters," 2016.

[17] M. H. Rahman, "Earthquakes don't kill, built environment does: Evidence from cross-country data," *Econ Model*, vol. 70, pp. 458–468, Apr. 2018, doi: 10.1016/j.econmod.2017.08.027.

[18] J. P. Newman *et al.*, "Review of literature on decision support systems for natural hazard risk reduction: Current status and future research directions," *Environmental Modelling & Software*, vol. 96, pp. 378–409, Oct. 2017, doi: 10.1016/j.envsoft.2017.06.042.

[19] L. Bosher and A. Dainty, "Disaster risk reduction and 'built-in' resilience: towards overarching principles for construction practice," *Disasters*, vol. 35, no. 1, pp. 1–18, Jan. 2011, doi: 10.1111/j.1467-7717.2010.01189.x.

[20] S. B. Miles, R. A. Green, and W. Svekla, "Disaster risk reduction capacity assessment for precarious settlements in Guatemala City," *Disasters*, vol. 36, no. 3, pp. 365–381, Jul. 2012, doi: 10.1111/j.1467-7717.2011.01267.x.

[21] D. E. Alexander, "Resilience and disaster risk reduction: An etymological journey," *Natural Hazards and Earth System Sciences*, vol. 13, no. 11, pp. 2707–2716, 2013, doi: 10.5194/nhess-13-2707-2013.

[22] H. V. Burton, G. Deierlein, D. Lallemant, and T. Lin, "Framework for Incorporating Probabilistic Building Performance in the Assessment of Community Seismic Resilience," *Journal of Structural Engineering*, vol. 142, no. 8, pp. 1–11, 2016, doi: 10.1061/(asce)st.1943-541x.0001321.

[23] L. Diana, J. Thiriot, Y. Reuland, and P. Lestuzzi, "Application of association rules to determine building typological classes for seismic damage predictions at regional scale: The case study of basel," *Front Built Environ*, vol. 5, no. April, pp. 1–17, 2019, doi: 10.3389/fbuil.2019.00051.

[24] M. L. Carreño, O. D. Cardona, and A. H. Barbat, “Urban seismic risk evaluation: A holistic approach,” *Natural Hazards*, vol. 40, no. 1, pp. 137–172, 2007, doi: 10.1007/s11069-006-0008-8.

[25] C. & Andrew and R. Spence, *Earthquake Protection*. 2002.

[26] A. Guettiche, P. Guéguen, and M. Mimoune, “Seismic vulnerability assessment using association rule learning: application to the city of Constantine, Algeria,” *Natural Hazards*, vol. 86, no. 3, pp. 1223–1245, 2017, doi: 10.1007/s11069-016-2739-5.

[27] B. & V. P. D., “On seismic vulnerability of masonry buildings: proposal of an evaluation procedure,” *L’industria delle Costruzioni*, vol. 18, pp. 66–78, 1984.

[28] C. A. Kircher, R. V. Whitman, and W. T. Holmes, “HAZUS Earthquake Loss Estimation Methods,” *Nat Hazards Rev*, vol. 7, no. 2, pp. 45–59, 2006, doi: 10.1061/(asce)1527-6988(2006)7:2(45).

[29] S. Lagomarsino and S. Giovinazzi, “Macroseismic and mechanical models for the vulnerability and damage assessment of current buildings,” *Bulletin of Earthquake Engineering*, vol. 4, no. 4, pp. 415–443, 2006, doi: 10.1007/s10518-006-9024-z.

[30] P. Mouroux and B. le Brun, “Risk-Ue Project: An Advanced Approach to Earthquake Risk Scenarios With Application to Different European Towns,” *Assessing and Managing Earthquake Risk*, pp. 479–508, 2008.

[31] S. Brzev *et al.*, “GEM Building Taxonomy (Version 2.0),” 2013. [Online]. Available: http://pubs.er.usgs.gov/publication/70058718

[32] H. Stone, “Exposure and vulnerability for seismic risk evaluations,” 2017.

[33] Gottfried. Grünthal, *European macroseismic scale 1998 : EMS-98*. European Seismological Commission, Subcommission on Engineering Seismology, Working Group Macroseismic scales, 1998.

[34] L. Abrahamczyk, D. H. Lang, and J. Schwarz, “WHE-REPORTS AS A COMPLEMENTARY DATABASE TOWARDS THE DEVELOPMENT OF AN INTERNATIONAL MACROSEISMIC SCALE,” 2017. [Online]. Available: http://db.world-housing.net/

[35] M. Ulmi *et al.*, “Hazus-MH 2.1 Canada user and technical manual: earthquake module,” 2014. doi: 10.4095/293800.

[36] A. Bendito, J. Rozelle, and D. Bausch, “Assessing Potential Earthquake Loss in Mérida State, Venezuela Using Hazus,” *International Journal of Disaster Risk Science*, vol. 5, no. 3, pp. 176–191, Jan. 2014, doi: 10.1007/s13753-014-0027-0.

[37] B. Gulati, “Earthquake Risk Assessment of Buildings: Applicability of HAZUS in Dehradun, India,” 2006.

[38] H. Miura, S. Midorikawa, K. Fujimoto, B. M. Pacheco, and H. Yamanaka, "Earthquake damage estimation in Metro Manila, Philippines based on seismic performance of buildings evaluated by local experts' judgments," *Soil Dynamics and Earthquake Engineering*, vol. 28, no. 10–11, pp. 764–777, Oct. 2008, doi: 10.1016/j.soildyn.2007.10.011.

[39] U. Hancilar, E. Çaktö, M. Erdik, G. E. Franco, and G. Deodatis, "Earthquake vulnerability of school buildings: Probabilistic structural fragility analyses," *Soil Dynamics and Earthquake Engineering*, vol. 67, pp. 169–178, Dec. 2014, doi: 10.1016/j.soildyn.2014.09.005.

[40] UN, "Global Assessment Report on Disaster Risk Reduction. Geneva: UN.," 2013.

[41] L. E. Yamin, A. I. Hurtado, A. H. Barbat, and O. D. Cardona, "Seismic and wind vulnerability assessment for the GAR-13 global risk assessment," *International Journal of Disaster Risk Reduction*, vol. 10, no. PB, pp. 452–460, Dec. 2014, doi: 10.1016/j.ijdrr.2014.05.007.

[42] K. A. Porter, K. S. Jaiswal, D. J. Wald, M. Greene, C. Comartin, and A. Res, "WHE-PAGER PROJECT: A NEW INITIATIVE IN ESTIMATING GLOBAL BUILDING INVENTORY AND ITS SEISMIC VULNERABILITY." [Online]. Available: http://www.world-housing.net/

[43] U. Hancilar, F. Taucer, H. Crowley, and A. M. Kaynia, "Guidelines for typology definition of European physical assets for earthquake risk assessment Soil-Structure Interaction (SSI) View project Towards the revision of EC8 soil classification system and elastic response spectra View project," 2013, doi: 10.2788/68751.

[44] D. Lang, S. Molina, J. Crempien, and E. Erduran, "Earthquake Risk Reduction in Guatemala, El Salvador, and Nicaragua with Regional Cooperation to Honduras, Costa Rica, and Panama: Mapping of Typical Buildings. Kjeller, Norway: NORSAR," 2009.

[45] M. M. Kassem, F. Mohamed Nazri, and E. Noroozinejad Farsangi, "The seismic vulnerability assessment methodologies: A state-of-the-art review," *Ain Shams Engineering Journal*, vol. 11, no. 4, pp. 849–864, 2020, doi: 10.1016/j.asej.2020.04.001.

[46] T. Rossetto, "Existing Empirical Fragility and Vulnerability Functions: Compendium and Guide for Selection Urban Waves: evaluating structure vulnerability to tsunami and earthquakes View project Mega Quakes: Cascading Earthquake Hazards and Compounding Risks View project," 2015, doi: 10.13117/GEM.VULNSMOD.TR2015.01.

[47] O. S. Kwon and A. Elnashai, "The effect of material and ground motion uncertainty on the seismic vulnerability curves of RC structure," *Eng Struct*, vol. 28, no. 2, pp. 289–303, Jan. 2006, doi: 10.1016/j.engstruct.2005.07.010.

[48] H. Groningen and F. G. Gulay, "A NEW APPROACH FOR THE PRELIMINARY SEISMIC ASSESSMENT OF RC A NEW APPROACH FOR THE PRELIMINARY SEISMIC ASSESSMENT OF RC BUILDINGS : P25 SCORING METHOD," no. July, 2008.

[49] T. Edition, “Rapid Visual Screening of Buildings for Potential Seismic Hazards: A Handbook,” no. January, 2015.

[50] İ. Engin Bal Hanzehogeschool Groningen, F. Gulten Gulay, S. Tezcan Bursa Teknik Üniversitesi, and I. Bal, “A NEW APPROACH FOR THE PRELIMINARY SEISMIC ASSESSMENT OF RC BUILDINGS: P25 SCORING METHOD Emerging Technologies in Earthquake and Structural Engineering View project Seismic Risk in Historical Structures View project A NEW APPROACH FOR THE PRELIMINARY SEISMIC ASSESSMENT OF RC BUILDINGS: P25 SCORING METHOD,” 2008. [Online]. Available: https://www.researchgate.net/publication/265823118

[51] A. Masi, L. Chiauzzi, G. Nicodemo, and V. Manfredi, “Correlations between macroseismic intensity estimations and ground motion measures of seismic events,” *Bulletin of Earthquake Engineering*, vol. 18, no. 5, pp. 1899–1932, Mar. 2020, doi: 10.1007/s10518-019-00782-2.

[52] G. M. Calvi, R. Pinho, G. Magenes, and J. Bommer, “Development of seismic vulnerability assessment methodologies over the past 30 years CA’REDIVIVUS View project SERA JRA4 (Risk modelling framework for Europe) View project,” 2006. [Online]. Available: https://www.researchgate.net/publication/241826044

[53] FEMA, “FEMA273, NEHRP Guidelines for the seismic rehabilitation of buildings. Federal Emergency Management Agency; 1997”.

[54] FEMA, “FEDERAL EMERGENCY MANAGEMENT AGENCY FEMA 356 / November 2000 PRESTANDARD AND COMMENTARY FOR THE SEISMIC REHABILITATION OF BUILDINGS.”

[55] V. v. Bertero, “Strength and deformation capacities of buildings under extreme environments,” *Structural engineering and structural mechanics*, pp. 29–79.

[56] P. Bazzurro and C. A. Cornell, “Seismic Hazard Analysis of Nonlinear Structures. I: Methodology,” *Journal of Structural Engineering*, vol. 120, no. 11, pp. 3320–3344, 1994, doi: 10.1061/(asce)0733-9445(1994)120:11(3320).

[57] P. Bazzurro, C. A. Cornell, N. Shome, and J. E. Carballo, “Three Proposals for Characterizing MDOF Nonlinear Seismic Response,” *Journal of Structural Engineering*, vol. 124, no. 11, pp. 1281–1289, 1998, doi: 10.1061/(asce)0733-9445(1998)124:11(1281).

[58] D. Vamvatsikos and C. A. Cornell, “Incremental dynamic analysis,” *Earthq Eng Struct Dyn*, vol. 31, no. 3, pp. 491–514, Mar. 2002, doi: 10.1002/eqe.141.

[59] S.-Y. Yun, R. O. Hamburger, C. A. Cornell, and D. A. Foutch, “Seismic Performance Evaluation for Steel Moment Frames,” *Journal of Structural Engineering*, vol. 128, no. 4, pp. 534–545, Apr. 2002, doi: 10.1061/(ASCE)0733-9445(2002)128:4(534).

[60] C. Grützner *et al.*, “Assessing the activity of faults in continental interiors: Palaeoseismic insights from SE Kazakhstan,” *Earth Planet Sci Lett*, vol. 459, pp. 93–104, Feb. 2017, doi: 10.1016/j.epsl.2016.11.025.

[61] N. v. Silacheva, U. K. Kulbayeva, and N. A. Kravchenko, “On the realization of seismic microzonation of Almaty (Kazakhstan) in ground accelerations based on the ‘continual’ approach,” *Geod Geodyn*, vol. 11, no. 1, pp. 56–63, Jan. 2020, doi: 10.1016/j.geog.2019.07.006.

[62] M. S. Rashid, D. Zhang, S.-W. Moon, D. Sarkulova, Y. Shokbarov, and J. Kim, “Macro-Seismic Assessment for Residential Buildings Constructed in the Soviet Union Era in Almaty, Kazakhstan,” *Buildings*, vol. 13, no. 4, p. 1053, Apr. 2023, doi: 10.3390/buildings13041053.

[63] “SP RK 2.03-30-2017. Construction in seismic zones. Nur-Sultan, AO KazNIISA.,” 2019.

[64] A. C. I. C. 318, “318-19(22): Building Code Requirements for Structural Concrete and Commentary (Reapproved 2022),” *Technical Documents*.

[65] F. McKenna, G. L. Fenves, M. H. Scott, and B. Jeremic, “Open system for earthquake engineering simulation (OpenSees),” *Pacific Earthquake Engineering Research Center, University of California, Berkeley, CA*, 2000.

[66] R. Park and T. Paulay, *Reinforced Concrete Structures*. Wiley, 1975. doi: 10.1002/9780470172834.

[67] “Pacific Earthquake Engineering Research. (2005). ‘NGA Database.’ from http://peer.berkeley.edu/nga/.”.

[68] Mohiuddin. Ali Khan, *Earthquake-resistant structures : design, build and retrofit*. Butterworth-Heinemann, 2009.

[69] H.-S. Lee, “Revised Rule for Concept of Strong-Column Weak-Girder Design,” *Journal of Structural Engineering*, vol. 122, no. 4, pp. 359–364, Apr. 1996, doi: 10.1061/(ASCE)0733-9445(1996)122:4(359).

[70] N. Shome and C. A. Cornell, “Probabilistic Seismic Demand Analysis of Nonlinear Structures. Reliability of Marine Structures Program Technical Report RMS-35.,” Stanford Digital Repository, 1999.

[71] C. A. Kircher, A. A. Nassar, O. Kustu, and W. T. Holmes, “Development of Building Damage Functions for Earthquake Loss Estimation,” *Earthquake Spectra*, vol. 13, pp. 663–682, 1997.

[72] A. W. Smyth *et al.*, “Probabilistic Benefit-Cost Analysis for Earthquake Damage Mitigation: Evaluating Measures for Apartment Houses in Turkey,” *Earthquake Spectra*, vol. 20, no. 1. Earthquake Engineering Research Institute, pp. 171–203, 2004. doi: 10.1193/1.1649937.

[73] M. Serdar Kirçil and Z. Polat, “Fragility analysis of mid-rise R/C frame buildings,” *Eng Struct*, vol. 28, no. 9, pp. 1335–1345, Jul. 2006, doi: 10.1016/j.engstruct.2006.01.004.

[74] D. Vamvatsikos and C. A. Cornell, “Incremental dynamic analysis,” *Earthq Eng Struct Dyn*, vol. 31, no. 3, pp. 491–514, Mar. 2002, doi: 10.1002/eqe.141.

[75] F. Emergency and M. Agency, “FEMA356, commentary for the seismic rehabilitation of buildings,” no. November, 2000.

[76] M. G. Flenga and M. J. Favvata, “Fragility curves and probabilistic seismic demand models on the seismic assessment of RC frames subjected to structural pounding,” *Applied Sciences (Switzerland)*, vol. 11, no. 17, Sep. 2021, doi: 10.3390/app11178253.